Membrane Trafficking and Signaling of the Delta Opioid Receptor Within the Biosynthetic Pathway

by

Stephanie E. Crilly

A dissertation submitted in partial fulfillment
of the requirements for the degree of
Doctor of Philosophy
(Cellular and Molecular Biology)
in the University of Michigan
2022

Doctoral Committee:

Associate Professor Manojkumar Puthenveedu, Chair
Professor Alan Smrcka
Professor Lois Weisman
Professor Bing Ye

Stephanie E. Crilly
secrilly@umich.edu
ORCID iD: 0000-0002-8151-290X

Acknowledgements

I would first like to acknowledge my advisor Dr. Manoj Puthenveedu. Without your influence, I would not be where I am today! Thank you for the opportunity to pursue the research questions most interesting to me and to grow as a scientist in your lab. The PhD journey has been a long and winding road with many twists and turns, and I am grateful for your encouragement, enthusiasm, and limitless optimism along the way.

I would next like to acknowledge all the members of the Puthenveedu lab, past and present. Through knowing each of you, I have grown both scientifically and personally. Special thanks to Dr. Dan Shiwarski for being an essential resource and mentor during my first years in the lab and for always being eager to offer advice to set me on a path to success. I would also like to give special thanks to Dr. Zara Weinberg whom I am thankful to call both a mentor and one of my dearest friends. Thank you for always believing in me and inspiring me by your example both in science and life. Thank you to Dr. Jenny Kunselman, Elena Shuvaeva, and Wooree Ko, who in addition to Zara, formed a valued support network during the transition from Carnegie Mellon University to University of Michigan. Thank you to Candilianne Serrano Zayas for being a wonderful friend and collaborator and for the energy and excitement you bring to science and those around you. I would also like to thank Josh Lott for countless insights and perspectives which have helped me stay grounded both inside and outside the lab. Thank you to Hao Chen, Ian Chronis, Caroline Hernandez-Casner, and Loyda Morales Rodriguez for your brilliant questions and even more brilliant spirits. Thank you to Dr. Aditya Kumar, Dr. Kasun Ratnayake, and Dr. Prahatha Venkatraman for being sources of wise advice, kind words, and enthusiastic support.

Thank you to my dissertation committee, Dr. Alan Smrcka, Dr. Lois Weisman, and Dr. Bing Ye, for enthusiastically supporting my development as a scientist and sharing your unique scientific insights.

Thank you to the scientific communities and people who have supported me at various stages of my graduate career: CMU Department of Biological Sciences (especially Dr. Aryn Gittis, Dr. Tina Lee, and Dr. Jon Minden), University of Michigan Cellular & Molecular Biology Program (especially Dr. Roberta Fuller for welcoming me to the CMB community), UMich OGPS (especially Dr. Shoba Subramanian). Thank you as well to Dr. Madan Babu and Dr. Maria Marti-Solano for productive collaborations.

Thank you to the mentors and educators who set me on this path and nurtured my scientific interest and curiosity: Margaret Ayers, Bob Foell, Drs. Claire Thomas, Floyd Mattie, and Kristen Browder, among many others.

Finally, I would like to thank my support system behind all the science. Thank you to my family and friends whose unconditional support has made this journey possible.

Table of Contents

List of Figures

Abstract

G protein-coupled receptors (GPCRs) transduce diverse signals, including light, ions, hormones, and neurotransmitters, into equally diverse cellular responses. These cellular responses underlie complex physiological processes, including sensation, learning and memory, cardiac function, and immune function. Understanding the variables which contribute to GPCR signaling diversity at a cellular level is essential to understanding the role of GPCRs in physiology and disease. The subcellular location from which GPCR signaling occurs is an increasingly recognized variable which contributes to signaling diversity.

I have used the delta opioid receptor (DOR) as a prototype GPCR to investigate mechanisms regulating GPCR localization and the effects of subcellular location on GPCR function. DOR is an ideal and therapeutically relevant prototype GPCR to study these questions. In neuronal cells, DOR localizes to multiple membrane compartments, including the plasma membrane and the Golgi apparatus. Relocation of DOR from intracellular sites to the plasma membrane is associated with enhanced pain-relieving effects of DOR agonists, which highlights the therapeutically relevant link between DOR localization and function.

I first investigated the mechanisms which regulate DOR localization to the Golgi in a rat neuroendocrine cell line which shares common mechanisms with primary neurons in regulation of DOR trafficking. Through systematic mutagenesis of the DOR C-terminal primary amino acid sequence and high-resolution imaging, we identified conserved dual RXR amino acid motifs which are required for signal-regulated retention of DOR in the Golgi. Using biochemical approaches, we showed that these RXR motifs also mediate interaction with the coatomer protein I (COPI) complex. These data support a model in which DOR retention in the Golgi is mediated by active retrograde trafficking within the biosynthetic pathway.

I next explored the effect of subcellular location on DOR activation. GPCR activation and coupling to effectors is driven by conformational changes in the receptor upon agonist binding. We used fluorescently tagged biosensors which recognize these conformational changes and high-resolution imaging to visualize DOR activation in different subcellular locations. We found that DOR in the plasma membrane and the Golgi differentially recruit two active conformation biosensors in response to the same agonist. These results indicate that subcellular location drives distinct engagement of effectors and suggest the exciting possibility that subcellular location may alter GPCR conformational landscapes upon ligand binding.

I also determined the effect of subcellular location on DOR signaling using biosensors for second messenger signaling molecules cAMP and calcium. We found that DOR activation in both the plasma membrane and the Golgi inhibits cAMP production, suggesting that DOR couples to inhibitory G proteins regardless of compartment-specific effects on effector engagement or conformational landscapes. In a rat neuroendocrine cell line, DOR activation at the plasma membrane modulates calcium release from intracellular stores in a Gi/o, Gq/11, and phospholipase C-dependent manner. Modulation of calcium is specific to DOR signaling from the plasma membrane and is not observed upon DOR activation in the Golgi. These data suggest that DOR subcellular location influences the signaling profile of active receptors.

Together this work adds to our understanding of how GPCR subcellular localization is regulated and how subcellular location can drive distinct GPCR activation and signaling. In the future, this mechanistic understanding could be applied to tune localization of therapeutically relevant GPCRs like DOR or to target GPCRs in specific subcellular compartments for desired therapeutic effects.

Chapter 1: An Introduction to Compartmentalized GPCR Signaling From Intracellular Membranes

This chapter is published as[1]**:**

Crilly, SE, and Puthenveedu, MA (2020). Compartmentalized GPCR Signaling from Intracellular Membranes. J Membr Biol, 1–13.

Abstract

G protein-coupled receptors (GPCRs) are integral membrane proteins that transduce a wide array of inputs including light, ions, hormones, and neurotransmitters into intracellular signaling responses which underlie complex processes ranging from vision to learning and memory. Although traditionally thought to signal primarily from the cell surface, GPCRs are increasingly being recognized as capable of signaling from intracellular membrane compartments, including endosomes, the Golgi apparatus, and nuclear membranes. Remarkably, GPCR signaling from these membranes produces functional effects that are distinct from signaling from the plasma membrane (PM), even though the same G protein effectors and second messengers are often activated. In this review we will discuss the emerging idea of a "spatial bias" in signaling. We will present the evidence for GPCR signaling through G protein effectors from intracellular membranes, and the ways in which this signaling differs from canonical PM signaling with important implications for physiology and pharmacology. We also highlight the potential mechanisms underlying spatial bias of GPCR signaling, including how intracellular membranes and their associated lipids and proteins affect GPCR activity and signaling.

[1] Statement of others' contributions to this work:
I wrote the published manuscript with input from Manoj Puthenveedu. Puthenveedu lab members provided helpful feedback on the final draft of the published manuscript as stated in the acknowledgements.

Introduction

G protein-coupled receptor (GPCR) signaling which underlies complex processes ranging from smell and taste to immune responses to vision, learning, and memory, is being reconsidered in the context of the membranes from which GPCRs signal. GPCRs are the largest class of transmembrane signaling receptors and are activated by a wide array of inputs including light, ions, peptide and non-peptide hormones and neurotransmitters. GPCRs transduce these inputs through conformational changes in their seven transmembrane domains. Conformational changes are driven and stabilized by interaction with classical heterotrimeric G protein effectors, which modulate diverse downstream signaling pathways and second messengers, including adenylyl cyclase and cAMP, ion channels, phospholipases, GTPases, and kinase cascades (Weis and Kobilka, 2018; Wu *et al.*, 2019). GPCRs were originally thought to activate these signaling pathways primarily from the plasma membrane (PM). However, GPCRs also localize to other membranes in the cell and can signal from these membranes, suggesting an important spatial component of signaling.

GPCRs signaling from intracellular membranes can occur through both non-G protein and G protein effectors. The first evidence of GPCR signaling from intracellular membranes suggested that this signaling is mediated by non-G protein effectors, specifically β-arrestins. β-arrestins interact with GPCRs and scaffold kinase signaling pathways in endosomes and at the PM, in addition to their roles in G protein signaling termination and GPCR internalization from the PM (Lohse *et al.*, 1990; Luttrell and Lefkowitz, 2002). Subsequent studies have demonstrated that a number of other non-G protein effectors could promote differential GPCR signaling at locations other than the PM (Varsano *et al.*, 2012; Jean-Alphonse *et al.*, 2014; Grimsey *et al.*, 2015; Alekhina and Marchese, 2016). However, research over the past decade supports the exciting new idea that signaling by a GPCR through the *same* G protein effector in *different* locations produces distinct signaling responses. In this review we will focus on how G protein signaling from GPCRs in intracellular membrane compartments differs from classical PM signaling **(Figure 1.1)**. We will also discuss potential mechanisms by which components of different cellular membranes may shape this “spatial bias” in signaling.

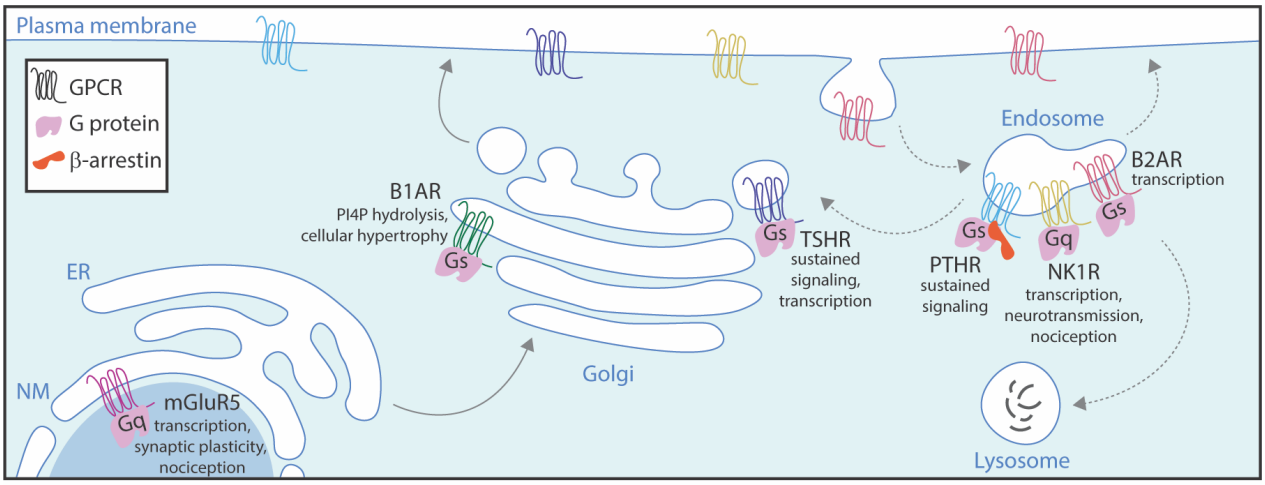

Figure 1.1. Examples of localization and signaling of GPCRs from intracellular membranes.
In addition to the plasma membrane GPCRs localize and signal through G proteins in compartments along the biosynthetic pathway (solid arrows) and the endolysosomal pathway (dashed arrows). Non-canonical GPCR signaling through G proteins in these membranes can proceed by distinct interactions, such as a PTHR-G protein-arrestin signaling complex, and produce distinct downstream signaling effects, including but not limited to sustained signaling, transcriptional responses, and effects on cell growth, neurotransmission, and the perception of pain.

GPCR signaling in endosomes

GPCR localization to the endosomal pathway

Many GPCRs enter and cycle within the endosomal pathway after activation and internalization from the PM. GPCR internalization is predominantly mediated by clathrin and β-arrestin-1 or β-arrestin-2 which interacts with clathrin via clathrin adaptor protein AP-2 (Laporte *et al.*, 1999; Weinberg and Puthenveedu, 2019). Within the endosomal pathway, GPCRs can enter recycling pathways which return receptors to the PM or degradative pathways which sort receptors to the lysosome. GPCR sorting to these different endosomal pathways is often an active process (Puthenveedu *et al.*, 2010; Bowman and Puthenveedu, 2015). Sorting can be regulated by amino acid trafficking motifs on a receptor, post-translational modifications like phosphorylation or ubiquitination, and interactions with endosome-associated proteins (Hanyaloglu and von Zastrow, 2008).

Regulated trafficking of GPCRs has clear consequences for their signaling. Classically, relocation of GPCRs from the PM to endosomes was proposed to serve as a mechanism of terminating signaling from the PM and desensitizing the cell to extracellular ligands (Lefkowitz *et al.*, 1980; Hertel and Perkins, 1984). However, the discovery of endosomal G protein signaling indicates that receptor endocytosis and localization to endosomal compartments contributes to "spatial bias" in GPCR signaling. We will now examine the early evidence for GPCR G protein signaling from endosomes, and how this signaling differs from signaling at the PM at a cellular and organismal level.

Evidence for GPCR activation and signaling from endosomes

Building on a report of endosomal G protein signaling by the yeast GPCR Ste2 (Slessareva *et al.*, 2006), early insights into endosomal G protein signaling in mammalian cells stemmed from prolonged signaling responses even after receptors had internalized from the PM. Activation of parathyroid hormone receptor (PTHR) and the thyroid stimulating hormone receptor (TSHR), which both couple to Gαs, elevates cellular cAMP even after robust internalization of receptors from the PM (Calebiro *et al.*, 2009; Ferrandon *et al.*, 2009). These observations were inconsistent with the hypothesis that removal of GPCRs from the PM serves mainly to terminate G protein signaling. Indeed, prolonged cAMP signaling persists even when agonist is removed from the extracellular media, and fluorescently labeled peptide ligands colocalize with receptors in endosomal compartments, suggesting that ligands can traffic with the receptor to endosomes and continue to signal (Calebiro *et al.*, 2009; Ferrandon *et al.*, 2009). Critically, prolonged elevation of cellular cAMP is disrupted by inhibition of endocytosis by pharmacological or genetic approaches, indicating endocytosis is required for sustained cAMP production by these GPCRs (Calebiro *et al.*, 2009; Ferrandon *et al.*, 2009).

Receptor endocytosis might contribute to distinct cAMP signaling profiles for different GPCRs. For example, inhibiting endocytosis partially decreases cAMP production by the activated Gαs-coupled dopamine receptor D1 (DRD1) and the β_2-adrenergic receptor (B2AR) (Kotowski *et al.*, 2011; Irannejad *et al.*, 2013). In the case of

DRD1, inhibiting endocytosis measurably decreases cAMP as early as one to two minutes after agonist addition (Kotowski *et al.*, 2011). In the case of B2AR, inhibiting endocytosis decreases cAMP production mainly at later time points, greater than five minutes after agonist treatment (Irannejad *et al.*, 2013). This later time may reflect the time required for B2AR sorting to the specific endosomal domain from which it initiates endosomal G protein signaling (Bowman *et al.*, 2016), as we discuss in more detail in section 5.2. Therefore, some GPCRs might require components of the endocytic process for acute signaling, whereas others require endocytosis for a second wave of cAMP signaling after desensitization of the initial PM cAMP signaling.

Conformational biosensors based on nanobodies have recently emerged as a powerful method that complements conventional signaling assays to study spatially restricted signaling. These nanobodies are a single protein domain derived from the antigen-binding region of heavy-chain only antibodies produced in camelid species (Manglik *et al.*, 2017). Several generated nanobodies specifically bind the active conformation of a specific GPCR or family of GPCRs (Manglik *et al.*, 2017). Additionally, another nanobody, referred to as Nb37, recognizes a nucleotide-free Gαs conformation as a readout of GDP exchange by the Gαs subunit of the activated G protein (Westfield *et al.*, 2011; Irannejad *et al.*, 2013). Nanobodies have greatly aided in vitro and in vivo studies of GPCR biology (Manglik *et al.*, 2017). When tagged with a fluorescent protein and expressed in live cells, nanobody biosensors localize to membranes containing active GPCR or Gαs protein, providing a highl spatiotemporal readout of GPCR activation **(Figure 1.2A)**. Indeed, fluorescently-tagged β-adrenergic receptor active conformation nanobody (Nb80) and nucleotide-free Gαs nanobody (Nb37) are recruited to B2AR at the PM and in endosomal compartments upon agonist treatment, highlighting the presence of both active GPCR and G protein in endosomes (Irannejad *et al.*, 2013; Bowman *et al.*, 2016). Similar nanobodies which recognize the active conformation of opioid receptors (Nb33 and Nb39) colocalize with internalized μ-opioid receptor (MOR), δ-opioid receptor (DOR), and κ-opioid receptors (KOR) in endosomes upon agonist treatment (Stoeber *et al.*, 2018; Kunselman *et al.*, 2020). Beyond the examples highlighted here, signaling assays and biosensor imaging have demonstrated signaling of internalized Gαs, Gαi, and Gαq-coupled GPCRs, including the sphingosine-

1-phosphate receptor, glucagon-like peptide-1 receptor, cannabinoid receptor 1, luteinizing hormone receptor (LHR), and the calcium-sensing receptor (CaSR), across a range of endosomal compartments ranging from very early endosomes, to early endosomes marked by EEA1/Rab5, to potentially even late endosomes/lysosomes marked by Rab7 (Rozenfeld and Devi, 2008; Ferrandon *et al.*, 2009; Mullershausen *et al.*, 2009; Kuna *et al.*, 2013; Sposini *et al.*, 2017; Gorvin *et al.*, 2018; Stoeber *et al.*, 2018; Jimenez-Vargas *et al.*, 2020; Kunselman *et al.*, 2020).

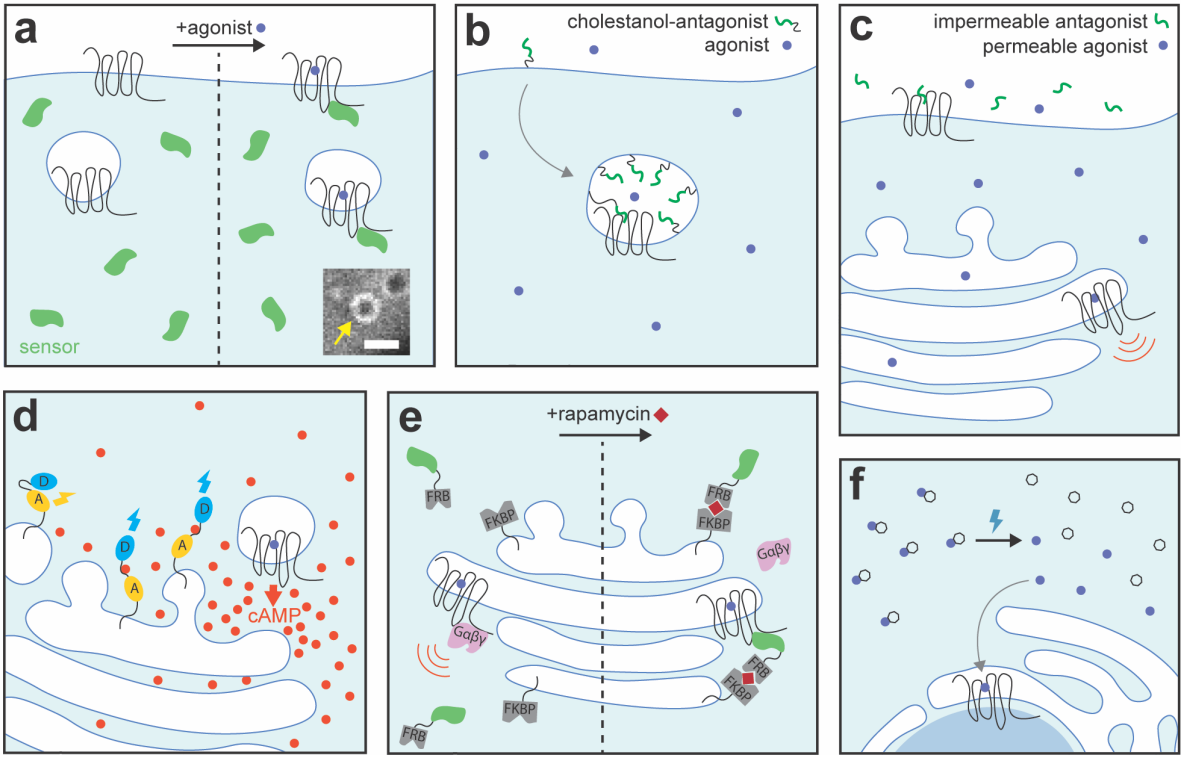

Figure 1.2. Tools for studying GPCR spatial signaling bias.
(A) Conformational biosensors including nanobodies and miniG proteins recognize active GPCR or Gs conformations. When expressed in cells these sensors will translocate from the cytosol to membranes containing active GPCR or G protein. If tagged with a fluorescent protein, translocation of the sensor can be visualized by confocal microscopy. *Inset:* HEK cell expressing Flag-DOR and venus-miniGsi and treated with 10μM SNC80 agonist. Accumulation of the miniG sensor is visible on endosomal membranes (yellow arrow), scale bar=1.5μm. **(B)** Cholestanol-conjugated ligands incorporate into the lipid bilayer, are internalized, and accumulate in endosomes. When concentrated in endosomes, these ligands can provide prolonged and specific agonism or antagonism of endosomal GPCRs. Whether these endosomally-targeted antagonists also inhibit plasma membrane GPCRs over prolonged time periods, and if so, to what levels is not clear. **(C)** To isolate GPCR signaling from intracellular sites, cells can be treated with a membrane

permeable agonist along with a membrane impermeable antagonist. The permeable agonist can access and activate intracellular GPCRs, while the impermeable antagonist acts only on GPCRs in the plasma membrane, preventing agonist from binding to these sites. **(D)** Fluorescent FRET sensors for PKA phosphorylation events or second messengers like cAMP produced downstream of GPCR activation can be targeted to specific cellular membranes. Localization of these sensors to specific membranes provides a readout of local signaling events. Second messenger like cAMP or phosphorylation of a kinase motif on the sensor leads to a conformational change in the sensor. Changes in cellular levels of cAMP or kinase activity are measured as the ratio between donor fluorophore (D) and acceptor fluorophore (A) emission for a ratiometric FRET sensor, like the one depicted. **(E)** Nanobodies which recognize the active conformation of GPCRs specifically inhibit GPCR signaling from intracellular sites. Rapamycin induces dimerization of FRB and FKBP domains fused to a nanobody or targeted to the organelle of interest, respectively. Dimerization leads to a high local concentration of nanobody which binds to active GPCRs. These nanobodies compete with endogenous G proteins for interaction with the active receptor, interfering with G protein activation and signaling in the organelle of interest. **(F)** Caged ligands are chemically modified so that they are inactive at the target receptor until uncaging. Local uncaging of caged ligands by a specific wavelength of light leads to photolysis of the caged ligand, freeing the active ligand. The free ligand can then bind to the target receptor.

Distinct consequences of endosomal G protein signaling

Illustrating the concept of “spatial bias,” G protein signaling from GPCRs in endosomes diverges from PM signaling in a number of ways at the molecular and cellular level. Sustained G protein signaling by PTHR and the vasopressin receptor 2 (V2R) is associated with prolonged arrestin-Gβγ, GPCR-Gβγ, or GPCR-arrestin interactions on endosomes (Ferrandon *et al.*, 2009; Feinstein *et al.*, 2011, 2013; Wehbi *et al.*, 2013). These data, coupled with single-particle electron microscopy structure of a chimeric GPCR simultaneously bound to β-arrestin-1 and a heterotrimeric G protein, support a hypothesis in which a subset of GPCRs which strongly bind β-arrestins sustain endosomal signaling from stabilized arrestin-Gβγ complexes which could support multiple rounds of Gαs activation (Wehbi *et al.*, 2013; Thomsen *et al.*, 2016). Whether this complex is uniquely stabilized in the endosomal compartment remains to be explored.

The role of arrestins in endosomal signaling has been extensively reviewed recently in more detail (Peterson and Luttrell, 2017; Ranjan *et al.*, 2017; Weinberg and

Puthenveedu, 2019). Endosomal GPCR-arrestin-G protein complexes likely function differently than GPCR-arrestin signaling complexes. The observation that some GPCRs remain associated with arrestin on the endosome and the detection of GPCR-arrestin-kinase complexes were some of the earliest evidence of potential GPCR signaling from endosomes (Déry *et al.*, 1999; Luttrell *et al.*, 1999; DeFea *et al.*, 2000a; Oakley *et al.*, 2000; Wei *et al.*, 2003). β-arrestins bound to a GPCR can scaffold a number of kinases, and kinases, including Src, Raf, JNK, and ERK, can also be visualized on endosomes containing GPCRs and/or arrestin (DeFea *et al.*, 2000a, 2000b; McDonald *et al.*, 2000; Luttrell *et al.*, 2001). GPCR signaling through arrestins is an excellent example of how GPCRs can also signal through *different* effectors in *different* locations.

Spatial bias shapes downstream transcriptional responses, either as a consequence of, or in addition to differential interactions with G protein effectors. In the case of B2AR, a prototypical Gαs-coupled receptor, endosomal cAMP production is required and sufficient for transcription of genes not upregulated by B2AR signaling from the PM (Tsvetanova and von Zastrow, 2014; Bowman *et al.*, 2016). Similarly, CaSR and neurokinin 1 receptor (NK1R) also require endosomal signaling to induce gene transcription from serum response elements (Jensen *et al.*, 2017; Gorvin *et al.*, 2018). How endosomal signaling drives transcriptional responses is an ongoing area of research and may result from spatiotemporal regulation of GPCR-effector interactions and second messengers.

Endosomal GPCR signaling is linked to physiology and can be specifically modulated by new spatially-targeted pharmacology. Sustained cAMP signaling and endocytosis of the LHR are required for meiosis in the oocyte of ovarian follicles, suggesting an important link between LHR endosomal signaling and fertility (Lyga *et al.*, 2016). Exciting new work in the context of pain neurotransmission by NK1R and the calcitonin receptor-like receptor (CLR) uses spatially-targeted ligands to specifically inhibit endosomal signaling. NK1R or CLR antagonists conjugated to the lipid cholestanol incorporate into the outer leaflet of the membrane bilayer, are internalized, and accumulate in endosomes **(Figure 1.2B)** (Jensen *et al.*, 2017; Yarwood *et al.*, 2017). These endosomally-targeted antagonists inhibit sustained signaling in spinal

cord neurons and provide greater and longer lasting pain relief in animal models of inflammatory pain than traditional antagonists (Jensen *et al.*, 2017; Yarwood *et al.*, 2017). A similar approach using lipoparticles to deliver DOR agonist to endosomes supports a role for endosomal DOR signaling in promoting sustained suppression of neuronal excitability and antinociception (Jimenez-Vargas *et al.*, 2020). These compartment-targeted ligands demonstrate the contribution of endosomal signaling to pain pathologies and highlight potential therapeutic approaches which exploit spatial bias in signaling.

GPCR signaling in the Golgi

GPCR localization to the Golgi

GPCRs can sort retrogradely from endosomes to the Golgi after internalization from the PM or be retained in the Golgi during biosynthetic trafficking en route to the PM after synthesis at the endoplasmic reticulum (ER). Retrograde sorting from endosomes to the most distal compartment and "sorting station" of the Golgi, the *trans*-Golgi network (TGN), is often mediated by the retromer complex (Chen *et al.*, 2019). GPCRs including, PTHR and TSHR, internalize and traffic retrogradely to the TGN (Feinstein *et al.*, 2011; Godbole *et al.*, 2017). Though not all GPCRs recycle through the TGN, as integral membrane proteins all GPCRs are expected to transit through the Golgi where they receive important modifications like glycosylation before initial insertion into the PM (Dong *et al.*, 2007). For many GPCRs Golgi residence is transient, but some receptors like DOR and β_1-adrenergic receptor (B1AR) exhibit steady-state Golgi localization (Irannejad *et al.*, 2017; Shiwarski *et al.*, 2017b). Golgi export of these receptors is highly regulated by amino acid trafficking motifs in receptors themselves, protein interactions, and even phospholipids (Mittal *et al.*, 2013; Koliwer *et al.*, 2015; Shiwarski *et al.*, 2017a, 2019; St-Louis *et al.*, 2017). Here we present new and emerging evidence supporting GPCR activation in the Golgi, as well as differential signaling by B1AR and TSHR in the Golgi.

Evidence for GPCR activation and signaling in the Golgi

Regardless of the mechanisms by which GPCRs localize to the Golgi, GPCRs can be activated by ligands and signal from Golgi compartments. Conformational biosensors including the nanobodies already described, as well as mini-G protein biosensors which mimic Gα subunit interactions with active GPCR conformations (Nehmé *et al.*, 2017; Wan *et al.*, 2018), reveal activation of GPCRs or Gαs proteins in the Golgi (Godbole *et al.*, 2017; Irannejad *et al.*, 2017; Stoeber *et al.*, 2018; Nash *et al.*, 2019). The nucleotide-free Gαs nanobody (Nb37) localizes to compartments containing both labeled TSH internalized with endogenous TSHR, and a TGN marker, as well as compartments containing a component of the retromer complex (Godbole *et al.*, 2017). Together these data suggest TSHR signals from retrograde endocytic compartments at the TGN (Godbole *et al.*, 2017). Activation of B1AR, DOR, MOR, and KOR by ligands in the Golgi have similarly been revealed by conformational biosensors recognizing active receptor conformations (Irannejad *et al.*, 2017; Stoeber *et al.*, 2018; Nash *et al.*, 2019; Che *et al.*, 2020).

Notably, for GPCRs not internalizing from the cell surface with their associated ligand, activation in the Golgi is limited to agonists which can readily cross multiple cell membranes either by diffusion or active transport by transporters like the organic cation transporter 3 (OCT3) catecholamine transporter (Irannejad *et al.*, 2017; Stoeber *et al.*, 2018). For both B1AR and DOR, membrane impermeable antagonists inhibit signaling responses induced by cell impermeable agonists, but fail to completely block signaling downstream of cell permeable agonists **(Figure 1.2C)**, with this residual signaling attributed to Golgi GPCRs (Irannejad *et al.*, 2017; Stoeber *et al.*, 2018). The dependence of intracellular GPCR activation on ligand permeability forms the basis of many approaches to assay signaling from both Golgi and nuclear membrane-localized GPCRs, which will be discussed in more detail later.

Distinct consequences of GPCR signaling in the Golgi

GPCR signaling from the Golgi mediates differential and spatially-restricted cellular signaling effects. Förster resonance energy transfer (FRET) sensors can be

targeted to both the PM and Golgi to measure local cAMP or protein kinase A (PKA) activity **(Figure 1.2D)** (Dipilato and Zhang, 2009; Depry *et al.*, 2011; Godbole *et al.*, 2017). In the case of TSHR, Golgi-localized FRET sensors reveal Golgi-localized cAMP and PKA signaling up to ten minutes after receptor internalization, which is lost when cells are treated with an endocytosis inhibitor (Godbole *et al.*, 2017). This signaling is linked to cAMP response element-binding protein (CREB) phosphorylation and transcription of cAMP-regulated genes. Golgi membrane integrity and anchoring of PKA at the Golgi through interactions with A-kinase-anchoring proteins (AKAPs) are required for TSH-induced CREB phosphorylation, suggesting the spatial organization of these signaling components at the Golgi regulates downstream signaling effects (Godbole *et al.*, 2017).

In the case of B1AR, activation of Golgi B1AR signaling in cardiac myocytes is required and sufficient to induce phospholipase C epsilon (PLCε)-dependent hydrolysis of phosphatidylinositol 4-phosphate (PI4P), the primary phospholipid at the Golgi (Nash *et al.*, 2019). In an interesting parallel to TSHR, PLCε interaction with muscle specific AKAP, mAKAP, is required for B1AR-dependent PI4P hydrolysis, suggesting that localization of signaling effectors may be a major component in regulating Golgi signaling pathways (Nash *et al.*, 2019). In addition to traditional pharmacological approaches using ligands with different membrane permeability, B1AR signaling from the Golgi was inhibited by a novel non-pharmacological approach, developed by Irannejad, et al., 2017. β-adrenergic receptor active conformation nanobody Nb80, is recruited to the Golgi via chemically induced dimerization and competes with endogenous G proteins for binding to the active receptor, effectively preventing local G protein activation **(Figure 1.2E)** (Irannejad *et al.*, 2017). Inhibition of B1AR Golgi signaling not only decreases PI4P hydrolysis, but also decreases cellular hypertrophy and atrial natriuretic factor (ANF) expression, both of which are hallmarks of cardiac hypertrophy often preceding heart failure (Nash *et al.*, 2019). These data provide rationale for specifically targeting Golgi B1AR signaling for treatment of heart failure and could guide new pharmacological approaches.

GPCR signaling in the nuclear membrane

GPCR localization to the nuclear membrane and endoplasmic reticulum

Similar to GPCRs localized to the Golgi, GPCRs can localize to nuclear membranes and connected ER membranes after synthesis or after internalizing from the PM. Localization to nuclear membranes can be mediated by a classical nuclear localization sequence (NLS) and/or importins. Nuclear targeting via an NLS or importins can occur after GPCR internalization, as observed for the protease-activated receptor 2 and the oxytocin receptor, or directly after synthesis, as observed for for α1-adrenergic receptors and the platelet-activating factor receptor (Wright *et al.*, 2012; Di Benedetto *et al.*, 2014; Joyal *et al.*, 2014; Bhosle *et al.*, 2016). In contrast, other GPCRs such as the metabotropic glutamate receptor 5 (mGluR5) utilize non-NLS sequences to direct nuclear localization and may interact with chromatin to retain these receptors in the nucleus (Sergin *et al.*, 2017). Among ER-targeted GPCRs, like the protease-activated receptor 4, ER localization can be regulated by classical RXR motifs, which are recognized by the COPI protein complex to retain receptors in the biosynthetic pathway (Brock *et al.*, 2005; Cunningham *et al.*, 2012). These same COPI interacting motifs also are found in some Golgi-localized GPCRs, like DOR (St-Louis *et al.*, 2017; Shiwarski *et al.*, 2019). Here we will focus on common themes and signaling of the particularly well-studied mGluR5 from nuclear membranes, but the diverse and varied signaling from these membranes has been well reviewed recently (Jong *et al.*, 2018).

Evidence for GPCR signaling from nuclear membranes

GPCR signaling from nuclear membranes has been demonstrated by both pharmacological approaches using membrane permeable and impermeable ligands, as well as assaying GPCR signaling in isolated nuclei. In a number of different neuronal cell types, activation of Gq-coupled mGluR5 by membrane permeable agonists promotes sustained calcium signaling (Jong *et al.*, 2009; Purgert *et al.*, 2014; Vincent *et al.*, 2016). These responses persist even when surface receptors are blocked by an impermeable antagonist, suggesting surface receptor activation and internalization are not required for sustained calcium signaling (Jong *et al.*, 2009; Purgert *et al.*, 2014; Vincent *et al.*, 2016). Agonist application to isolated nuclei containing mGluR5 or the

endothelin type B receptor (ETBR) produces calcium release from these membranes, suggesting that nuclear membranes contain GPCRs and downstream signaling components, including Gαq, PLC, and inositol trisphosphate receptors (IP3Rs), sufficient to stimulate calcium release (Kumar *et al.*, 2008; Merlen *et al.*, 2013; Vincent *et al.*, 2016).

In addition to traditional ligands, “caged” ligands which consist of an agonist or antagonist chemically modified to be inactive until light-induced photolysis allows local uncaging, have been used to study signaling from nuclear membranes **(Figure 1.2F)**. Uncaging of intracellular caged agonists of mGluR5, angiotensin receptor, or ETBR promotes activation of the respective intracellular and intracellular calcium release (Merlen *et al.*, 2013; Purgert *et al.*, 2014; Tadevosyan *et al.*, 2015; Jong and O’Malley, 2017).

Distinct consequences of GPCR signaling from nuclear membranes by mGluR5

Signaling of intracellular mGluR5 in neurons is a particularly well studied example of how signaling from nuclear membranes diverges from signaling at the PM and influences physiology. In striatal neurons, signaling from PM-localized or intracellular mGluR5 is sufficient to activate CREB transcription factor, whereas intracellular mGluR5 signaling is required and sufficient to activate Elk1 transcription factor and transcription of associated serum-response element target genes, including several genes linked to neuronal plasticity (Jong *et al.*, 2009; Kumar *et al.*, 2012). In hippocampal neurons, intracellular mGluR5 mediates one form of synaptic plasticity, long term depression, whereas PM-localized mGluR5 mediates both long term depression and long term potentiation, suggesting that intracellular mGluR5 signaling may be relevant to complex processes like learning and memory (Purgert *et al.*, 2014). Endogenous glutamate activation of intracellular mGluR5 in spinal cord neurons contributes to pain pathologies linked to neuronal hypersensitivity after nerve injury (Vincent *et al.*, 2016). Inhibiting intracellular mGluR5 signaling with a membrane permeable antagonist or inhibiting the neuronal transporter which allows glutamate to access intracellular receptors produces greater pain relief than membrane impermeable

antagonists (Vincent *et al.*, 2016). Future approaches using ligands specifically targeted to nuclear membranes, similar to the approach described for endosomally-targeted antagonists (Jensen *et al.*, 2017; Yarwood *et al.*, 2017), could further clarify the role of mGluR5 in these complex neural processes and pathologies.

Mechanisms of GPCR spatial signaling bias

Despite evidence supporting "spatial bias" in GPCR signaling through G proteins in different cellular membranes, the mechanisms driving spatially biased signaling are not fully understood. Understanding how GPCR signaling from *different* cellular membranes drives distinct downstream responses while signaling through the *same* G protein effectors will be essential to understanding GPCR biology and designing new spatially-targeted therapeutic approaches. Temporal and spatial organization of signaling emerge as common themes differentiating GPCR signaling through G proteins in intracellular membranes from signaling in the PM. We will propose potential mechanisms of spatial bias with emphasis on how spatial bias may be shaped by the kinetics of signaling, spatial organization of signaling effectors, as well as the lipid composition of membranes.

Temporal component of intracellular signaling

Sustained signaling responses are associated with GPCR signaling from non-canonical locations. However, the factors driving sustained signaling and the consequences of "second waves" of intracellular signaling are unclear (Lohse and Calebiro, 2013; Stoeber *et al.*, 2018). PTHR, TSHR, and mGluR5 signaling from endosomes, Golgi, and nuclear membranes, are all associated with prolonged cAMP or calcium signaling over longer time scales than those observed for PM signaling of these receptors (Calebiro *et al.*, 2009; Ferrandon *et al.*, 2009; Jong *et al.*, 2009; Godbole *et al.*, 2017). The mechanisms which terminate G protein signaling at the PM, such as GPCR phosphorylation by G protein-coupled receptor kinases (GRKs) and β-arrestin binding (Luttrell and Lefkowitz, 2002), have not yet been definitively demonstrated to terminate G protein signaling at other membranes. Indeed, other proteins present on

endosomes and at the TGN can regulate and terminate G protein signaling from these membranes (see section 5.2).

Regarding the consequences of intracellular signaling, it is difficult to fully dissociate the contribution of temporal and spatial components. Signaling for several GPCRs from endosomes, the TGN/Golgi, or nuclear membranes is associated with gene transcription (Jong *et al.*, 2009; Tsvetanova and von Zastrow, 2014; Godbole *et al.*, 2017; Jensen *et al.*, 2017; Yarwood *et al.*, 2017; Gorvin *et al.*, 2018). How intracellular signaling may drive transcriptional responses is not clear, and it is unlikely that intracellular signaling alone produces these responses. A direct consequence of sustained intracellular signaling may be a larger integrated, or total, signaling response. However, in the case of transcriptional responses downstream of B2AR signaling through Gs at endosomes, magnitude of the cAMP signaling response alone does not directly correlate with transcription of endosomally regulated genes (Tsvetanova and von Zastrow, 2014; Tsvetanova *et al.*, 2017). Additionally, production of cAMP at the endosomal membrane is sufficient to produce the same transcriptional responses (Tsvetanova and von Zastrow, 2014). Golgi-localized PKA is also required for TSHR transcriptional responses, making a strong case for a spatial component of these signaling responses which we will now consider (Godbole *et al.*, 2017).

Spatial component of intracellular signaling: Proteins

Spatial organization of GPCR effectors and downstream signaling components is a possible mechanism driving spatially biased signaling. Signaling effectors like G proteins and adenylyl cyclases, a common downstream effector of Gs and Gi-coupled receptors, localize to multiple membrane locations, including endosomes and the Golgi, consistent with GPCR signaling from these locations (Calebiro *et al.*, 2009; Ferrandon *et al.*, 2009; Kotowski *et al.*, 2011; Cancino *et al.*, 2014). These GPCR effectors, including G protein subunits and adenylyl cyclases, also dynamically traffic to different membranes and cellular compartments in response to GPCR signaling (Wedegaertner *et al.*, 1996; Hynes *et al.*, 2004; Allen *et al.*, 2005; Saini *et al.*, 2007; Lazar *et al.*, 2020). In a recent example of this phenomenon, GPCR signaling promotes isoform-specific

internalization of adenylyl cyclase 9 (AC9) to endosomes (Lazar *et al.*, 2020). AC9 is also required for endosomal cAMP production by B2AR (Lazar *et al.*, 2020), highlighting the potential link between effector localization and endosomal signaling. As illustrated for B1AR and TSHR, AKAPs are essential for mediating spatially biased signaling of these GPCRs in the Golgi (Godbole *et al.*, 2017; Nash *et al.*, 2019). AKAPs scaffold a variety of signaling effectors including adenylyl cyclases, phosphodiesterases, kinases, and phospholipases at multiple cellular membranes and facilitate efficient interactions between effectors to promote localized signaling responses (Welch *et al.*, 2010; Zhang *et al.*, 2011; Kapiloff *et al.*, 2014).

Interestingly, spatial organization of effectors into microdomains, even within the same intracellular membrane compartment, can influence GPCR signaling. B2AR in the active conformation, visualized by an active conformation nanobody (Nb80), localizes throughout the endosomal membrane (Irannejad *et al.*, 2013; Bowman *et al.*, 2016). However, the nucleotide-free Gαs nanobody (Nb37) is restricted to recycling tubules on the endosome (Bowman *et al.*, 2016). These data suggest that although B2AR is active throughout the endosome, G protein coupling and activation is restricted to a specific endosomal domain. B2AR localization to these endosomal microdomains is required for endosomal transcriptional responses (Bowman *et al.*, 2016). The mechanisms restricting receptor localization or G protein activation to these specific domains are not yet known and is an exciting area for future study.

Microdomains are best studied at the PM where lipid rafts, caveolae, clathrin-coated pits, and primary cilia can compartmentalize and organize GPCR signaling (Patel *et al.*, 2008; Hilgendorf *et al.*, 2016; Mykytyn and Askwith, 2017; Weinberg and Puthenveedu, 2019). These domains often have distinct protein and lipid compositions, including cholesterol and phospholipids, and can localize GPCRs and specific effectors to produce distinct signaling outputs or maintain specific local signaling environments (Russo *et al.*, 2009; Marley *et al.*, 2013; Mukhopadhyay *et al.*, 2013; Garcia-Gonzalo *et al.*, 2015; Singh *et al.*, 2015; Bachmann *et al.*, 2016; Moore *et al.*, 2016; Weinberg *et al.*, 2017). As we increase our understanding of how microdomains organize GPCR

signaling in the PM, we will likely be able to identify analogous mechanisms that regulate GPCR signaling from microdomains in intracellular compartments.

In addition to classical signaling molecules, membrane trafficking proteins can play dual roles in regulating both GPCR trafficking and signaling. The retromer complex, which has been linked to TSHR, PTHR, and B2AR trafficking (Feinstein *et al.*, 2011; Temkin *et al.*, 2011; Godbole *et al.*, 2017), plays divergent roles in regulating GPCR signaling. PTHR endosomal signaling is terminated by retromer, whereas TSHR signals from compartments containing retromer components at the TGN (Feinstein *et al.*, 2011; Godbole *et al.*, 2017). B2AR actively sorts to retromer-containing recycling tubules in the endosome, which are the site of G protein activation and initiation of endosomal transcriptional responses (Temkin *et al.*, 2011; Bowman *et al.*, 2016). APPL1, a protein associated with very early endosomes and GPCR recycling, also negatively regulates cAMP production by LHR, B1AR, and the follicle-stimulating hormone receptor (FSHR) (Sposini *et al.*, 2017).

Spatial component of intracellular signaling: Membrane lipids

At a more fundamental level, the lipid composition of different cellular membranes may drive spatial differences in GPCR signaling. Lipids and expression of lipid modifying enzymes vary across cell types (Chattopadhyay and Paila, 2007; Balla, 2013). Cellular membranes within the same cell are heterogeneous and differ not only in protein composition, but in lipid composition, including cholesterol and phospholipids, both of which can influence GPCR signaling (Ikonen, 2008; Van Meer *et al.*, 2008; Balla, 2013). Cholesterol is most enriched at the PM but can also be found in endosomal compartments and the TGN (Mukherjee *et al.*, 1998; Ikonen, 2008; Van Meer *et al.*, 2008). Cholesterol interacts with GPCRs and modulates GPCR activity in a variety of ways including but not limited to receptor dimerization, ligand binding, G protein coupling, and signaling (Xiang *et al.*, 2002; Pucadyil and Chattopadhyay, 2004; Cherezov *et al.*, 2007; Hanson *et al.*, 2008; Levitt *et al.*, 2009; Oates *et al.*, 2012; Prasanna *et al.*, 2014).

Phospholipids which vary in cellular membrane distribution also directly and indirectly modulate GPCR and effector activity. Negatively charged phospholipid phosphatidylglycerol (PG) acts as an allosteric modulator at B2AR and promotes agonist binding (Dawaliby *et al.*, 2016). PG and phosphatidylserine (PS) decrease B2AR coupling to Gi over Gs. This selectivity was attributed to a negatively charged amino acid motif present on the Gαi protein. This motif may be repelled from a negatively charged membrane, and interestingly can be regulated by acute changes in local membrane charge such as through the influx of calcium ions (Strohman *et al.*, 2019). PG similarly promotes interaction of the neurotensin receptor 1 (NTSR1) with Gαq and Gβ1γ1 and increases GDP exchange by the G protein (Inagaki *et al.*, 2012). Phosphatidylinositol-4,5-bisphosphate ($PI(4,5)P_2$), which is enriched in the PM, can also stabilize G protein interactions with GPCRs and promote GPCR-stimulated GTP hydrolysis (Yen *et al.*, 2018). Beyond their direct effects on GPCR-G protein activity and coupling, membrane lipids also bind to GPCR interacting partners and effectors, including arrestins, GRKs, adenylyl cyclases, and AKAPs, (Gaidarov *et al.*, 1999; Ostrom *et al.*, 2002; Vögler *et al.*, 2008; Homan *et al.*, 2013; Kapiloff *et al.*, 2014). Taken together, these data suggest that spatial signaling bias may be influenced by the effect of local membrane lipids on GPCR activity.

Conclusion and future perspectives

Our understanding of GPCR biology and pharmacology has been transformed by the discovery that GPCRs can signal from multiple cellular locations. GPCRs can activate the same G protein effectors on intracellular membranes, including endosomes, the Golgi, and nuclear membranes, as are activated at the PM, yet produce distinct signaling effects **(Figure 1.1)**. In addition to these compartments in the membrane trafficking pathway, GPCR signaling has also been reported on unexpected cellular compartments including the mitochondria and melanosomes (reviewed in Jong et al., 2018). These discoveries, enabled by the development of new tools allowing for activation of GPCRs and measurement of conformational changes and signaling with high spatial and temporal resolution, have changed our view of GPCRs from being

simple on-off switches at the PM, to being master regulators of multiple spatially and temporally distinct phases of signaling **(Figure 1.2)**.

These new ideas and advances point to an exciting time ahead for studying the cell biology of GPCRs. From a fundamental perspective, the idea that the intracellular location of GPCRs is a key determinant of signaling provides a revised appreciation for the role of membranes and trafficking in regulating GPCR function. Classically thought of as a mechanism to add or remove GPCRs from the cell surface, trafficking might also be a critical mechanism to transport GPCRs between distinct spatially separated signaling complexes. Further, selectively modulating signaling from specific compartments is an exciting and emerging prospect for developing therapeutics with greater efficacy and fewer adverse effects. Future quantitative analysis of GPCR localization and signaling in cell types of interest, and of how signaling events in different membranes contribute to a net signaling response will allow us to leverage GPCR location to fine-tune targeting of GPCRs for better therapeutics.

Acknowledgements

SEC and MAP would like to thank Ian Chronis, Josh Lott, Loyda Morales Rodriguez, Dr. Kasun Ratnayake, Dr. Prahatha Venkatraman, and Dr. Zara Weinberg for invaluable feedback and discussion on this manuscript. MAP was supported by National Institutes of Health GM117425 and National Science Foundation 1517776.

References

Alekhina, O, and Marchese, A (2016). β-arrestin1 and Signal-transducing Adaptor Molecule 1 (STAM1) cooperate to promote focal adhesion kinase autophosphorylation and chemotaxis via the chemokine receptor CXCR4. J Biol Chem 291, 26083–26097.

Allen, JA, Yu, JZ, Donati, RJ, and Rasenick, MM (2005). Beta-adrenergic receptor stimulation promotes G(alpha)s internalization through lipid rafts: A study in living cells. Mol Pharmacol 67, 1493–1504.

Bachmann, VA et al. (2016). Gpr161 anchoring of PKA consolidates GPCR and cAMP signaling. Proc Natl Acad Sci U S A 113, 7786–7791.

Balla, T (2013). Phosphoinositides: Tiny lipids with giant impact on cell regulation. Physiol Rev 93, 1019–1137.

Di Benedetto, A et al. (2014). Osteoblast regulation via ligand-activated nuclear trafficking of the oxytocin receptor. Proc Natl Acad Sci U S A 111, 16502–16507.

Bhosle, V et al. (2016). Nuclear localization of platelet-activating factor receptor controls retinal neovascularization. Cell Discov 2, 1–18.

Bowman, SL, and Puthenveedu, MA (2015). Postendocytic Sorting of Adrenergic and Opioid Receptors: New Mechanisms and Functions. Prog Mol Biol Transl Sci 132, 189–206.

Bowman, SL, Shiwarski, DJ, and Puthenveedu, MA (2016). Distinct G protein-coupled receptor recycling pathways allow spatial control of downstream G protein signaling. J Cell Biol 214, 797–806.

Brock, C, Boudier, L, Maurel, D, Blahos, J, and Pin, J-P (2005). Assembly-dependent surface targeting of the heterodimeric GABAB Receptor is controlled by COPI but not 14-3-3. Mol Biol Cell 16, 5572–5578.

Calebiro, D, Nikolaev, VO, Gagliani, MC, de Filippis, T, Dees, C, Tacchetti, C, Persani, L, and Lohse, MJ (2009). Persistent cAMP-signals triggered by internalized G-protein-coupled receptors. PLoS Biol 7, e1000172.

Cancino, J et al. (2014). Control systems of membrane transport at the interface between the endoplasmic reticulum and the Golgi. Dev Cell 30, 280–294.

Chattopadhyay, A, and Paila, YD (2007). Lipid-protein interactions, regulation and dysfunction of brain cholesterol. Biochem Biophys Res Commun 354, 627–633.

Che, T et al. (2020). Nanobody-enabled monitoring of kappa opioid receptor states. Nat Commun 11.

Chen, KE, Healy, MD, and Collins, BM (2019). Towards a molecular understanding of endosomal trafficking by Retromer and Retriever. Traffic 20, 465–478.

Cherezov, V et al. (2007). High-resolution crystal structure of an engineered human β2-adrenergic G protein-coupled receptor. Science (80-) 318, 1258–1265.

Cunningham, MR, McIntosh, KA, Pediani, JD, Robben, J, Cooke, AE, Nilsson, M, Gould, GW, Mundell, S, Milligan, G, and Plevin, R (2012). Novel role for proteinase-activated receptor 2 (PAR2) in membrane trafficking of proteinase-activated receptor 4 (PAR4). J Biol Chem 287, 16656–16669.

Dawaliby, R, Trubbia, C, Delporte, C, Masureel, M, Van Antwerpen, P, Kobilka, BK, and Govaerts, C (2016). Allosteric regulation of G protein-coupled receptor activity by phospholipids. Nat Chem Biol 12, 35–39.

DeFea, KA, Vaughn, ZD, O'Bryan, EM, Nishijima, D, Déry, O, and Bunnett, NW (2000a). The proliferative and antiapoptotic effects of substance P are facilitated by formation of a β-arrestin-dependent scaffolding complex. Proc Natl Acad Sci U S A 97, 11086–11091.

DeFea, KA, Zalevsky, J, Thoma, MS, Dery, O, Mullins, RD, and Bunnett, NW (2000b). β-Arrestin-dependent endocytosis of proteinase-activated receptor 2 is required for intracellular targeting of activated ERK1/2. J Cell Biol 148, 1267–1281.

Depry, C, Allen, MD, and Zhang, J (2011). Visualization of PKA activity in plasma membrane microdomains. Mol Biosyst 7, 52–58.

Déry, O, Thoma, MS, Wong, H, Grady, EF, and Bunnett, NW (1999). Trafficking of proteinase-activated receptor-2 and β-arrestin-1 tagged with green fluorescent protein. β-Arrestin-dependent endocytosis of a proteinase receptor. J Biol Chem 274, 18524–18535.

Dipilato, LM, and Zhang, J (2009). The role of membrane microdomains in shaping β 2-adrenergic receptor-mediated cAMP dynamics. Mol Biosyst 5, 832–837.

Dong, C, Filipeanu, CM, Duvernay, MT, and Wu, G (2007). Regulation of G protein-coupled receptor export trafficking. Biochim Biophys Acta 1768, 853–870.

Feinstein, TN, Wehbi, VL, Ardura, JA, Wheeler, DS, Ferrandon, S, Gardella, TJ, and Vilardaga, JP (2011). Retromer terminates the generation of cAMP by internalized PTH receptors. Nat Chem Biol 7, 278–284.

Feinstein, TN, Yui, N, Webber, MJ, Wehbi, VL, Stevenson, HP, King, JD, Hallows, KR, Brown, D, Bouley, R, and Vilardaga, JP (2013). Noncanonical control of vasopressin receptor type 2 signaling by retromer and arrestin. J Biol Chem 288, 27849–27860.

Ferrandon, S, Feinstein, TN, Castro, M, Wang, B, Bouley, R, Potts, JT, Gardella, TJ, and Vilardaga, J-P (2009). Sustained cyclic AMP production by parathyroid hormone receptor endocytosis. Nat Chem Biol 5, 734–742.

Gaidarov, I, Krupnick, JG, Falck, JR, Benovic, JL, and Keen, JH (1999). Arrestin function in G protein-coupled receptor endocytosis requires phosphoinositide binding.

Garcia-Gonzalo, FR, Phua, SC, Roberson, EC, Garcia, G, Abedin, M, Schurmans, S, Inoue, T, and Reiter, JF (2015). Phosphoinositides Regulate Ciliary Protein Trafficking to Modulate Hedgehog Signaling. Dev Cell 34, 400–409.

Godbole, A, Lyga, S, Lohse, MJ, and Calebiro, D (2017). Internalized TSH receptors en route to the TGN induce local Gs-protein signaling and gene transcription. Nat Commun 8, 443.

Gorvin, CM et al. (2018). AP2σ Mutations Impair Calcium-Sensing Receptor Trafficking and Signaling, and Show an Endosomal Pathway to Spatially Direct G-Protein Selectivity. Cell Rep 22, 1054–1066.

Grimsey, NJ, Aguilar, B, Smith, TH, Le, P, Soohoo, AL, Puthenveedu, MA, Nizet, V, and Trejo, JA (2015). Ubiquitin plays an atypical role in GPCR-induced p38 MAP kinase activation on endosomes. J Cell Biol 210, 1117–1131.

Hanson, MA, Cherezov, V, Griffith, MT, Roth, CB, Jaakola, VP, Chien, EYT, Velasquez, J, Kuhn, P, and Stevens, RC (2008). A Specific Cholesterol Binding Site Is Established by the 2.8 Å Structure of the Human β2-Adrenergic Receptor. Structure 16, 897–905.

Hanyaloglu, AC, and von Zastrow, M (2008). Regulation of GPCRs by Endocytic Membrane Trafficking and Its Potential Implications. Annu Rev Pharmacol Toxicol 48, 537–568.

Hertel, C, and Perkins, JP (1984). Receptor-specific mechanisms of desensitization of β-adrenergic receptor function. Mol Cell Endocrinol 37, 245–256.

Hilgendorf, KI, Johnson, CT, and Jackson, PK (2016). The primary cilium as a cellular receiver: Organizing ciliary GPCR signaling. Curr Opin Cell Biol 39, 84–92.

Homan, KT, Glukhova, A, and Tesmer, JJG (2013). Regulation of G Protein-Coupled Receptor Kinases by Phospholipids. Curr Med Chem 20, 39–46.

Hynes, TR, Mervine, SM, Yost, EA, Sabo, JL, and Berlot, CH (2004). Live cell imaging of Gs and the β2-adrenergic receptor demonstrates that both αs and β 1γ7 internalize upon stimulation and exhibit similar trafficking patterns that differ from that of the β2-adrenergic receptor. J Biol Chem 279, 44101–44112.

Ikonen, E (2008). Cellular cholesterol trafficking and compartmentalization. Nat Rev Mol

Cell Biol 9, 125–138.

Inagaki, S, Ghirlando, R, White, JF, Gvozdenovic-Jeremic, J, Northup, JK, and Grisshammer, R (2012). Modulation of the interaction between neurotensin receptor NTS1 and Gq protein by lipid. J Mol Biol 417, 95–111.

Irannejad, R et al. (2013). Conformational biosensors reveal GPCR signalling from endosomes. Nature 495, 534–538.

Irannejad, R, Pessino, V, Mika, D, Huang, B, Wedegaertner, PB, Conti, M, and von Zastrow, M (2017). Functional selectivity of GPCR-directed drug action through location bias. Nat Chem Biol 13, 799–806.

Jean-Alphonse, F, Bowersox, S, Chen, S, Beard, G, Puthenveedu, MA, and Hanyaloglu, AC (2014). Spatially restricted G protein-coupled receptor activity via divergent endocytic compartments. J Biol Chem 289, 3960–3977.

Jensen, DD et al. (2017). Neurokinin 1 receptor signaling in endosomes mediates sustained nociception and is a viable therapeutic target for prolonged pain relief. Sci Transl Med 9.

Jimenez-Vargas, NN et al. (2020). Endosomal signaling of delta opioid receptors is an endogenous mechanism and therapeutic target for relief from inflammatory pain. Proc Natl Acad Sci, 202000500.

Jong, Y-JI, and O'Malley, KL (2017). Mechanisms Associated with Activation of Intracellular Metabotropic Glutamate Receptor, mGluR5. Neurochem Res 42, 166–172.

Jong, YJI, Harmon, SK, and O'Malley, KL (2018). GPCR signalling from within the cell. Br J Pharmacol 175, 4026–4035.

Jong, YJI, Kumar, V, and O'Malley, KL (2009). Intracellular metabotropic glutamate receptor 5 (mGluR5) activates signaling cascades distinct from cell surface counterparts. J Biol Chem 284, 35827–35838.

Joyal, JS et al. (2014). Subcellular localization of coagulation factor II receptor-like 1 in neurons governs angiogenesis. Nat Med 20, 1165–1173.

Kapiloff, MS, Rigatti, M, and Dodge-Kafka, KL (2014). Architectural and functional roles of a kinase-anchoring proteins in camp microdomains. J Gen Physiol 143, 9–15.

Koliwer, J, Park, M, Bauch, C, Von Zastrow, M, and Kreienkamp, HJ (2015). The golgi-associated PDZ domain protein PIST/GOPC stabilizes the β1-Adrenergic receptor in intracellular compartments after internalization. J Biol Chem 290, 6120–6129.

Kotowski, SJ, Hopf, FW, Seif, T, Bonci, A, and von Zastrow, M (2011). Endocytosis

Promotes Rapid Dopaminergic Signaling. Neuron 71, 278–290.

Kumar, V, Fahey, PG, Jong, YJI, Ramanan, N, and O'Malley, KL (2012). Activation of intracellular metabotropic glutamate receptor 5 in striatal neurons leads to up-regulation of genes associated with sustained synaptic transmission including Arc/Arg3.1 protein. J Biol Chem 287, 5412–5425.

Kumar, V, Jong, YJI, and O'Malley, KL (2008). Activated nuclear metabotropic glutamate receptor mGlu5 couples to nuclear Gq/11 proteins to generate inositol 1,4,5-trisphosphate-mediated nuclear Ca2+ release. J Biol Chem 283, 14072–14083.

Kuna, RS, Girada, SB, Asalla, S, Vallentyne, J, Maddika, S, Patterson, JT, Smiley, DL, DiMarchi, RD, and Mitra, P (2013). Glucagon-like peptide-1 receptor-mediated endosomal cAMP generation promotes glucose-stimulated insulin secretion in pancreatic β-cells. Am J Physiol - Endocrinol Metab 305.

Kunselman, JM, Gupta, A, gomes, I, Devi, LA, and Puthenveedu, MA (2020). Compartment-specific opioid receptor signaling is selectively modulated by Dynorphin subtypes. BioRxiv Cell Biol, 2020.06.21.162206.

Laporte, SA, Oakley, RH, Zhang, J, Holt, JA, Ferguson, SSG, Caron, MG, and Barak, LS (1999). The β2-adrenergic receptor/βarrestin complex recruits the clathrin adaptor AP-2 during endocytosis. Proc Natl Acad Sci U S A 96, 3712–3717.

Lazar, AM, Irannejad, R, Baldwin, TA, Sundaram, AB, Gutkind, JS, Inoue, A, Dessauer, CW, and Von Zastrow, M (2020). G protein-regulated endocytic trafficking of adenylyl cyclase type 9. Elife 9.

Lefkowitz, RJ, Wessels, MR, and Stadel, JM (1980). Hormones, Receptors, and Cyclic AMP: Their Role in Target Cell Refractoriness. Curr Top Cell Regul 17, 205–230.

Levitt, ES, Clark, MJ, Jenkins, PM, Martens, JR, and Traynor, JR (2009). Differential effect of membrane cholesterol removal on μ- and δ-opioid receptors. A parallel comparison of acute and chronic signaling to adenylyl cyclase. J Biol Chem 284, 22108–22122.

Lohse, MJ, Benovic, JL, Codina, J, Caron, MG, and Lefkowitz, RJ (1990). β-arrestin: A protein that regulates β-adrenergic receptor function. Science (80-) 248, 1547–1550.

Lohse, MJ, and Calebiro, D (2013). Cell biology: Receptor signals come in waves. Nature 495, 457–458.

Luttrell, LM et al. (1999). β-arrestin-dependent formation of β2 adrenergic receptor-src protein kinase complexes. Science (80-) 283, 655–661.

Luttrell, LM, and Lefkowitz, RJ (2002). The role of β-arrestins in the termination and

transduction of G-protein-coupled receptor signals. J Cell Sci 115, 455–465.

Luttrell, LM, Roudabush, FL, Choy, EW, Miller, WE, Field, ME, Pierce, KL, and Lefkowitz, RJ (2001). Activation and targeting of extracellular signal-regulated kinases by β-arrestin scaffolds. Proc Natl Acad Sci U S A 98, 2449–2454.

Lyga, S, Volpe, S, Werthmann, RC, Götz, K, Sungkaworn, T, Lohse, MJ, and Calebiro, D (2016). Persistent cAMP Signaling by Internalized LH Receptors in Ovarian Follicles. Endocrinology 157, 1613–1621.

Manglik, A, Kobilka, BK, and Steyaert, J (2017). Nanobodies to Study G Protein-Coupled Receptor Structure and Function. Annu Rev Pharmacol Toxicol 57, 19–37.

Marley, A, Choy, RWY, and von Zastrow, M (2013). GPR88 Reveals a Discrete Function of Primary Cilia as Selective Insulators of GPCR Cross-Talk. PLoS One 8, 70857.

McDonald, PH, Chow, C-W, Miller, WE, Laporte, SA, Field, ME, Lin, F-T, Davis, RJ, and Lefkowitz, RJ (2000). beta -Arrestin 2: A Receptor-Regulated MAPK Scaffold for the Activation of JNK3. Science (80-) 290, 1574–1577.

Van Meer, G, Voelker, DR, and Feigenson, GW (2008). Membrane lipids: Where they are and how they behave. Nat Rev Mol Cell Biol 9, 112–124.

Merlen, C et al. (2013). Intracrine endothelin signalling evokes IP3-dependent increases in nucleoplasmic Ca 2+ in adult cardiac myocytes *. J Mol Cell Cardiol 62, 189–202.

Mittal, N et al. (2013). Select G-protein-coupled receptors modulate agonist-induced signaling via a ROCK, LIMK, and β-arrestin 1 pathway. Cell Rep 5, 1010–1021.

Moore, BS, Stepanchick, AN, Tewson, PH, Hartle, CM, Zhang, J, Quinn, AM, Hughes, TE, and Mirshahi, T (2016). Cilia have high cAMP levels that are inhibited by Sonic Hedgehog-regulated calcium dynamics. Proc Natl Acad Sci U S A 113, 13069–13074.

Mukherjee, S, Zha, X, Tabas, I, and Maxfield, FR (1998). Cholesterol distribution in living cells: Fluorescence imaging using dehydroergosterol as a fluorescent cholesterol analog. Biophys J 75, 1915–1925.

Mukhopadhyay, S, Wen, X, Ratti, N, Loktev, A, Rangell, L, Scales, SJ, and Jackson, PK (2013). The ciliary G-protein-coupled receptor Gpr161 negatively regulates the sonic hedgehog pathway via cAMP signaling. Cell 152, 210–223.

Mullershausen, F, Zecri, F, Cetin, C, Billich, A, Guerini, D, and Seuwen, K (2009). Persistent signaling induced by FTY720-phosphate is mediated by internalized S1P1 receptors. Nat Chem Biol 5, 428–434.

Mykytyn, K, and Askwith, C (2017). G-Protein-Coupled receptor signaling in cilia. Cold Spring Harb Perspect Biol 9.

Nash, CA, Wei, W, Irannejad, R, and Smrcka, A V. (2019). Golgi localized βi-adrenergic receptors stimulate golgi PI4P hydrolysis by PLCε to regulate cardiac hypertrophy. Elife 8.

Nehmé, R, Carpenter, B, Singhal, A, Strege, A, Edwards, PC, White, CF, Du, H, Grisshammer, R, and Tate, CG (2017). Mini-G proteins: Novel tools for studying GPCRs in their active conformation. PLoS One 12.

Oakley, RH, Laporte, SA, Holt, JA, Caron, MG, and Barak, LS (2000). Differential affinities of visual arrestin, βarrestin1, and βarrestin2 for G protein-coupled receptors delineate two major classes of receptors. J Biol Chem 275, 17201–17210.

Oates, J, Faust, B, Attrill, H, Harding, P, Orwick, M, and Watts, A (2012). The role of cholesterol on the activity and stability of neurotensin receptor 1. Biochim Biophys Acta - Biomembr 1818, 2228–2233.

Ostrom, RS, Liu, X, Head, BP, Gregorian, C, Seasholtz, TM, and Insel, PA (2002). Localization of adenylyl cyclase isoforms and G protein-coupled receptors in vascular smooth muscle cells: Expression in caveolin-rich and noncaveolin domains. Mol Pharmacol 62, 983–992.

Patel, HH, Murray, F, and Insel, PA (2008). G-Protein-Coupled Receptor-Signaling Components in Membrane Raft and Caveolae Microdomains. In: Handbook of Experimental Pharmacology, Handb Exp Pharmacol, 167–184.

Peterson, YK, and Luttrell, LM (2017). The Diverse Roles of Arrestin Scaffolds in G Protein-Coupled Receptor Signaling. Pharmacol Rev 69, 256–297.

Prasanna, X, Chattopadhyay, A, and Sengupta, D (2014). Cholesterol modulates the dimer interface of the β2- adrenergic receptor via cholesterol occupancy sites. Biophys J 106, 1290–1300.

Pucadyil, TJ, and Chattopadhyay, A (2004). Cholesterol modulates ligand binding and G-protein coupling to serotonin1A receptors from bovine hippocampus. Biochim Biophys Acta - Biomembr 1663, 188–200.

Purgert, CA, Izumi, Y, Jong, YJI, Kumar, V, Zorumski, CF, and O'Malley, KL (2014). Intracellular mGluR5 can mediate synaptic plasticity in the hippocampus. J Neurosci 34, 4589–4598.

Puthenveedu, MA, Lauffer, B, Temkin, P, Vistein, R, Carlton, P, Thorn, K, Taunton, J, Weiner, OD, Parton, RG, and Zastrow, M Von (2010). Sequence-Dependent Sorting of Recycling Proteins by Actin-Stabilized Endosomal Microdomains. Cell 143, 761–773.

Ranjan, R, Dwivedi, H, Baidya, M, Kumar, M, and Shukla, AK (2017). Novel Structural Insights into GPCR–β-Arrestin Interaction and Signaling. Trends Cell Biol 27, 851–862.

Rozenfeld, R, and Devi, LA (2008). Regulation of CB $_1$ cannabinoid receptor trafficking by the adaptor protein AP-3. FASEB J 22, 2311–2322.

Russo, A, Soh, UJK, Paing, MM, Arora, P, and Trejo, JA (2009). Caveolae are required for protease-selective signaling by protease-activated receptor-1. Proc Natl Acad Sci U S A 106, 6393–6397.

Saini, DK, Kalyanaraman, V, Chisari, M, and Gautam, N (2007). A family of G protein βγ subunits translocate reversibly from the plasma membrane to endomembranes on receptor activation. J Biol Chem 282, 24099–24108.

Sergin, I, Jong, YJI, Harmon, SK, Kumar, V, and O'Malley, KL (2017). Sequences within the C terminus of the metabotropic glutamate receptor 5 (mGluR5) are responsible for inner nuclear membrane localization. J Biol Chem 292, 3637–3655.

Shiwarski, DJ, Crilly, SE, Dates, A, and Puthenveedu, MA (2019). Dual RXR motifs regulate nerve growth factor–mediated intracellular retention of the delta opioid receptor. Mol Biol Cell 30, 680–690.

Shiwarski, DJ, Darr, M, Telmer, CA, Bruchez, MP, and Puthenveedu, MA (2017a). PI3K class II α regulates δ-opioid receptor export from the trans-Golgi network. Mol Biol Cell 28, 2202–2219.

Shiwarski, DJ, Tipton, A, Giraldo, MD, Schmidt, BF, Gold, MS, Pradhan, AA, and Puthenveedu, MA (2017b). A PTEN-regulated checkpoint controls surface delivery of σ opioid receptors. J Neurosci 37, 3741–3752.

Singh, J, Wen, X, and Scales, SJ (2015). The orphan G protein-coupled receptor Gpr175 (Tpra40) enhances Hedgehog signaling by modulating cAMP levels. J Biol Chem 290, 29663–29675.

Slessareva, JE, Routt, SM, Temple, B, Bankaitis, VA, and Dohlman, HG (2006). Activation of the Phosphatidylinositol 3-Kinase Vps34 by a G Protein α Subunit at the Endosome. Cell 126, 191–203.

Sposini, S, Jean-Alphonse, FG, Ayoub, MA, Oqua, A, West, C, Lavery, S, Brosens, JJ, Reiter, E, and Hanyaloglu, AC (2017). Integration of GPCR Signaling and Sorting from Very Early Endosomes via Opposing APPL1 Mechanisms. Cell Rep 21, 2855–2867.

St-Louis, É, Degrandmaison, J, Grastilleur, S, Génier, S, Blais, V, Lavoie, C, Parent, J-L, and Gendron, L (2017). Involvement of the coatomer protein complex I in the intracellular traffic of the delta opioid receptor. Mol Cell Neurosci 79, 53–63.

Stoeber, M, Jullié, D, Lobingier, BT, Laeremans, T, Steyaert, J, Schiller, PW, Manglik, A, and von Zastrow, M (2018). A Genetically Encoded Biosensor Reveals Location Bias of Opioid Drug Action. Neuron 98, 963-976.e5.

Strohman, MJ, Maeda, S, Hilger, D, Masureel, M, Du, Y, and Kobilka, BK (2019). Local membrane charge regulates β2 adrenergic receptor coupling to Gi3. Nat Commun 10, 1–10.

Tadevosyan, A et al. (2015). Photoreleasable ligands to study intracrine angiotensin II signalling. J Physiol 593, 521–539.

Temkin, P, Lauffer, B, Jäger, S, Cimermancic, P, Krogan, NJ, and Von Zastrow, M (2011). SNX27 mediates retromer tubule entry and endosome-to-plasma membrane trafficking of signalling receptors. Nat Cell Biol 13, 715–723.

Thomsen, ARB et al. (2016). GPCR-G Protein-β-Arrestin Super-Complex Mediates Sustained G Protein Signaling. Cell 166, 907–919.

Tsvetanova, NG, Trester-Zedlitz, M, Newton, BW, Riordan, DP, Sundaram, AB, Johnson, JR, Krogan, NJ, and Von Zastrow, M (2017). G protein-coupled receptor endocytosis confers uniformity in responses to chemically distinct ligands. Mol Pharmacol 91, 145–156.

Tsvetanova, NG, and von Zastrow, M (2014). Spatial encoding of cyclic AMP signaling specificity by GPCR endocytosis. Nat Chem Biol 10, 1061–1065.

Varsano, T, Taupin, V, Guo, L, Baterina, OY, and Farquhar, MG (2012). The PDZ Protein GIPC Regulates Trafficking of the LPA1 Receptor from APPL Signaling Endosomes and Attenuates the Cell's Response to LPA. PLoS One 7.

Vincent, K et al. (2016). Intracellular mGluR5 plays a critical role in neuropathic pain. Nat Commun 7, 10604.

Vögler, O, Barceló, JM, Ribas, C, and Escribá, P V. (2008). Membrane interactions of G proteins and other related proteins. Biochim Biophys Acta - Biomembr 1778, 1640–1652.

Wan, Q, Okashah, N, Inoue, A, Nehmé, R, Carpenter, B, Tate, CG, and Lambert, NA (2018). Mini G protein probes for active G protein-coupled receptors (GPCRs) in live cells. J Biol Chem, jbc.RA118.001975.

Wedegaertner, PB, Bourne, HR, and Von Zastrow, M (1996). Activation-induced subcellular redistribution of G(sα). Mol Biol Cell 7, 1225–1233.

Wehbi, VL, Stevenson, HP, Feinstein, TN, Calero, G, Romero, G, and Vilardaga, JP (2013). Noncanonical GPCR signaling arising from a PTH receptor-arrestin- Gβγ

complex. Proc Natl Acad Sci U S A 110, 1530–1535.

Wei, H, Ahn, S, Shenoy, SK, Karnik, SS, Hunyady, L, Luttrell, LM, and Lefkowitz, RJ (2003). Independent β-arrestin 2 and G protein-mediated pathways for angiotensin II activation of extracellular signal-regulated kinases 1 and 2. Proc Natl Acad Sci U S A 100, 10782–10787.

Weinberg, ZY, and Puthenveedu, MA (2019). Regulation of G protein-coupled receptor signaling by plasma membrane organization and endocytosis. Traffic 20, 121–129.

Weinberg, ZY, Zajac, AS, Phan, T, Shiwarski, DJ, and Puthenveedu, MA (2017). Sequence-Specific Regulation of Endocytic Lifetimes Modulates Arrestin-Mediated Signaling at the μ Opioid Receptor. Mol Pharmacol 91, 416–427.

Weis, WI, and Kobilka, BK (2018). The Molecular Basis of G Protein–Coupled Receptor Activation. Annu Rev Biochem 87, 897–919.

Welch, EJ, Jones, BW, and Scott, JD (2010). Network with the AKAPs context-dependent regulation of anchored Enzymes. Mol Interv 10, 86–97.

Westfield, GH et al. (2011). Structural flexibility of the G alpha s alpha-helical domain in the beta2-adrenoceptor Gs complex. Proc Natl Acad Sci U S A 108, 16086–16091.

Wright, CD, Wu, SC, Dahl, EF, Sazama, AJ, and O'Connell, TD (2012). Nuclear localization drives α1-adrenergic receptor oligomerization and signaling in cardiac myocytes. Cell Signal 24, 794–802.

Wu, V, Yeerna, H, Nohata, N, Chiou, J, Harismendy, O, Raimondi, F, Inoue, A, Russell, RB, Tamayo, P, and Gutkind, JS (2019). Illuminating the Onco-GPCRome: Novel G protein-coupled receptor-driven oncocrine networks and targets for cancer immunotherapy. J Biol Chem 294, 11062–11086.

Xiang, Y, Rybin, VO, Steinberg, SF, and Kobilka, B (2002). Caveolar localization dictates physiologic signaling of β2-adrenoceptors in neonatal cardiac myocytes. J Biol Chem 277, 34280–34286.

Yarwood, RE et al. (2017). Endosomal signaling of the receptor for calcitonin gene-related peptide mediates pain transmission. Proc Natl Acad Sci U S A 114, 12309–12314.

Yen, HY et al. (2018). PtdIns(4,5)P2 stabilizes active states of GPCRs and enhances selectivity of G-protein coupling. Nature 559, 423–427.

Zhang, L, Malik, S, Kelley, GG, Kapiloff, MS, and Smrcka, A V. (2011). Phospholipase Cε scaffolds to muscle-specific A kinase anchoring protein (mAKAPβ) and integrates multiple hypertrophic stimuli in cardiac myocytes. J Biol Chem 286, 23012–23021.

Chapter 2: Dual RXR Motifs Mediate Nerve Growth Factor and Phosphoinositide 3-Kinase-Regulated Intracellular Retention of the Delta Opioid Receptor

This chapter was published in part as and adapted from[2]:

Shiwarski, DJ*, Crilly, SE*, Dates, A, and Puthenveedu, MA (2019). Dual RXR motifs regulate nerve growth factor–mediated intracellular retention of the delta opioid receptor. Mol Biol Cell 30, 680–690.

*co-first authors

Abstract

G protein-coupled receptor (GPCR) localization to the plasma membrane (PM) influences both the ability of a cell to respond to extracellular ligands and the GPCR signaling profile in response to these ligands. Despite the importance of GPCR PM localization in shaping cell signaling, the mechanisms which regulate delivery of newly synthesized GPCRs to the PM are not fully understood. Here we used the delta opioid receptor (DOR) as a physiologically relevant prototype GPCR to investigate these mechanisms. In neuronal cells, DOR is retained in intracellular compartments, including the *trans*-Golgi network, by a nerve growth factor (NGF) and phosphoinositide 3-kinase (PI3K)-regulated checkpoint that delays DOR export from the *trans*-Golgi network. Through systematic mutational analysis of the DOR primary amino acid sequence, we identified conserved dual RXR motifs required for NGF and PI3K-regulated DOR Golgi retention in neuroendocrine cells. These motifs were required to bind the coatomer

[2] Statement of others' contributions to this work:
Daniel Shiwarski generated DOR deletion mutants, alanine scanning mutants, and alanine point mutants and performed experiments assessing their localization. Daniel Shiwarski and I performed data analysis of mutant receptor localization. I performed GST pull down experiments with assistance from Andrew Dates and co-immunoprecipitation experiments. I wrote part of the published manuscript with Daniel Shiwarski and Manoj Puthenveedu and performed revision experiments. I adapted the published manuscript for this dissertation. I generated the DOR lysine point mutant and SSTR5 mutants and performed and analyzed experiments assessing their localization. Candilianne Serrano Zayas performed and analyzed experiments assessing B2AR localization. Aditya Kumar provided helpful feedback on this written chapter.

protein I (COPI) complex, a vesicle coat complex that mediates retrograde cargo traffic within the biosynthetic pathway. Our results suggest that interactions of DOR with COPI, via C-terminal RXR motifs, retain DOR in the Golgi. These mechanisms could allow for acute regulation of DOR PM availability and associated signaling responses by both natural physiology and future therapeutic interventions. Lastly, we investigated whether C-terminal RXR motifs could serve as a general mechanism of signal-regulated biosynthetic trafficking of other GPCRs. Preliminary data suggest that the somatostatin receptor 5 is a candidate GPCR with shared mechanisms of signal-regulated Golgi localization.

Introduction

G protein-coupled receptor (GPCR) localization to the plasma membrane (PM) shapes receptor signaling in multiple ways. Removal of GPCRs from the PM through endocytosis desensitizes cells to extracellular ligands (Sorkin and Von Zastrow, 2002). Reinsertion of GPCRs to the PM through either endosomal recycling or insertion of newly synthesized receptors from the biosynthetic pathway resensitizes cells to these ligands (Böhm *et al.*, 1996; Sorkin and Von Zastrow, 2002). Additionally, GPCRs can signal from both the PM and intracellular compartments (Crilly and Puthenveedu, 2020). Signaling at the PM versus intracellular compartments like endosomes or the Golgi produces distinct downstream cellular responses ranging from altered second messenger signaling, to distinct transcriptional responses, to neurotransmission and behavior (Tsvetanova and von Zastrow, 2014; Godbole *et al.*, 2017; Jensen *et al.*, 2017; Nash *et al.*, 2019).

Though both endosomal recycling and biosynthetic trafficking regulate GPCR localization to the PM, GPCR biosynthetic trafficking is less well studied. Amino acid sequences within the GPCR itself regulate GPCR internalization, endosomal sorting, and recycling of GPCRs (Puthenveedu and von Zastrow, 2006; Marchese *et al.*, 2008; Bowman and Puthenveedu, 2015; Weinberg *et al.*, 2017). These sequences can also be acutely regulated by other cellular signaling pathways to dynamically regulate GPCR endosomal sorting (Bowman *et al.*, 2015; Kunselman *et al.*, 2019, 2021). In contrast, though a handful of sequence motifs and associated protein interactors, such as COPII, COPI, GGA proteins, and golgin-160, function in constitutive biosynthetic trafficking of GPCRs to the PM (Dong *et al.*, 2007; Zhang *et al.*, 2011, 2016; Gilbert *et al.*, 2014; St-Louis *et al.*, 2017), whether sequence elements mediating GPCR biosynthetic trafficking can be dynamically regulated by extracellular signals is an important unanswered question.

DOR is a physiologically relevant GPCR to study regulated biosynthetic trafficking to the PM. In neuronal cells, DOR localizes to intracellular compartments including the Golgi (Roth *et al.*, 1981; Cahill *et al.*, 2001a; Wang and Pickel, 2001; Kim and von Zastrow, 2003; Shiwarski *et al.*, 2017b). DOR trafficking to the PM from

intracellular pools to the PM can be acutely regulated by a number of signals including inflammation, PM receptor activation, and kinase activity (Cahill *et al.*, 2001b; Bao *et al.*, 2003; Patwardhan *et al.*, 2005; Bie *et al.*, 2010; Mittal *et al.*, 2013; Pettinger *et al.*, 2013; Shiwarski *et al.*, 2017a). DOR relocation from intracellular sites to the PM is correlated with enhanced pain-relieving effects of DOR agonists (Cahill *et al.*, 2003; Pradhan *et al.*, 2013; Shiwarski *et al.*, 2017b). Furthermore, once DOR reaches the PM and is activated and endocytosed, it primarily sorts to degradative pathways in the lysosome, meaning recovery of signal is primarily mediated by new receptor delivery from biosynthetic pathways (Tsao and Von Zastrow, 2000; Whistler *et al.*, 2002). Despite the clear relevance of this signal-regulated trafficking to DOR pharmacology, the mechanisms which specifically regulate DOR biosynthetic trafficking are not fully understood.

We performed systematic mutagenesis of the DOR C-terminal primary amino acid sequence and quantitative microscopy to identify the amino acids required for NGF and PI3K-regulated DOR Golgi retention. We identified two C-terminal RXR motifs required for signal-regulated DOR Golgi retention. Additionally, using biochemical approaches we found that C-terminal RXR motifs are required and sufficient for interaction with the COPI retrograde trafficking machinery. Together these data support a model in which sequence-specific interactions of DOR with COPI modulate DOR Golgi export and delivery to the PM. Lastly, we explored whether NGF and PI3K can regulate Golgi localization of other GPCRs through a similar mechanism. We identified somatostatin receptor 5 (SSTR5) as a candidate GPCR with shared mechanisms of regulated trafficking.

Results

DOR C-terminal amino acids 345–359 contain sequence determinants required for NGF and PI3K-regulated DOR Golgi retention

The last 27 amino acids of the DOR C-terminal tail confer nerve growth factor (NGF)-regulated Golgi retention to other transmembrane proteins (Kim and von Zastrow, 2003), suggesting this region contains a minimal amino acid sequence sufficient for signal-regulated retention. We first performed systematic deletions in the

DOR C-terminal tail to identify the amino acid residues required for NGF-regulated DOR Golgi retention **(Figure 2.1A)**.

PC12 cells expressing Flag-tagged wild-type DOR (DOR WT) or one of four C-terminal deletion mutants (∆345–352, ∆353–359, ∆360–366, ∆367 TGA) were treated with NGF for 1 hour before fixation and staining for Flag and *trans*-Golgi network (TGN) marker TGN-38, followed by confocal imaging. DOR WT localizes to the PM in untreated control (Ctrl) cells **(Figure 2.1B)**. After acute NGF treatment, newly synthesized DOR was retained in a compartment colocalizing with TGN-38 **(Figure 2.1B, yellow arrow)**. The four deletion mutants also localized to the PM in Ctrl cells and were retained in the Golgi following NGF treatment **(Figure 2.1B)**.

To quantify any differences in Golgi retention of the deletion mutants compared to DOR WT, we used a method described previously to calculate the percentage of total DOR that was retained in the Golgi (Shiwarski *et al.*, 2017a, 2017b). Briefly, we used TGN-38 staining to create a mask defining the *trans*-Golgi network area in the cell. We applied this mask to the DOR channel to quantify DOR signal in the Golgi. This Golgi DOR signal was then expressed as a percentage of total DOR signal in the cell and normalized to DOR WT in untreated Ctrl cells. In addition to this single-cell measure to quantify retention, we also determined the percentage of cells that showed DOR localized to the Golgi under each condition at a population level.

Following NGF treatment, the percentage of total receptor retained in the Golgi increased for all DOR constructs **(Figure 2.1C)**, indicating that none of these regions was fully required for NGF-regulated DOR Golgi retention. However, ∆345–352 and ∆353–359 deletion mutants displayed reduced NGF-regulated DOR Golgi retention compared to DOR WT. Additionally, a decreased percentage of cells expressing ∆345–352 and ∆353–359 deletion displayed DOR localized to the Golgi following NGF treatment compared to cells expressing DOR WT **(Figure 2.1D)**. These data suggest that the region between amino acids 345-359 of the DOR C-terminal tail may play a role in NGF-regulated DOR Golgi retention.

In addition to regulation by NGF, the DOR C-terminal tail is also sufficient to confer PI3K-regulated Golgi retention to a transmembrane protein (Shiwarski *et al.*,

2017a). Inhibition of Class II PI3Ks leads to DOR Golgi retention, and PI3K Class II α isoform specifically regulates DOR export from the TGN in both PC12 cells and neurons (Shiwarski *et al.*, 2017a). We tested whether the ∆345–352 and ∆353–359 deletion mutants showing reduced Golgi retention following NGF also showed reduced Golgi retention following PI3K inhibition.

PC12 cells expressing Flag-tagged DOR WT, DOR Δ345–352, or DOR Δ353–359 were treated with PI3K inhibitors (PI3Ki) Wortmannin (Wort, 10 μM) or LY294002 (LY, 10 μM) for 1 hour before fixation and staining for Flag and TGN-38, followed by confocal imaging. As expected, DOR WT was retained in the Golgi following PI3K inhibition **(Figure 2.1E)**. Δ345–352 and Δ353–359 deletion mutants displayed small, but significant decreases in Golgi retention compared to DOR WT by both single cell and population level measures **(Figure 2.1E-G)**. These data further suggest that the region between amino acids 345-359 of the DOR C-terminal contains sequence determinants required for NGF and PI3K-regulated DOR Golgi retention. The partial effect of each of the two deletion mutants (Δ345–352 and Δ353–359) raises the possibility that the signal-regulated retention motif spans the two deletion regions.

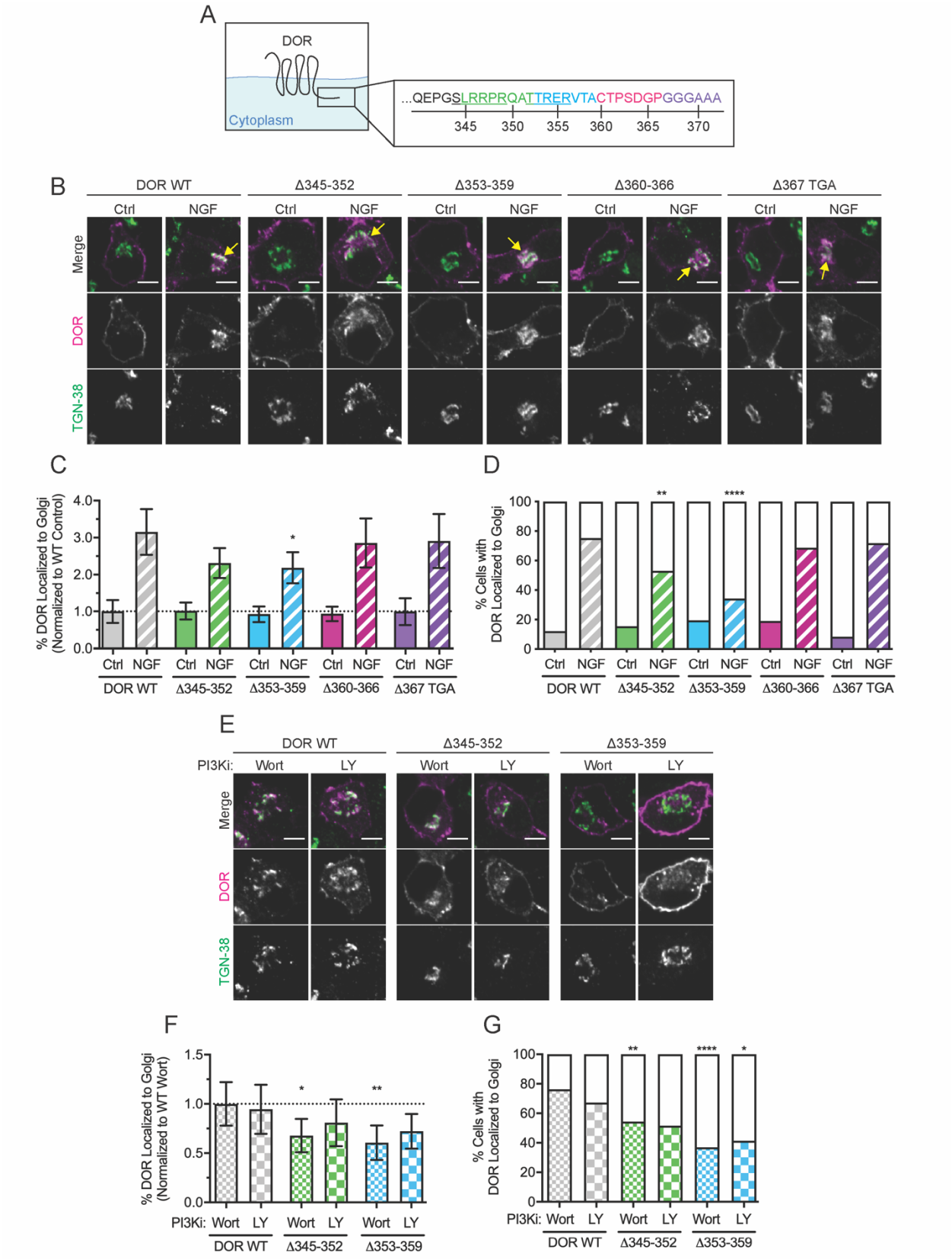
A
DOR
Cytoplasm
...QEPGSLRRPRQATTRERVTACTPSDGPGGGAAA
345
350
355
360
365
370
B
DOR WT
Δ345-352
Δ353-359
Δ360-366
Δ367 TGA
Ctrl
NGF
Merge
DOR
TGN-38
C
% DOR Localized to Golgi (Normalized to WT Control)
4.0
3.0
2.0
1.0
0.0
*
Ctrl NGF Ctrl NGF Ctrl NGF Ctrl NGF Ctrl NGF
DOR WT
Δ345-352
Δ353-359
Δ360-366
Δ367 TGA
D
% Cells with DOR Localized to Golgi
100
80
60
40
20
0
**
****
Ctrl NGF Ctrl NGF Ctrl NGF Ctrl NGF Ctrl NGF
DOR WT
Δ345-352
Δ353-359
Δ360-366
Δ367 TGA
E
DOR WT
Δ345-352
Δ353-359
PI3Ki:
Wort
LY
Merge
DOR
TGN-38
F
% DOR Localized to Golgi (Normalized to WT Wort)
1.5
1.0
0.5
0.0
*
**
PI3Ki: Wort LY Wort LY Wort LY
DOR WT
Δ345-352
Δ353-359
G
% Cells with DOR Localized to Golgi
100
80
60
40
20
0
**
****
*
PI3Ki: Wort LY Wort LY Wort LY
DOR WT
Δ345-352
Δ353-359

Figure 2.1. Deletions Δ345–352 and Δ353–359 partially reduce DOR Golgi retention induced by NGF treatment and PI3K inhibition.
(A) The last 27 amino acids of the DOR C-terminal tail were subdivided into four regions, indicated by color, which were systematically deleted to create four DOR deletion mutants (Δ345–352, Δ353–359, Δ360–366, and Δ367 TGA). **(B)** PC12 cells expressing either wild-type Flag-tagged DOR (DOR WT) or one of the Flag-tagged DOR deletion mutants were left untreated (Ctrl) or treated with 100 ng/mL nerve growth factor (NGF) for 1 hour, then fixed and stained for Flag (magenta in merge) and *trans*-Golgi network marker TGN-38 (green in merge) (scale bars=5 μm). DOR WT and deletion mutants localized primarily to the plasma membrane in Ctrl cells and colocalized with TGN-38 following NGF treatment (white in merge, yellow arrows). **(C)** The percentage of DOR fluorescence within the region defined by TGN-38 staining, normalized to the mean of DOR WT expressing Ctrl cells, was quantified. NGF-induced increases in retention of deletion mutants were compared to the increase observed for DOR WT (Bars indicate mean ± 95% CI; one-way ANOVA ($p=0.0443$) of NGF conditions with significance from Dunnett's multiple comparisons test of DOR WT NGF condition versus deletion mutant NGF conditions indicated in the figure; WT vs Δ345–352, $p=0.0791$; WT vs Δ353–359, $p=0.0295$; WT vs Δ360–366, $p=0.8574$; WT vs Δ367 TGA, $p=0.9623$). **(D)** The percentage of cells with DOR localized to the Golgi was quantified and compared between NGF-treated deletion mutants and DOR WT (significance from two-tailed Chi-square test of DOR WT NGF condition versus deletion mutant NGF conditions indicated in the figure with Bonferroni correction for multiple comparisons: WT vs Δ345–352, $p=0.0084$; WT vs Δ353–359, $p<0.0001$; WT vs Δ360–366, $p>1$; WT vs Δ367 TGA, $p>1$). (For **C** and **D**, WT, Ctrl=82 cells, NGF=77; Δ345–352, Ctrl=97, NGF=98; Δ353–359, Ctrl=77, NGF=105; Δ360–366, Ctrl=84, NGF=80; Δ367 TGA, Ctrl=34, NGF=39, across a minimum of two biological replicates). **(E)** PC12 cells expressing either Flag-tagged DOR WT, Δ345–352, or Δ353–359 were treated with a PI3K inhibitor (PI3Ki), 10 μM Wortmannin (Wort) or 10 μM LY294002 (LY), for 1 hour, then fixed and stained for Flag (magenta in merge) and TGN-38 (green in merge) (scale bars=5 μm). DOR WT colocalized with TGN-38 (white in merge) following Wort or LY treatment. Δ345–352 and Δ353–359 deletion mutants also colocalized with TGN-38 following Wort or LY treatment. **(F)** The percentage of DOR fluorescence within the region defined by TGN-38 staining was normalized to the mean of Wort-treated cells expressing DOR WT, and compared between DOR WT and deletion mutants for each treatment condition (Bars indicate mean ± 95% CI; Among Wort-treated cells, significance from one-way ANOVA ($p=0.0088$) with Dunnett's multiple comparisons test of DOR WT Wort vs deletion mutants indicated in the figure: WT Wort vs Δ345–352 Wort, $p=0.0308$; WT Wort vs Δ353–359 Wort, $p=0.0079$; Among LY-treated cells, significance from one-way ANOVA ($p=0.3974$) with Dunnett's multiple comparisons test of DOR WT LY vs deletion mutants indicated in the figure: WT LY vs Δ345–352 LY, $p=0.5896$; WT LY vs Δ353–359 LY, $p=0.3047$). **(G)** Percentage of cells with DOR localized to the Golgi after treatment with Wort or LY was quantified and compared between DOR WT and deletion mutants for each treatment condition (significance from two-tailed Chi-square test of DOR WT Wort or LY versus deletion mutant Wort or LY

indicated in the figure with Bonferroni correction for multiple comparisons: WT Wort vs Δ345–352 Wort, p=0.0086; WT Wort vs Δ353–359 Wort, p<0.0001; WT LY vs Δ345–352 LY, p=0.1714; WT LY vs Δ353–359 LY, p=0.0442). (For **F** and **G**, WT, Wort=76 cells, LY=55; Δ345–352, Wort=79, LY=62; Δ353–359, Wort=73, LY=50, across three biological replicates).

RXR motifs within the DOR C-terminal tail are required for NGF and PI3K-regulated DOR Golgi retention

Given that two deletion mutants (Δ345–352 and Δ353–359, **Figure 2.1**) and two alanine scanning mutants (SLRRPRΔAla and TTRERΔAla, **Figure 2.S1**) showed only partial reduction in DOR Golgi retention, we hypothesized that the retention motif may span these two regions. To aid in identifying residues of interest we evaluated the evolutionary conservation of DOR C-terminal tail amino acid sequences across human, mouse, and rat species. We identified two conserved RXR motifs, 347–349 (RPR) and 354–356 (RER) **(Figure 2.2A)**. In addition to conservation of these residues, amino acid sequences containing arginine (R)–any amino acid (X)–arginine (R), or 'RXR', motifs retain ion channels and GPCRs in the endoplasmic reticulum (Zerangue *et al.*, 1999; Margeta-Mitrovic *et al.*, 2000; Ma *et al.*, 2001; Cunningham *et al.*, 2012).

To specifically test the role of these arginine motifs in signal-regulated DOR Golgi retention, we mutated all five arginine residues spanning amino acids 345-359 to alanine (DOR 2AXA). PC12 cells expressing Flag-tagged DOR WT or arginine mutant DOR 2AXA were treated with NGF or PI3Ki for 1 hour before fixation and staining for Flag and TGN-38, followed by confocal imaging. DOR WT and DOR 2AXA both localized to the PM in untreated Ctrl cells **(Figure 2.2B)**. Following 1 hour of NGF or PI3Ki (LY, 10 μM) treatment, DOR WT was retained in the Golgi as expected, whereas DOR 2AXA remained localized primarily to the PM **(Figure 2.2B)**. The percentage of total DOR 2AXA retained in the Golgi following NGF or PI3Ki treatment significantly decreased compared to DOR WT **(Figure 2.2C)**. Additionally, the percentage of cells expressing DOR 2AXA localized to the Golgi following NGF or PI3Ki treatment was significantly decreased compared to cells expressing DOR WT **(Figure 2.2D)**. Both DOR WT and DOR 2AXA total receptor levels were consistent across treatment

conditions, indicating the absence of DOR 2AXA Golgi retention is not due to enhanced receptor degradation **(Figure 2.S2A)**. Together these results indicate that C-terminal arginine residues comprising two RXR motifs are required for NGF and PI3K-regulated DOR Golgi retention.

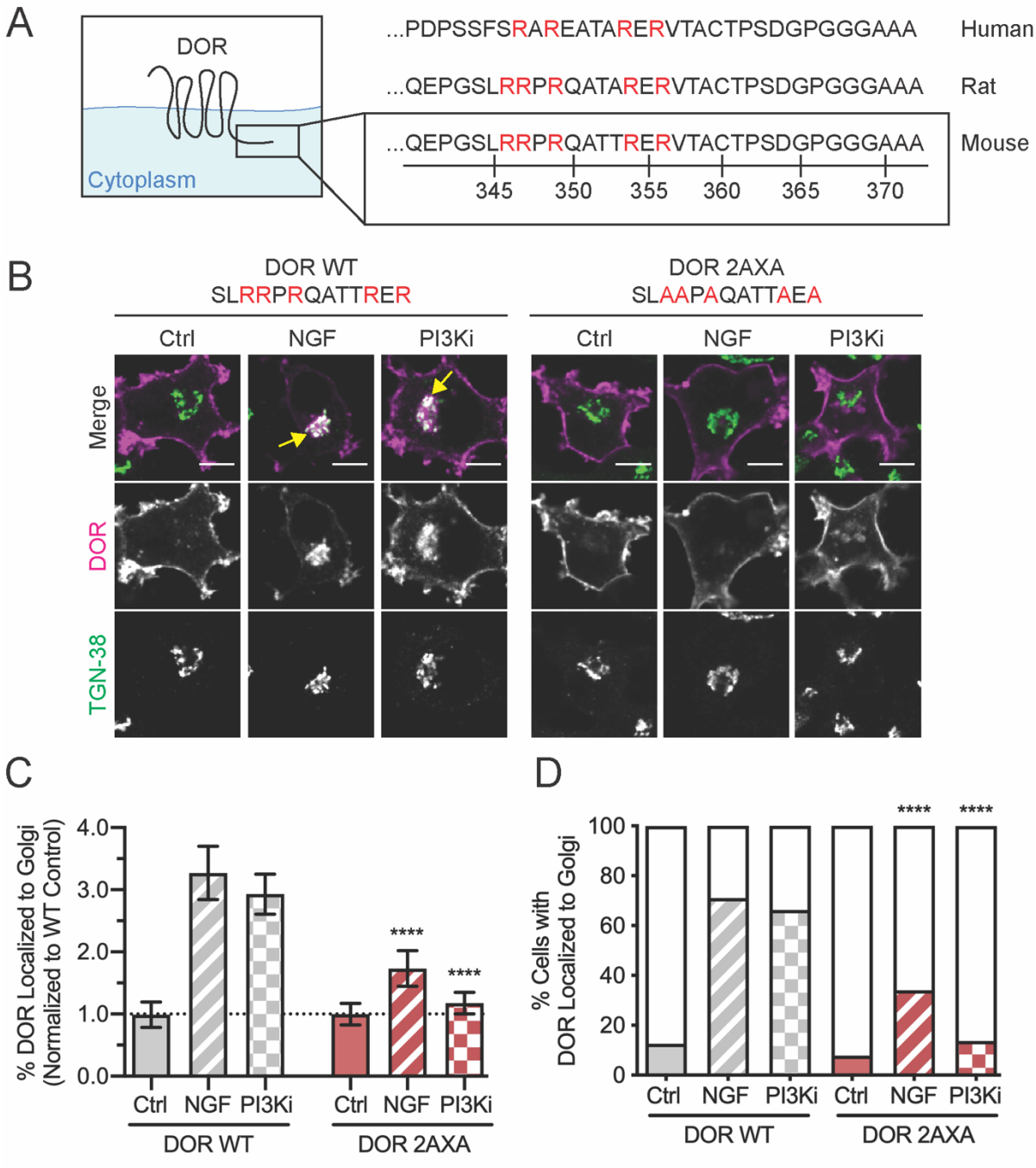

Figure 2.2. DOR C-terminal RXR motifs are required for DOR Golgi retention by NGF treatment and PI3K inhibition.

(A) Five arginine residues (red) composing two RXR motifs which span the Δ345–352 and Δ353–359 deletion regions were substituted with alanine to generate the DOR 2AXA mutant. **(B)** PC12 cells expressing either Flag-tagged DOR WT or DOR 2AXA were left untreated (Ctrl) or treated with NGF or PI3Ki (LY, 10 μM) for 1 hour, then fixed and stained for Flag (magenta in merge) and TGN-38 (green in merge) (scale bars=5 μm). Both DOR WT and DOR 2AXA localized primarily to the plasma membrane in Ctrl cells. DOR WT colocalized with TGN-38 (white in merge, yellow arrow) following NGF or PI3Ki treatment, whereas DOR 2AXA continued to localize primarily to the plasma membrane. **(C)** The percentage of DOR fluorescence within the region defined by TGN-38 staining, normalized to the mean of DOR WT expressing Ctrl cells, was quantified and compared between DOR WT and 2AXA for each treatment condition (Bars indicate mean ± 95% CI; significance from two-tailed Student's t-test of WT NGF vs 2AXA NGF, $p<0.0001$, or WT PI3Ki vs 2AXA PI3Ki, $p<0.0001$ indicated in the figure). **(D)** Percentage of cells with DOR localized to the Golgi was quantified and compared between DOR WT and 2AXA for each treatment condition (significance from two-tailed Chi-square tests of WT NGF vs 2AXA NGF, $p<0.0001$ or WT PI3Ki vs 2AXA PI3Ki, $p<0.0001$). (For **C** and **D**, DOR WT, Ctrl=86 cells, NGF=75, PI3Ki=159; DOR 2AXA, Ctrl=87, NGF=94, PI3Ki=123, across two biological replicates).

To further probe the properties of C-terminal arginine motifs required to mediate DOR Golgi retention, we next tested whether positively charged residues are sufficient to preserve DOR Golgi retention. We mutated the five arginine residues spanning amino acids 345-359 to lysine (DOR 2KXK). DOR 2KXK localized to the PM in untreated control cells and was retained in the Golgi following NGF and PI3Ki treatment **(Figure 2.S3A, yellow arrows)**. The percentage of total DOR 2KXK localized to the Golgi, as well as the percentage of cells with DOR KXK localized to the Golgi, did not significantly differ from DOR WT following NGF and PI3Ki treatment **(Figure 2.S3B-C)**. These data indicate that both arginine and lysine-based C-terminal motifs are sufficient to confer signal-regulated DOR Golgi retention.

RXR motifs in the DOR C-terminal tail are required and sufficient for interaction with COPI

Given that C-terminal RXR motifs are required for DOR retention, we next asked whether these residues serve as interacting motifs for machinery that could cause cargo to localize to the Golgi by retention or retrieval. Because RXR motifs in ion channels

were originally described as binding coat protein complex I (COPI) and retrieving unassembled subunits to the ER (Yuan *et al.*, 2003; Michelsen *et al.*, 2005), we focused on COPI as a potential interacting factor for the DOR RXR motifs. PC12 cells expressing Flag-tagged DOR WT or DOR 2AXA were treated with 0.5 mM DSP crosslinker to capture transient and local interactions of DOR with COPI components prior to cell lysis and immunoprecipitation of the Flag-tagged receptor and immunoblotting for the β-COP subunit of COPI. β-COP coimmunoprecipitated with DOR WT **(Figure 2.3A)**, suggesting that these two proteins may interact in cells. We observed a significant decrease in β-COP coimmunoprecipitation with DOR 2AXA compared with DOR WT **(Figure 2.3A-B)**. We did not see a complete loss of β-COP binding, consistent with a conventional lysine-based motif in an intracellular loop of DOR that was identified as binding COPI (St-Louis *et al.*, 2017). However, the reduction in β-COP coimmunoprecipitation with DOR 2AXA suggests that C-terminal RXR motifs contribute to COPI binding.

To test whether C-terminal RXR motifs are sufficient for interaction with COPI machinery, we next used an affinity purification approach. PC12 cell lysate was incubated with GST fusion proteins consisting of either GST fused to the last 27 amino acids of the DOR C-terminal tail (GST-DOR) or a mutant in which the five arginine residues in the tail were mutated to alanine (GST-2AXA). Both β-COP and ε-COP copurified with GST-DOR but not with GST-2AXA or GST alone, at 10- and 3.3-μM concentrations, as shown by immunoblotting for each subunit **(Figure 2.3C, 2.S4)**. These results suggest that the DOR C-terminal tail is sufficient to bind COPI and C-terminal RXR motifs are required to bind β-COP and ε-COP in this context. Taken together, our results suggest a model in which RXR motifs in the DOR C-terminal tail, by binding the COPI retrograde trafficking machinery, can regulate the export of DOR from the Golgi in response to extracellular signals.

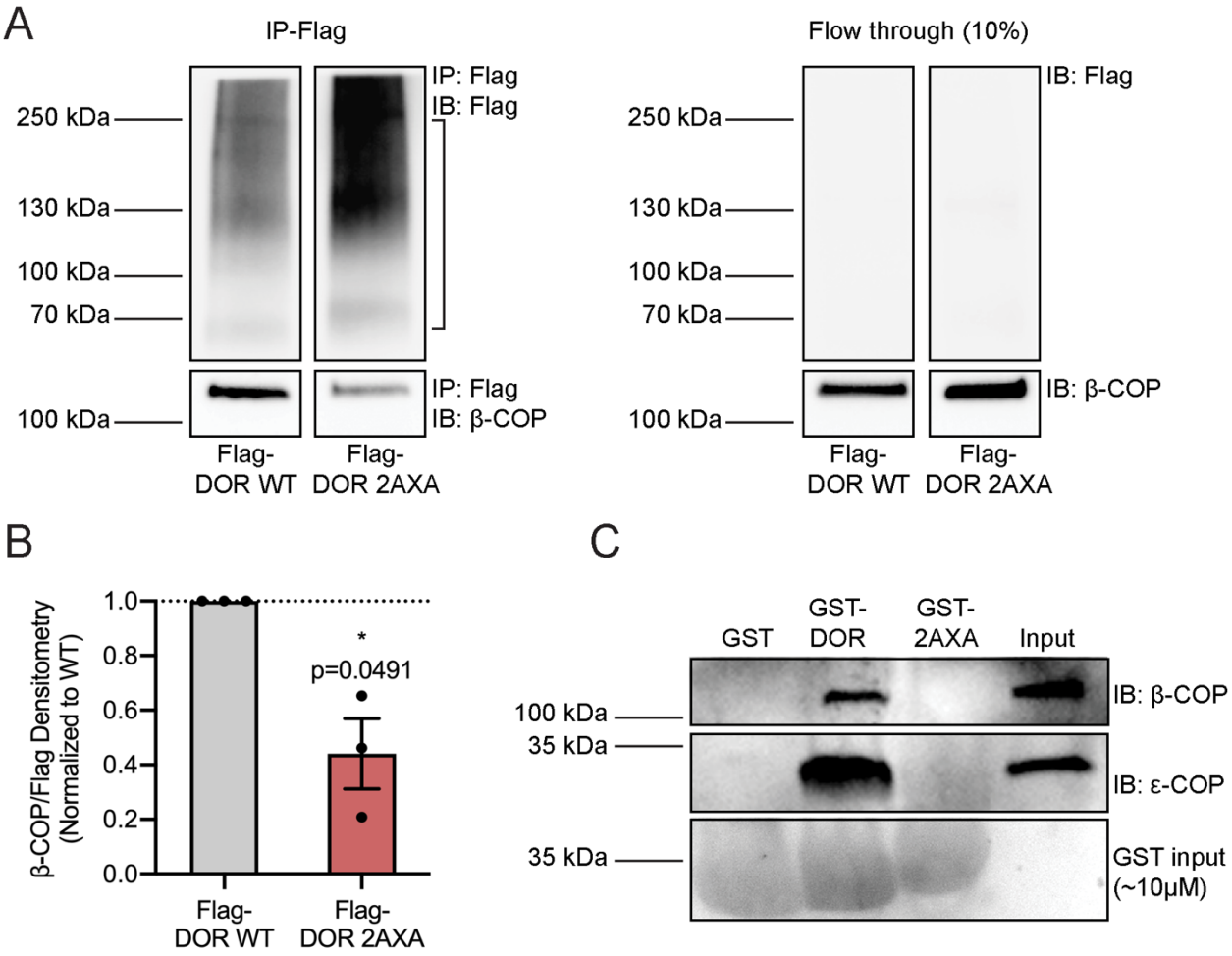

Figure 2.3. DOR C-terminal RXR motifs are required and sufficient for interaction with COPI coat proteins.

(A) PC12 cells expressing Flag-tagged DOR WT or DOR 2AXA were cross-linked with 0.5 mM DSP, which was followed by immunoprecipitation (IP) with an anti-Flag antibody and immunoblotting (IB) for β-COP or Flag. Representative immunoblot (n=3) for β-COP shows more β-COP interacting with Flag-DOR WT. Immunoblotting for Flag indicates expression of the tagged receptor and efficient depletion of the tagged receptor from the supernatant after immunoprecipitation. **(B)** The difference in β-COP associated with the WT and mutant receptor quantitated by densitometry. β-COP in the IP was normalized to Flag-DOR WT or 2AXA. The region used for quantitation is noted by square brackets. There was a statistically significant decrease in the amount of β-COP that immunoprecipitated with DOR 2AXA compared to DOR WT (n=3, mean ± SEM; significance from one sample t-test to a theoretical mean of 1 reported in the figure). **(C)** PC12 cell lysate was incubated with 150 μg (~10 μM) GST fusion proteins bound to glutathione agarose beads, followed by immunoblotting (IB) for β-COP or ε-COP. The 110-kDa band corresponding to β-COP or the 34-kDa band corresponding to ε-COP

coprecipitates with the wild-type DOR tail (GST-DOR), but not with GST or the tail lacking RXR motifs (GST-2AXA). β-COP and ε-COP are also present in 10 μg whole-cell lysate (Input). A Ponceau-S staining for the respective GST proteins is shown in the bottom panel. Blot is representative of three separate experiments.

NGF and PI3K regulate Golgi localization of SSTR5

The identification of signal-regulated RXR motifs which modulate DOR delivery to the PM raises the possibility that this mechanism could regulate subcellular localization of other GPCRs. RXR motifs regulate trafficking of several other GPCRs, including vasopressin 2 receptor, protease activated receptor 4, kappa opioid receptor, alpha$_{2c}$ adrenergic receptor, and GABA$_B$ receptor (Margeta-Mitrovic *et al.*, 2000; Hermosilla *et al.*, 2004; Cunningham *et al.*, 2012; Li *et al.*, 2012; Filipeanu *et al.*, 2015), though to our knowledge signal-regulated RXR motifs in a GPCR have been described for DOR only. Regulation of RXR motifs by the NGF and PI3K-regulated trafficking checkpoint we have described for DOR in neuronal cells is directly relevant to GPCRs in systems where NGF plays an important role, such as the nervous system and immune system (Aloe *et al.*, 2012).

We first tested whether the signal-regulated trafficking mechanisms we have identified for DOR apply to other GPCRs. We were particularly interested in GPCR families expressed in the nervous system and GPCRs previously reported to localize intracellularly to the Golgi. Among the somatostatin receptor family, somatostatin receptor 5 (SSTR5) has been reported to localize to the Golgi in specific expression contexts (Sarret *et al.*, 2004; Wente *et al.*, 2005; Bauch *et al.*, 2014). Though most enriched in endocrine tissues, SSTR5 is expressed in multiple brain regions (Bruno *et al.*, 1993; Stroh *et al.*, 1999; Ramírez *et al.*, 2002).

To test whether SSTR5 Golgi localization is regulated similarly to DOR, we expressed Flag-tagged DOR, SSTR5, or β2-adrenergic receptor (B2AR), as a negative control, in PC12 cells and assessed their localization. PC12 cells expressing Flag-tagged DOR, SSTR5, or B2AR were treated with NGF or PI3Ki (10μM LY) for 1 hour before fixation and staining for Flag and TGN-38, followed by confocal imaging. Each receptor localized to the PM in untreated Ctrl cells **(Figure 2.4A)**. Following NGF or PI3Ki treatment, both DOR and SSTR5 were retained in the Golgi **(Figure 2.4A, yellow arrows)**. Compared to DOR, intracellular SSTR5 appeared more broadly distributed, both colocalized with and adjacent to TGN-38 staining. B2AR, which lacks RXR motifs

in all intracellular regions, localized primarily to the PM, consistent with its known subcellular distribution in unstimulated cells (Von Zastrow and Kobilka, 1992). Following NGF or PI3Ki treatment the percentage of receptor localized to the Golgi and percentage of cells with receptor localized to the Golgi significantly increased for both DOR and SSTR5, though the magnitude of the effect was lower for SSTR5 compared to DOR **(Figure 2.4B-C)**. Together these data indicate that like DOR, SSTR5 Golgi retention is regulated by NGF and PI3K in neuronal cells.

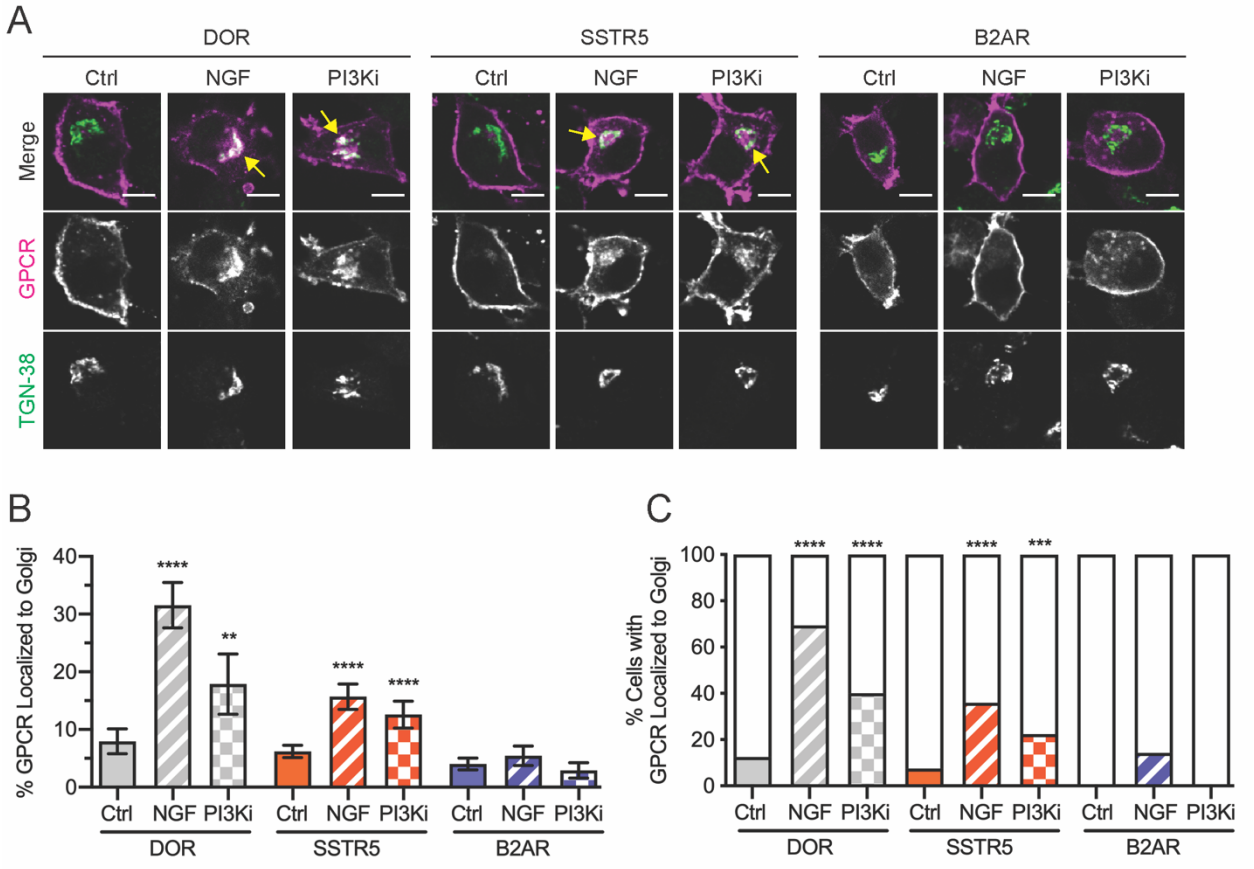

Figure 2.4. NGF and PI3K regulate Golgi localization of SSTR5.
(A) PC12 cells expressing either Flag-tagged DOR, SSTR5, or B2AR were left untreated (Ctrl) or treated with NGF or PI3Ki (LY, 10 μM) for 1 hour, then fixed and stained for Flag (magenta in merge) and TGN-38 (green in merge) (scale bars=5 μm). All three receptors localized primarily to the plasma membrane in Ctrl cells. DOR and SSTR5 colocalized with TGN-38 (white in merge, yellow arrows) following NGF or PI3Ki treatment, whereas B2AR continued to localize primarily to the plasma membrane. **(B)** The percentage of GPCR fluorescence within the region defined by TGN-38 staining was quantified for each receptor and NGF and PI3Ki treatment conditions compared to Ctrl condition (Bars indicate mean ± 95% CI; Among DOR cells, significance from one-way ANOVA

(p<0.0001) with Dunnett's multiple comparisons test compared to DOR Ctrl reported in the figure: Ctrl vs NGF, p<0.0001, Ctrl vs PI3Ki, p=0.0014; Among SSTR5 cells, significance from one-way ANOVA (p<0.0001) with Dunnett's multiple comparisons test compared to SSTR5 Ctrl reported in the figure: Ctrl vs NGF, p<0.0001, Ctrl vs PI3Ki, p<0.0001; Among B2AR cells, significance from one-way ANOVA (p=0.0356) with Dunnett's multiple comparisons test compared to B2AR Ctrl reported in the figure: Ctrl vs NGF, p=0.2404, Ctrl vs PI3Ki, p=0.4418). **(C)** Percentage of cells with GPCR localized to the Golgi was quantified and compared between treatment conditions and the control condition for each receptor (significance from two-tailed Chi-square tests with Bonferroni correction for multiple comparisons of DOR Ctrl vs NGF, p<0.0001, Ctrl vs PI3Ki, p<0.0001; SSTR5 Ctrl vs NGF, p<0.0001, Ctrl vs PI3Ki, p=0.0002; B2AR Ctrl vs NGF, p=0.1044). (For **B** and **C**, DOR, Ctrl=136 cells, NGF=124, PI3Ki=54; SSTR5, Ctrl=186, NGF=192, PI3Ki=142; B2AR, Ctrl=17, NGF=21, PI3Ki=17, DOR and SSTR5 across a minimum of three biological replicates, B2AR from one biological replicate).

C-terminal sequences regulate Golgi localization of SSTR5

We next asked which sequence determinants contribute to signal-regulated SSTR5 Golgi retention. Informed by the requirement of RXR motifs for DOR Golgi retention, we first mutated three C-terminal arginine residues to alanine, which includes one potential RXR motif (SSTR5 AXA) (**Figure 2.5A**, residues in red). PC12 cells expressing Flag-tagged SSTR5 WT or SSTR5 AXA were treated with NGF or PI3Ki (LY, 10μM) for 1 hour before fixation and staining for Flag and TGN-38, followed by confocal imaging. Both SSTR5 WT and the AXA mutant localized to the PM in untreated Ctrl cells and localized to the Golgi after NGF or PI3Ki treatment **(Figure 2.5B)**. Both the percentage of SSTR5 localized to the Golgi and the percentage of cells with SSTR5 localized to the Golgi showed a small but significant decrease for SSTR5 AXA compared to SSTR5 WT after NGF treatment **(Figure 2.5C-D)**. Paradoxically, both measures *increased* for the AXA mutant after PI3Ki treatment **(Figure 2.5C-D)**. These opposing effects could indicate that NGF and PI3Ks modulate GPCR Golgi localization through multiple mechanisms.

SSTR5 C-terminal PDZ ligand (**Figure 2.5A**, underlined) mediates Golgi export or retention depending on relative expression levels of PDZ domain protein interactors in specific cellular contexts (Wente *et al.*, 2005; Bauch *et al.*, 2014). Given the importance of this C-terminal sequence determinant to Golgi localization, we wanted to

test its requirement for NGF and PI3K-regulated SSTR5 Golgi localization. Interestingly, deletion of the C-terminal PDZ ligand in SSTR5 leads to a two-fold increase in Golgi SSTR5 across all conditions, including in baseline control cells, suggesting that the normal function of the PDZ ligand may be in promoting Golgi export. Both the percentage of SSTR5 localized to the Golgi and the percentage of cells with SSTR5 localized to the Golgi in PC12 cells expressing a C-terminally truncated SSTR5 lacking the PDZ ligand (SSTR5ΔPDZ) significantly increased (a minimum of two-fold) in all treatment conditions, including untreated cells, compared to SSTR5 WT **(Figure 2.5E-F)**. However, increased Golgi localization upon NGF and PI3Ki was preserved for SSTR5ΔPDZ, suggesting the PDZ ligand is not directly required for NGF or PI3K-regulated Golgi localization. These data support a model in which multiple layers of regulation contribute to SSTR5 Golgi localization.

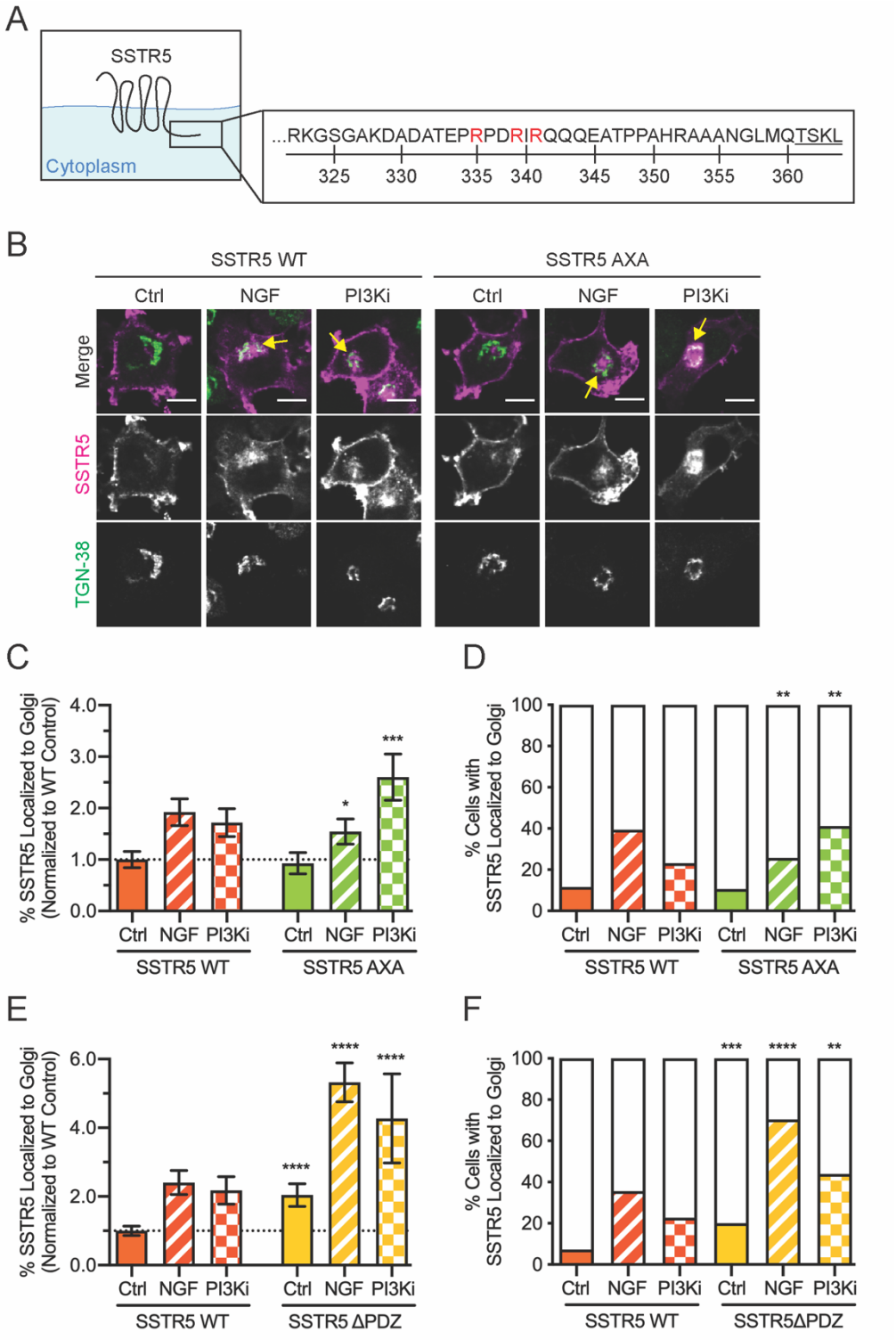

Figure 2.5. C-terminal sequence determinants mediate SSTR5 Golgi localization. **(A)** Two regions of interest in the SSTR5 C-terminal tail were mutated and evaluated separately. Three arginine residues (red) composing one RXR motif were substituted with

alanine to generate the SSTR5 AXA mutant. The C-terminal tail was also truncated before the last four amino acids (underlined) which comprise a PDZ ligand to generate the SSTR5ΔPDZ mutant. **(B)** PC12 cells expressing either Flag-tagged SSTR5 WT or SSTR5 AXA were left untreated (Ctrl) or treated with NGF or PI3Ki (LY, 10 μM) for 1 hour, then fixed and stained for Flag (magenta in merge) and TGN-38 (green in merge) (scale bars=5 μm). SSTR5 WT and AXA localized primarily to the plasma membrane in Ctrl cells and colocalized with TGN-38 (white in merge, yellow arrows) following NGF or PI3Ki treatment. **(C)** The percentage of SSTR5 fluorescence within the region defined by TGN-38 staining was quantified, normalized to SSTR5 WT Ctrl cells, and compared between WT and AXA for each treatment condition (Bars indicate mean ± 95% CI; significance from two-tailed Student's t-test of WT NGF vs AXA NGF, p=0.0398, or WT PI3Ki vs AXA PI3Ki, p=0.0006 indicated in the figure). **(D)** Percentage of cells with SSTR5 localized to the Golgi was quantified and compared between WT and AXA for each treatment condition (significance from two-tailed Chi-square tests indicated in the figure, WT NGF vs AXA NGF, p=0.0065; WT PI3Ki vs AXA PI3Ki, p=0.0021). (For **C** and **D**, SSTR5 WT, Ctrl=155 cells, NGF=188, PI3Ki=170; SSTR5 AXA, Ctrl=171, NGF=167, PI3Ki=131, across a minimum of three biological replicates). **(E)** The percentage of SSTR5 fluorescence within the region defined by TGN-38 staining was quantified, normalized to SSTR5 WT Ctrl cells, and compared between WT and SSTR5ΔPDZ for Ctrl and treatment conditions (Bars indicate mean ± 95% CI; significance from two-tailed Student's t-test of WT Ctrl vs ΔPDZ Ctrl, p<0.0001, WT NGF vs ΔPDZ NGF, p<0.0001, and WT PI3Ki vs ΔPDZ PI3Ki, p<0.0001 indicated in the figure). **(F)** Percentage of cells with SSTR5 localized to the Golgi was quantified and compared between WT and SSTR5ΔPDZ for Ctrl and treatment conditions (significance from two-tailed Chi-square tests indicated in the figure, WT Ctrl vs ΔPDZ Ctrl, p=0.0007, WT NGF vs ΔPDZ NGF, p<0.0001, WT PI3Ki vs ΔPDZ PI3Ki, p=0.0074). (For **E** and **F**, SSTR5 WT, Ctrl=178 cells, NGF=177, PI3Ki=141; SSTR5ΔPDZ, Ctrl=150, NGF=142, PI3Ki=41, across a minimum of one biological replicate).

Discussion

Here, we demonstrate that NGF and PI3K-regulated Golgi retention of DOR requires two bi-arginine motifs (RXR) within the DOR C-terminal tail. These C-terminal RXR motifs are required for interactions of DOR with COPI. Together these data suggest a model in which DOR interactions with COPI mediate signal-regulated DOR Golgi retention through active retrieval and retrograde trafficking of DOR within the biosynthetic pathway. We also presented evidence suggesting the signal-regulated Golgi localization observed for DOR may apply broadly to other GPCRs. Like DOR, SSTR5 localizes to the Golgi in an NGF and PI3K-regulated manner, with distinct

contributions of the C-terminal tail to this localization, suggesting signal-regulated GPCR Golgi localization may be mediated by overlapping but distinct mechanisms.

Active retention of cargo in the late Golgi or the *trans*-Golgi network presents an interesting challenge for cargo, considering the prevalent model that each compartment in the Golgi apparatus matures, and cargo transits and exits the Golgi as a "default" mechanism (Glick and Luini, 2011). Our results suggest that DOR is retained by a similar mechanism by which Golgi resident enzymes are retained in the Golgi—by constant COPI-mediated retrieval to earlier compartments (Glick and Luini, 2011). For DOR, the COPI interactions could be a mechanism to constantly retrieve receptors from the TGN to earlier Golgi compartments, allowing retention in the Golgi. In HEK293 cells, DOR interacts constitutively with COPI through traditional di-lysine or a combination of lysine and arginine motifs in the intracellular loops, and mutation of these motifs increases DOR levels at the PM (St-Louis *et al.*, 2017). In our experiments, the majority of DOR was delivered to the cell surface under basal conditions. Although it is possible that some amount of DOR was retained in the Golgi at baseline, this retention was significantly increased by NGF treatment or PI3K inhibition (Kim and von Zastrow, 2003; Shiwarski *et al.*, 2017a, 2017b). Further, this retention was abolished in receptors lacking the RXR motifs.

Our identification of RXR motifs that mediate Golgi retention of DOR is consistent with the role of these "atypical" arginine-based motifs in trafficking steps of multiple cargo. RXR motifs were first shown to mediate retrieval and retention of the ATP-sensitive potassium channel α (Kir6.1/2) and β (SUR1) subunits in the ER (Zerangue *et al.*, 1999). Complete assembly of subunits masks the RXR sequence and allows channel export from the ER. Amino acids between and flanking the arginine residues can influence the magnitude of retention and the compartment within which the channel was retained (Zerangue *et al.*, 2001; Michelsen *et al.*, 2005). RXR motifs also play roles in export of other membrane channels and GPCRs, such as the NMDA receptor, the vasopressin 2 receptor, the $GABA_B$ receptor, and the protease activated receptor 4, from the ER depending on protein folding state, dimerization, interaction with PDZ proteins, or phosphorylation (Margeta-Mitrovic *et al.*, 2000; Scott *et al.*, 2001; Hermosilla

et al., 2004; Cunningham *et al.*, 2012). Unlike these proteins, DOR exits the ER irrespective of the RXR motif (Figure 1A), and the primary role of DOR RXR motifs appears to be in signal-regulated retention in late Golgi compartments, from which regulated delivery to the PM can cause physiological changes in DOR signaling and antinociception (Shiwarski *et al.*, 2017b).

Consistent with our observation that DOR RXR motifs bind COPI coat subunits, RXR motifs which mediate retention of ion channels and other GPCRs within the biosynthetic pathway, also bind COPI subunits (Zerangue *et al.*, 2001; Yuan *et al.*, 2003; Brock *et al.*, 2005; Michelsen *et al.*, 2005; Cunningham *et al.*, 2012). RXR motifs interact with COPI through distinct sites (β-COP and δ-COP) from where canonical di-lysine motifs interact (α-COP and β'-COP) (Eugster *et al.*, 2004; Michelsen *et al.*, 2007; Jackson *et al.*, 2012; Ma and Goldberg, 2013). Lysines typically cannot substitute for arginines in other RXR motifs both in terms of COPI interaction and functional retention of proteins (Zerangue *et al.*, 1999; Yuan *et al.*, 2003; Michelsen *et al.*, 2005). However, lysine substitution in DOR RXR motifs preserves signal-regulated DOR retention, though we did not test the effect of lysine substitution on the DOR COPI interaction. Alternatively, lysine substitutions in the DOR tail could create di-lysine motifs similar to those which mediate COPI interaction and retention of GPCRs (Zhu *et al.*, 2015; St-Louis *et al.*, 2017). Mapping the specific interaction of DOR RXR motifs with COPI, including whether this interaction is direct, will be essential for understanding how these motifs mediate signal-regulated retention and for informing efforts to target this interaction to increase DOR at the PM.

How could signals regulate the interactions of the DOR RXR motif with COPI? Though we have not yet directly shown that the signals which increase DOR Golgi retention also increase RXR motif-dependent DOR-COPI interaction, it is interesting to speculate about how DOR-COPI interactions could be signal-regulated to modulate DOR levels at the PM. Direct posttranslational modification of DOR, such as phosphorylation, could modulate DOR-COPI interaction. PKA activation via adrenergic receptors dynamically modulates RXR interaction with COPI and PM localization of the SUR1/Kir6.2 channel (Arakel *et al.*, 2014). Additionally, PKC phosphorylation near the

C-terminal RXR motif of the NMDA receptor NR1 subunit decreases ER retention (Scott *et al.*, 2001). The DOR C-terminal tail contains several potential phosphorylation sites, including a known G protein-coupled receptor kinase (GRK) phosphorylation site downstream of the second RXR motif (Pei *et al.*, 1995; Gendron *et al.*, 2016). GPCR phosphorylation by GRKs typically follows agonist-induced receptor activation (Pei *et al.*, 1995), and how DOR phosphorylation at these sites may be regulated by NGF or PI3Ki remains unclear.

Signal-regulated interaction of DOR with another protein could mask the RXR motif and promote DOR export from the Golgi. RXR motifs can be masked by binding of proteins such as 14-3-3 or PDZ-interacting proteins near the RXR motif which sterically interferes with COPI binding (Yuan *et al.*, 2003; Michelsen *et al.*, 2005; Li *et al.*, 2012). DOR does not contain a PDZ ligand, but a complement of proteins that interact with its C-terminal tail have been identified, including canonical interacting proteins such as β-arrestins or G proteins (Georgoussi *et al.*, 2012). DOR can also form homodimers and heterodimers with other GPCRs, and while the C-terminal tail might play a role in this, most of this has been shown at the PM (Cvejic and Devi, 1997; Jordan and Devi, 1999; McVey *et al.*, 2001; Law *et al.*, 2005; Gendron *et al.*, 2016). Indeed, dimerization can control ER export and surface trafficking of other GPCRs (Margeta-Mitrovic *et al.*, 2000; Salahpour *et al.*, 2004; Décaillot *et al.*, 2008; Cunningham *et al.*, 2012). Proteomic approaches using proximity labeling methods, such as APEX, have identified novel GPCR interactors (Lobingier *et al.*, 2017; Paek *et al.*, 2017), and could reveal dynamic protein interactions which mediate signal-regulated DOR Golgi retention. Beyond protein interactors, the hypothesized role of phospholipid $PI(3,4)P_2$ in promoting DOR Golgi export (Shiwarski *et al.*, 2017a), raises the possibility that DOR interaction with phospholipids in the Golgi membrane could mask RXR motifs. The ability of the DOR C-terminal tail to bind phospholipids has not yet been directly tested and is an interesting direction for future study.

NGF and PI3K regulation of SSTR5 Golgi localization raises the interesting possibility that signal-regulated Golgi retention mechanisms characterized for DOR may apply broadly to other GPCRs. Though SSTR5 subcellular distribution clearly changes

in response to NGF and PI3Ki, the mechanisms that regulate this localization require further investigation. Previous work describing SSTR5 localization to the Golgi in a PDZ ligand-dependent manner suggests receptor internalization from the PM and new receptor synthesis can contribute to Golgi localization (Wente *et al.*, 2005; Bauch *et al.*, 2014). Whether SSTR5 we observe localized to the Golgi after NGF or PI3Ki is newly synthesized, like DOR (Kim and von Zastrow, 2003; Shiwarski *et al.*, 2017b), or is internalized from the PM is an important unanswered question.

The mechanisms that regulate SSTR5 Golgi localization may only partially overlap with those described for DOR. A potential C-terminal RXR motif in SSTR5 appears partially required for NGF-regulated SSTR5 Golgi localization **(Figure 2.5)**. SSTR5 contains another potential RXR motif in intracellular loop 3 which could also contribute to Golgi localization. Analysis of these additional sequence determinants and directly testing whether SSTR5 putative RXR motifs interact with COPI will further clarify the mechanism. In contrast to the role of C-terminal arginine residues in NGF-regulated Golgi localization, we observed that mutation of these residues increased PI3K-regulated Golgi retention. This difference could reflect distinct roles of NGF and PI3K signaling in regulating trafficking of different GPCRs. We used 10μM LY294002 for these experiments which is required to inhibit PI3K Class II α known to regulate DOR Golgi export (Domin *et al.*, 1997; Shiwarski *et al.*, 2017a). However, this concentration inhibits both Class I and Class II PI3Ks, and the broad effects of this inhibitor on PI3K signaling could directly or indirectly influence SSTR5 localization. Genetic approaches to specifically disrupt PI3K Class II α, which we have used to study DOR trafficking (Shiwarski *et al.*, 2017a), may help to clarify these differences. Lastly, the SSTR5 C-terminal PDZ ligand adds a layer of regulation to SSTR5 Golgi localization, independent of NGF and PI3K signaling. Whether protein interactions through the putative SSTR5 RXR motif or PDZ ligand reciprocally regulate each other to tune baseline SSTR5 localization, similar to other GPCRs interacting with PDZ domain proteins or 14-3-3 (Scott *et al.*, 2001; Yuan *et al.*, 2003; Li *et al.*, 2012), is an interesting direction for future study.

The emerging links between GPCR localization and signaling and physiology underscore the importance of understanding the mechanisms controlling GPCR localization. DOR localization to the PM is associated with enhanced pain-relieving effects (Cahill *et al.*, 2003; Pradhan *et al.*, 2013; Shiwarski *et al.*, 2017b; Abdallah and Gendron, 2018). Additionally, DOR, among a growing number of GPCRs, can be activated and signal from intracellular compartments, including the Golgi (Stoeber *et al.*, 2018; Crilly *et al.*, 2021). GPCR signaling from intracellular compartments like endosomes and the Golgi can have different consequences from signaling at the PM (Tsvetanova and von Zastrow, 2014; Bowman *et al.*, 2016; Godbole *et al.*, 2017; Nash *et al.*, 2019), and the remainder of this thesis explores how DOR activation and signaling profiles differ between PM and Golgi compartments. Although the physiological relevance of DOR signaling from the Golgi is not fully understood, interactions of the DOR RXR motif with COPI could modify spatially biased signaling. The identification of an amino acid motif and protein interaction regulating DOR PM localization provides an exciting and novel intervention point to modulate DOR localization and cell signaling.

Materials and Methods

DNA constructs and mutagenesis

The wild-type DOR construct consists of an N-terminal signal sequence Flag-tag in the pcDNA3.1 vector. All point mutants and deletion mutants were constructed using a modified QuickChange PCR protocol and confirmed via DNA sequencing. Primers for the alanine point mutants and deletion mutants were designed using the QuickChange Primer Design Tool from Agilent Technologies. Following the PCR with PfuTurbo high-fidelity polymerase (Agilent Technologies), a *Dpn*I digest was performed for 1 h, followed by bacterial transformation in *Escherichia coli* DH5α (Invitrogen). GST fusion protein plasmids were constructed from GST fused to the last 27 amino acids of DOR in the pGEX-4T1 vector. Alanine mutations were introduced into this construct via a QuickChange PCR protocol and confirmed via DNA sequencing.

Human SSTR5-Tango was a gift from Bryan Roth (Addgene plasmid #66506) (Kroeze *et al.*, 2015). SSTR5 was cloned via PCR and restriction enzyme cloning into pcDNA3.1 with an N-terminal signal sequence Flag-tag. All point mutants were created using a modified QuickChange PCR protocol and confirmed via DNA sequencing.

Human Flag-B2AR was a gift from Mark von Zastrow and cloned as described (Cao *et al.*, 1999).

Cell culture and transfection

The cell line used for experimentation was pheochromocytoma-12 (PC12; #CRL-1721) cells grown and cultured in F12K medium (Life Technologies 21127-022) supplemented with 10% horse serum and 5% fetal bovine serum (FBS) at 37°C with 5% CO_2. The medium was changed every 3 d to maintain proper cell health. Tissue culture flasks were coated with collagen IV (Sigma #C5533-5MG) to allow PC12 cells to adhere. Cells were passed at a ratio of 1:4 to ensure sufficient seeding density to facilitate growth. Cells were plated onto collagen IV–coated six-well plates and grown in 10% horse serum and 5% fetal bovine serum F12K media for 24 h before transfection. Cells were transiently transfected using the Lipofectamine 2000 lipofection reagent (Invitrogen 11668-019). DNA and Lipofectamine ratios (7.5 µl of Lipofectamine 2000 and 1.5µg of the appropriate plasmid DNA) were selected from the manufacturer's recommendations. Cells were left to incubate with the transfection mixture and Opti-MEM for 5 hours at 37°C, and the medium was then replaced. Experiments were conducted 48–72 hours following transfection.

Fixed cell immunofluorescence

PC12 cells expressing Flag-receptor mutants were plated on coverslips (Corning) coated with poly-d-lysine (Sigma, #P7280) and grown at 37°C for 48 hours. Following treatments with either NGF (100 ng/ml, BD Biosciences 356004 or Gibco #13527) or PI3K inhibition (Wortmannin, 10 µM, Enzo Life Sciences BML-ST415; LY294002, 10 µM, Tocris #1130) for 1 hour, cells were fixed in 4% paraformaldehyde, pH 7.4. The coverslips were blocked with 1 mM calcium and 1 mM magnesium–containing

phosphate-buffered saline (PBS) with 5% fetal bovine serum, 5% 1 M glycine, and 0.75% Triton X-100. For immunofluorescence imaging, cells were labeled for 1 hour in blocking buffer with anti-Flag M1 antibody (Sigma-Aldrich #F3040; 1:1000) conjugated with Alexa-647 (Molecular Probes #A20186) and anti–TGN-38 rabbit polyclonal antibody (1:1000; Sigma-Aldrich #T9826). Alexa-568 goat anti-rabbit secondary (1:1000; Sigma-Aldrich #A11011) antibody in blocking buffer was added for 1 hour to label the anti–TGN-38. Coverslips were again washed in calcium-magnesium PBS and mounted on glass slides using Prolong Diamond Reagent (Molecular Probes #P36962).

Cells were imaged using an Andor confocal imaging system (XDi spinning disk, Andor) at 60× magnification (Nikon CFI APO TIRF) on a Nikon TE-2000 inverted microscope with a mechanical Piezo XYZ-stage (Nikon), iXon 897 Ultra cameras (Andor), a laser combiner (Andor) containing 405-, 488-, 515-, 568-, and 647-nm excitation capabilities, IQ2 imaging software (Andor), and an isolation table (TMC).

Image analysis and quantification

All imaging analysis and data were quantified using ImageJ/Fiji (National Institutes of Health, Bethesda, MD) (Schindelin *et al.*, 2012; Rueden *et al.*, 2017). Custom macros using Golgi staining as a mask were written to allow unbiased measurements for the total receptor fluorescence for each cell and the fluorescence intensity of receptor within the Golgi for fixed cell analysis (Shiwarski *et al.*, 2017b). Briefly, the region defined by TGN-38 staining was used to define the Golgi area of the cell. Receptor fluorescence within this Golgi region is measured as a percentage of total receptor fluorescence in the whole cell. This ratio was calculated for each cell and then averaged across all cells. Further, the percentage of cells that visually displayed receptor localized to the Golgi was manually determined by binary quantification (1 = retention, 0 = no retention). The binary quantification results were averaged to determine the population percentage of cells with receptor localized to the Golgi. A more detailed procedure and a quantification example can be found in a previous publication (Shiwarski *et al.*, 2017b).

Immunoprecipitation, immunoblotting, and densitometry

PC12 cells were grown in 10-cm plates and transfected as described above using 5 μg Flag-DOR WT or Flag-DOR 2AXA DNA and 37.5 μl Lipofectamine 2000 per plate. Two days after transfection, plates were washed with PBS before crosslinking with 0.5 mM dithiobis succinimidyl propionate (DSP) for 2 hours at 4°C. DSP was quenched with 20 mM Tris, pH 7.4. Cells were scraped from the plate and incubated in lysis buffer (0.5% Triton X-100, 10 mM HEPES, 150 mM NaCl, 1 mM egtazic acid (EGTA), 0.1 mM MgCl2, pH 7.4, with 1 mM PMSF and Pierce protease inhibitor tab EDTA-free) on ice for 30 min with intermittent vortexing. Lysate was then spun at 13,200 × *g* for 15 min. A Pierce BCA Assay kit was used for protein estimation. Sheep anti-mouse immunoglobulin G dynabeads (30 μl, Invitrogen #1120) were prepared for immunoprecipitation by incubating them for 2 hours at room temperature with 1 μg mouse anti-Flag M2 antibody (Sigma, F1804). Prepared beads were rotated with 0.5–1.0 μg/μl PC12 cell lysate, fixed across conditions for each experiment, overnight at 4°C. The next day, beads were washed six times in a solution of 0.1% Triton, 10 mM HEPES, 150 mM NaCl, 1 mM EGTA, 0.1 mM MgCl2, pH 7.4. Elution was carried out in 20 μl lysis buffer with 1 mg/ml Flag peptide for 2 hours with gentle agitation at 4°C.

Samples were prepared for SDS–PAGE with reducing sample buffer (RSB) containing fresh 10% β-mercaptoethanol (BME), and 1 μl 1 M dithiothreitol (DTT) was added to each sample before it was heated at 75°C for 5 min. Proteins were transferred to a nitrocellulose membrane overnight at 4°C. Blots were blocked in 5% milk-TBST solution. Membranes were blotted with mouse anti–β-COP (1:200 overnight at 4°C, Santa Cruz, sc-393615) and rabbit anti-Flag (1:1000 1 hour room temperature, Bethyl Laboratories A190-101A) primary antibodies and goat anti-mouse or rabbit HRP secondary (1:1000 1 hour room temperature, BioRad #1706516 or #1706515). Blots were developed with Clarity Western ECL Substrate (BioRad #1705061) and imaged using the ChemiDoc Touch imager (BioRad) and iBrightFL1000 (ThermoFisher). Between immunoblotting for β-COP and Flag, blots were stripped for 30 min at room temperature and reblocked in 5% milk-TBST for 1 hour.

ImageLab software (BioRad) was used for densitometry. For β-COP, densitometry was performed on the band migrating at 110 kDa. β-COP levels were normalized to densitometric measurements of Flag-DOR WT or 2AXA, which was quantified as the volume between 70 and 250 kDa. Values were plotted using GraphPad Prism 9 software.

For whole cell receptor expression blots, PC12 cells were transfected with Flag-DOR WT or 2AXA. Three days after transfection, cells were left untreated (Ctrl) or treated with NGF (100 ng/mL), LY (10 μM), Wortmannin (10 μM), or 1uL DMSO for 1 hour. 50-60% confluent 6 wells were lysed in 75 μL 2x Laemmli sample buffer (2% SDS) and sonicated. 100 mM DTT was added to samples which were then heated at 37°C for 1 hour. Samples were then spun down at 20,000 x *g* for 5 min. 50 μL of each sample was loaded on a 4-20% SDS PAGE gel. Proteins were transferred overnight to nitrocellulose then blotted with Bethyl anti-Flag primary (1:1000, Bethyl Laboratories A190-101A) and goat anti-Rabbit HRP secondary (1:3000, BioRad #1706515), then developed with SuperSignal Femto substrate (ThermoFisher #34094). Blots were imaged on the iBrightFL1000 (ThermoFisher).

Recombinant protein purification

GST fusion proteins were produced in *E. coli* BL21 cells transformed with the appropriate pGEX-4T-1 plasmids containing GST fusion constructs. Cells were grown to A_{600} between 0.6 and 0.8 and then induced with 1 mM isopropyl β-d-1-thiogalactopyranoside for 3–4 hours at 30°C. Cells were spun down and pellets were washed with 150 mM NaCl before lysis in a buffer containing 50 mM Tris, 5 mM EDTA, 150 mM NaCl, 10% glycerol, 5 mM DTT, Pierce protease inhibitor tab, and 1 mM PMSF. Triton X-100 was added to cells in lysis buffer at a final concentration of 1%, and the lysate was incubated on ice for 30 min. The lysate was spun at 5200 × *g* for 30 min, followed by ultracentrifugation of the supernatant at 257,000 × *g* for 1 hour. Pierce glutathione agarose beads were equilibrated with PBS and 1 mM DTT, and lysate was incubated with beads for 2 hours at 4°C. Beads were washed once in wash buffer containing PBS, 1 mM DTT, and 0.1% Tween, followed by a wash in wash buffer with

300 mM NaCl, before a final wash in PBS + 1 mM DTT + 150 mM NaCl. GST fusion proteins were then eluted from the beads in 50 mM Tris, pH 8.0, 150 mM NaCl, 1 mM DTT, and 25 mM glutathione and dialyzed overnight against TBS to remove free glutathione.

GST pull down

GST fusion proteins were bound to glutathione magnetic agarose (Pierce #78601) as recommended by the manufacturer. Beads were washed three times with wash buffer of 1:1 TBS:lysis buffer (10 mM Tris-HCl, 50 mM NaCl, 1 mM EDTA, 10% glycerol, 0.5% Triton X-100, 2 mM DTT, and EDTA-free Pierce protease inhibitor, pH 7.4). GST fusion protein (150 µg) was incubated with beads with rotation for 2 hours at 4°C. Beads were washed five times, and then 150 µg PC12 cell lysate prepared using lysis buffer was added, and the beads were incubated an additional 2 hours at 4°C with rotation. Beads were washed five times with lysis buffer and then resuspended in RSB and heated for 5 min at 95°C to elute proteins. Samples were then analyzed by SDS–PAGE and immunoblotting with mouse anti–β-COP (1:200 overnight at 4°C, Santa Cruz, sc-393615) and mouse anti-ε-COP (1:200 overnight at 4°C, Santa Cruz, sc-133194).

Statistics and data analysis

Statistical and graphical analyses were performed using GraphPad Prism 9 software. Statistical tests were chosen based on the experimental sample size, distribution, and conditions. For statistical analysis of the fixed-cell immunofluorescence imaging data, two-tailed chi-square tests, one-way analysis of variance (ANOVA), and two-sided Student's *t* test were used as appropriate. Multiple comparisons were corrected by the Bonferroni method. A p value of <0.05 was considered statistically significant. The figures and visuals were assembled in Adobe Illustrator version 26.0.1.

Acknowledgements

We thank Marlena Darr and Drs. Zara Weinberg, Shanna Bowersox, and Cary Shiwarski for technical help and comments on the published manuscript. We thank Drs. Nathan Urban, Adam Linstedt, Tina Lee, Peter Friedman, Guillermo Romero, Jean-Pierre Vilardaga, and Alessandro Bisello for reagents, comments, and suggestions on the published manuscript. SEC thanks Dr. Aditya Kumar for helpful comments and feedback on this chapter. MAP was supported by National Institutes of Health DA036086 and GM117425. SEC was supported by a National Science Foundation Graduate Research Fellowship under Grant DGE 1256260.

Supplementary Figures

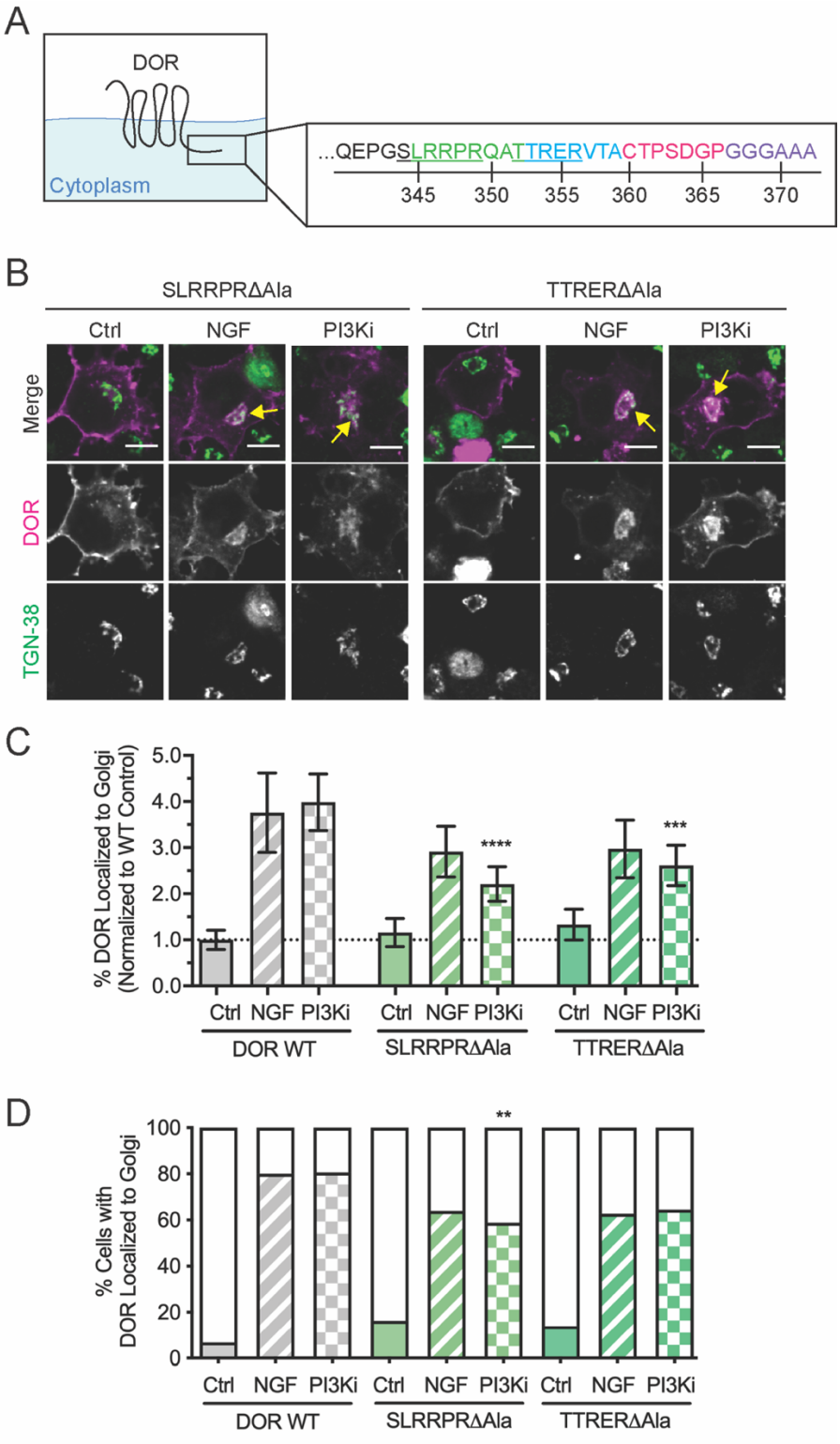

Figure 2.S1. Alanine mutations of single RXR motifs within the C-terminal tail of DOR partially reduce DOR Golgi retention induced by NGF treatment and PI3K inhibition.

(A) SLRRPR or TTRER residues (underlined) which span the Δ345–352 and Δ353–359 deletion regions were substituted with alanine to generate the DOR SLRRPRΔAla and TTRERΔAla mutants. **(B)** PC12 cells expressing Flag-tagged DOR WT, SLRRPRΔAla, or TTRERΔAla were left untreated (Ctrl) or treated with 100 ng/mL NGF or PI3K inhibitor (PI3Ki) (LY, 10 μM) for 1 hour, then fixed and stained for Flag (magenta in merge) and TGN-38 (green in merge) (scale bars=5 μm). DOR WT and mutants localize primarily to the plasma membrane in Ctrl cells and colocalize with TGN-38 (white in merge, yellow arrows) following NGF or PI3Ki treatment. **(C)** The percentage of DOR fluorescence within the region defined by TGN-38 staining, normalized to the mean of DOR WT expressing Ctrl cells, was quantified and compared between DOR WT and alanine scanning mutants within each treatment condition (Bars indicate mean ± 95% CI.; Among NGF-treated cells, significance from one-way ANOVA ($p=0.1610$) with Dunnett's multiple comparisons test of DOR WT NGF vs mutants NGF indicated in the figure: WT NGF vs SLRRPRΔAla NGF, $p=0.1225$; WT NGF vs TTRERΔAla NGF, $p=0.2317$; Among PI3Ki-treated cells, significance from one-way ANOVA ($p<0.0001$) with Dunnett's multiple comparisons test of DOR WT PI3Ki vs mutants PI3Ki indicated in the figure: WT PI3Ki vs SLRRPRΔAla PI3Ki, $p<0.0001$; WT PI3Ki vs TTRERΔAla PI3Ki, $p=0.0002$). **(D)** Percentage of cells with DOR localized to the Golgi after treatment with NGF or PI3Ki was quantified and compared between DOR WT and deletion mutants for each treatment condition (significance from two-tailed Chi-square test of DOR WT NGF or PI3Ki versus deletion mutant NGF or PI3Ki indicated in the figure with Bonferroni correction for multiple comparisons: WT NGF vs SLRRPRΔAla NGF, $p=0.1598$; WT NGF vs TTRERΔAla NGF, $p=0.1740$; WT PI3Ki vs SLRRPRΔAla PI3Ki, $p=0.0082$; WT PI3Ki vs TTRERΔAla PI3Ki, $p=0.0536$). (For **C** and **D**, DOR WT, Ctrl=58 cells, NGF=56; PI3Ki=67; SLRRPRΔAla, Ctrl=49; NGF=91; PI3Ki=85; TTRERΔAla, NT=43; NGF=51; PI3Ki=90, across a minimum of two biological replicates).

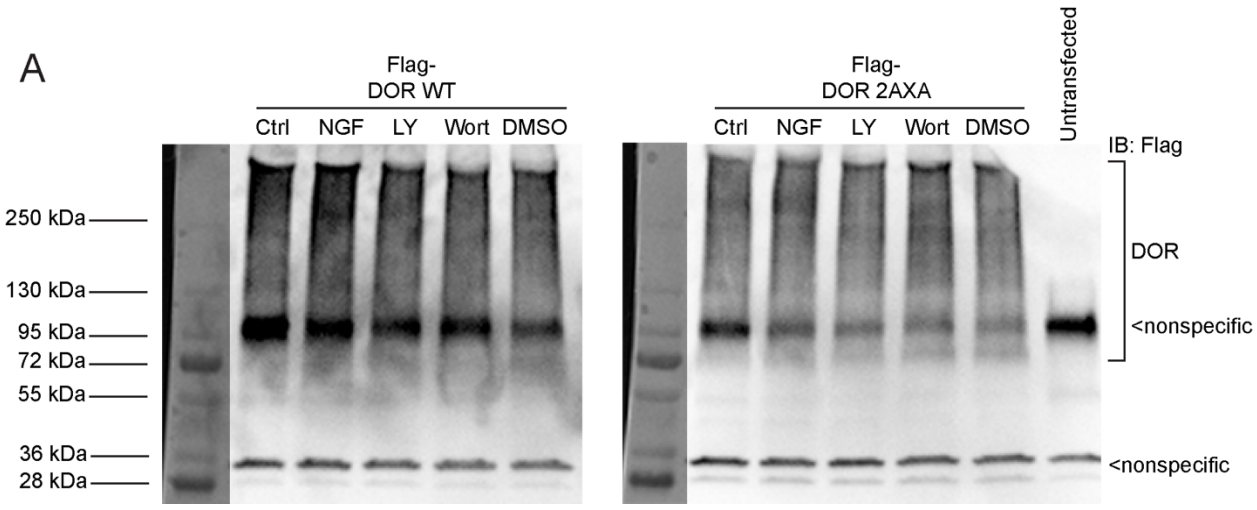

Figure 2.S2. DOR WT and 2AXA total receptor levels are not altered by NGF or PI3Ki treatment.

(A) Immunoblot of total receptor levels from PC12 cells expressing either DOR WT or DOR 2AXA. Total receptor levels are similar across untreated cells (Ctrl) and cells treated with NGF (100ng/mL), PI3Ki (10 μM Wort or 10 μM LY), or DMSO vehicle control for 1 hour.

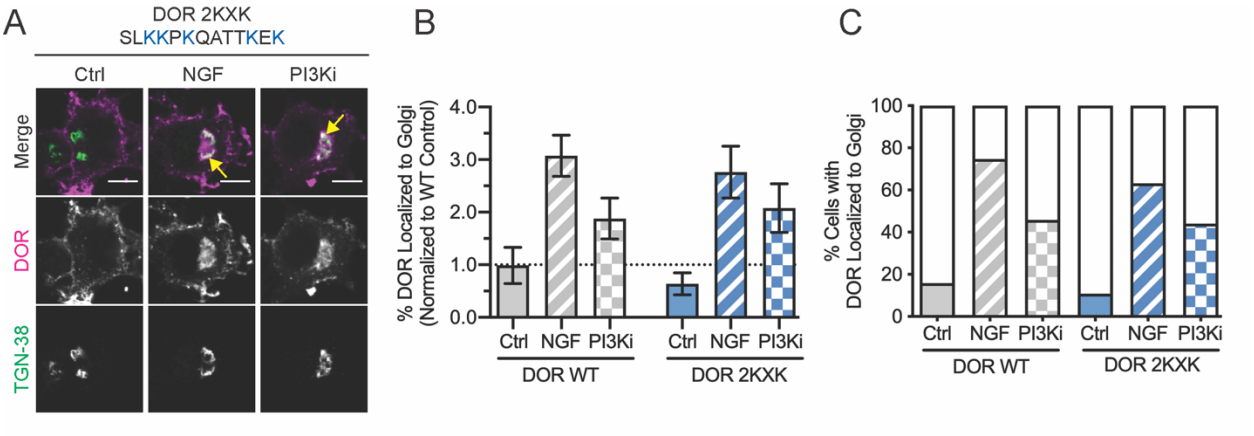

Figure 2.S3. Positive charge preserves function of C-terminal RXR motifs which regulate DOR Golgi retention by NGF treatment and PI3K inhibition.
(A) PC12 cells expressing Flag-tagged DOR 2KXK, in which the five C-terminal arginine residues described in Fig. 2 were mutated to lysine (blue), were left untreated (Ctrl) or treated with 100ng/mL NGF or PI3Ki (10μM LY) for 1 hour, then fixed and stained for Flag (magenta in merge) and TGN-38 (green in merge) (scale bars=5 μm). DOR 2KXK localizes primarily to the plasma membrane in Ctrl cells. DOR 2KXK colocalizes with TGN-38 (white in merge, yellow arrow) following NGF or PI3Ki treatment. **(B)** The percentage of DOR fluorescence within the region defined by TGN-38 staining, normalized to the mean of DOR WT expressing Ctrl cells, increased similarly for both DOR WT and DOR 2KXK following NGF or PI3Ki treatment (Bars indicate mean ± 95% CI; one-tailed Student's t-test of WT NGF vs 2KXK NGF, p=0.1627, or WT PI3Ki vs 2KXK PI3Ki, p=0.2547). **(C)** The percentage of cells with DOR localized to the Golgi increased similarly for cells expressing DOR WT or DOR 2KXK following NGF or PI3Ki treatment (significance from two-tailed Chi-square tests of WT NGF vs 2KXK NGF, p=0.1208 or WT PI3Ki vs 2KXK PI3Ki, p=0.8112). (For **B** and **C**, DOR WT, Ctrl=83 cells, NGF=80, PI3Ki=86; DOR 2KXK, Ctrl=74, NGF=76, PI3Ki=75, across two biological replicates)

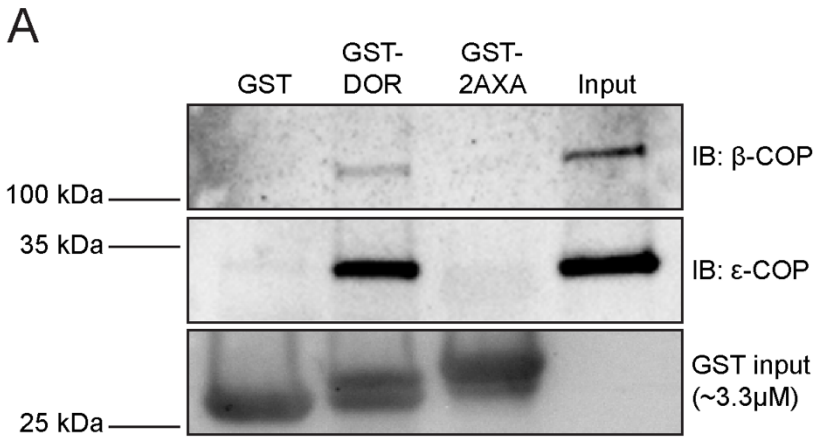

Figure 2.S4. Co-purification of β-COP and ε-COP with GST-DOR tail requires RXR motifs.

(A) PC12 cell lysate was incubated with 50 μg (~3.3 μM) GST fusion proteins bound to glutathione agarose beads, followed by immunoblotting (IB) for β-COP (110 kDa band) or ε-COP (34-kDa band). β-COP or ε-COP signal are visible in lanes in which wild-type DOR tail (GST-DOR) was used for the pull down and in the input lane containing 10 μg of whole cell lysate. No β-COP or ε-COP signal above background was detected for GST and GST-2AXA lanes. A Ponceau-S staining for the respective GST proteins is shown in the bottom panel.

References

Abdallah, K, and Gendron, L (2018). The delta opioid receptor in pain control. In: Handbook of Experimental Pharmacology, Springer New York LLC, 147–177.

Aloe, L, Rocco, ML, Bianchi, P, and Manni, L (2012). Nerve growth factor: From the early discoveries to the potential clinical use. J Transl Med 10.

Arakel, EC et al. (2014). Tuning the electrical properties of the heart by differential trafficking of KATP ion channel complexes. J Cell Sci 127, 2106–2119.

Bao, L et al. (2003). Activation of delta opioid receptors induces receptor insertion and neuropeptide secretion. Neuron 37, 121–133.

Bauch, C, Koliwer, J, Buck, F, and Ho, H (2014). Subcellular Sorting of the G-Protein Coupled Mouse Somatostatin Receptor 5 by a Network of PDZ-Domain Containing Proteins. 9, 1–10.

Bie, B, Zhang, Z, Cai, YQ, Zhu, W, Zhang, Y, Dai, J, Lowenstein, CJ, Weinman, EJ, and Pan, ZZ (2010). Nerve Growth Factor-Regulated Emergence of Functional -Opioid Receptors. J Neurosci 30, 5617–5628.

Böhm, SK, Khitin, LM, Grady, EF, Aponte, G, Payan, DG, and Bunnett, NW (1996). Mechanisms of desensitization and resensitization of proteinase- activated receptor-2. J Biol Chem 271, 22003–22016.

Bowman, SL, and Puthenveedu, MA (2015). Postendocytic Sorting of Adrenergic and Opioid Receptors: New Mechanisms and Functions. Prog Mol Biol Transl Sci 132, 189–206.

Bowman, SL, Shiwarski, DJ, and Puthenveedu, MA (2016). Distinct G protein-coupled receptor recycling pathways allow spatial control of downstream G protein signaling. J Cell Biol 214, 797–806.

Bowman, SL, Soohoo, AL, Shiwarski, DJ, Schulz, S, Pradhan, AA, and Puthenveedu, MA (2015). Cell-autonomous regulation of Mu-opioid receptor recycling by substance P. Cell Rep 10, 1925–1936.

Brock, C, Boudier, L, Maurel, D, Blahos, J, and Pin, J-P (2005). Assembly-dependent surface targeting of the heterodimeric GABAB Receptor is controlled by COPI but not 14-3-3. Mol Biol Cell 16, 5572–5578.

Bruno, JF, Xu, Y, Song, J, and Berelowitz, M (1993). Tissue distribution of somatostatin receptor subtype messenger ribonucleic acid in the rat. Endocrinology 133, 2561–2567.

Cahill, CM, McClellan, KA, Morinville, A, Hoffert, C, Hubatsch, D, O'Donnell, D, and

Beaudet, A (2001a). Immunohistochemical distribution of delta opioid receptors in the rat central nervous system: Evidence for somatodendritic labeling and antigen-specific cellular compartmentalization. J Comp Neurol 440, 65–84.

Cahill, CM, Morinville, A, Hoffert, C, O'Donnell, D, and Beaudet, A (2003). Up-regulation and trafficking of delta opioid receptor in a model of chronic inflammation: implications for pain control. Pain 101, 199–208.

Cahill, CM, Morinville, A, Lee, MC, Vincent, JP, Collier, B, and Beaudet, A (2001b). Prolonged morphine treatment targets delta opioid receptors to neuronal plasma membranes and enhances delta-mediated antinociception. J Neurosci 21, 7598–7607.

Cao, TT, Deacon, HW, Reczek, D, Bretscher, A, and Von Zastrow, M (1999). A kinase-regulated PDZ-domain interaction controls endocytic sorting of the β2-adrenergic receptor. Nature 401, 286–290.

Crilly, SE, Ko, W, Weinberg, ZY, and Puthenveedu, MA (2021). Conformational specificity of opioid receptors is determined by subcellular location irrespective of agonist. Elife 10.

Crilly, SE, and Puthenveedu, MA (2020). Compartmentalized GPCR Signaling from Intracellular Membranes. J Membr Biol, 1–13.

Cunningham, MR, McIntosh, KA, Pediani, JD, Robben, J, Cooke, AE, Nilsson, M, Gould, GW, Mundell, S, Milligan, G, and Plevin, R (2012). Novel role for proteinase-activated receptor 2 (PAR2) in membrane trafficking of proteinase-activated receptor 4 (PAR4). J Biol Chem 287, 16656–16669.

Cvejic, S, and Devi, LA (1997). Dimerization of the delta opioid receptor: implication for a role in receptor internalization. J Biol Chem 272, 26959–26964.

Décaillot, FM, Rozenfeld, R, Gupta, A, and Devi, LA (2008). Cell surface targeting of mu-delta opioid receptor heterodimers by RTP4. Proc Natl Acad Sci U S A 105, 16045–16050.

Domin, J, Pages, F, Volinia, S, Rittenhouse, SE, Zvelebil, MJ, Stein, RC, and Waterfield, MD (1997). Cloning of a human phosphoinositide 3-kinase with a C2 domain that displays reduced sensitivity to the inhibitor wortmannin. Biochem J 326, 139–147.

Dong, C, Filipeanu, CM, Duvernay, MT, and Wu, G (2007). Regulation of G protein-coupled receptor export trafficking. Biochim Biophys Acta 1768, 853–870.

Eugster, A, Frigerio, G, Dale, M, and Duden, R (2004). The α- and β′-COP WD40 Domains Mediate Cargo-selective Interactions with Distinct Di-lysine Motifs. Mol Biol Cell 15, 1011–1023.

Filipeanu, CM, Pullikuth, AK, and Guidry, JJ (2015). Molecular Determinants of the Human a 2C -Adrenergic Receptor Temperature-Sensitive Intracellular Traffic s. Mol Pharmacol Mol Pharmacol 87, 792–802.

Gendron, L, Cahill, CM, Zastrow, M Von, Schiller, PW, and Pineyro, G (2016). Molecular Pharmacology of d -Opioid Receptors. 68, 631–700.

Georgoussi, Z, Georganta, E-M, and Milligan, G (2012). The Other Side of Opioid Receptor Signalling: Regulation by Protein-Protein Interaction. Curr Drug Targets 13, 80–102.

Gilbert, CE, Zuckerman, DM, Currier, PL, and Machamer, CE (2014). Three basic residues of intracellular loop 3 of the beta-1 adrenergic receptor are required for golgin-160-dependent trafficking. Int J Mol Sci 15, 2929–2945.

Glick, BS, and Luini, A (2011). Models for Golgi traffic: A critical assessment. Cold Spring Harb Perspect Biol 3.

Godbole, A, Lyga, S, Lohse, MJ, and Calebiro, D (2017). Internalized TSH receptors en route to the TGN induce local Gs-protein signaling and gene transcription. Nat Commun 8, 443.

Hermosilla, R, Oueslati, M, Donalies, U, Schönenberger, E, Krause, E, Oksche, A, Rosenthal, W, and Schülein, R (2004). Disease-causing V2 Vasopressin Receptors are Retained in Different Compartments of the Early Secretory Pathway. Traffic 5, 993–1005.

Jackson, LP, Lewis, M, Kent, HM, Edeling, MA, Evans, PR, Duden, R, and Owen, DJ (2012). Molecular Basis for Recognition of Dilysine Trafficking Motifs by COPI. Dev Cell 23, 1255–1262.

Jensen, DD et al. (2017). Neurokinin 1 receptor signaling in endosomes mediates sustained nociception and is a viable therapeutic target for prolonged pain relief. Sci Transl Med 9.

Jordan, BA, and Devi, LA (1999). G-protein-coupled receptor heterodimerization modulates receptor function. Nature 399, 697–700.

Kim, K, and von Zastrow, M (2003). Neurotrophin-regulated sorting of opioid receptors in the biosynthetic pathway of neurosecretory cells. J Neurosci 23, 2075–2085.

Kroeze, WK, Sassano, MF, Huang, XP, Lansu, K, McCorvy, JD, Giguère, PM, Sciaky, N, and Roth, BL (2015). PRESTO-Tango as an open-source resource for interrogation of the druggable human GPCRome. Nat Struct Mol Biol 22, 362–369.

Kunselman, JM, Lott, J, and Puthenveedu, MA (2021). Mechanisms of selective G

protein–coupled receptor localization and trafficking. Curr Opin Cell Biol 71, 158–165.

Kunselman, JM, Zajac, AS, Weinberg, ZY, and Puthenveedu, MA (2019). Homologous regulation of mu opioid receptor recycling by Gβγ, protein kinase C, and receptor phosphorylation. Mol Pharmacol 96, 702–710.

Law, P-Y, Erickson-Herbrandson, LJ, Zha, QQ, Solberg, J, Chu, J, Sarre, A, and Loh, HH (2005). Heterodimerization of - and -Opioid Receptors Occurs at the Cell Surface Only and Requires Receptor-G Protein Interactions. J Biol Chem 280, 11152–11164.

Li, JG, Chen, C, Huang, P, Wang, Y, and Liu-Chen, LY (2012). 14-3-3ζ Protein regulates anterograde transport of the human κ-opioid receptor (hKOPR). J Biol Chem 287, 37778–37792.

Lobingier, BT, Hüttenhain, R, Eichel, K, Miller, KB, Ting, AY, von Zastrow, M, and Krogan, NJ (2017). An Approach to Spatiotemporally Resolve Protein Interaction Networks in Living Cells. Cell 169, 350-360.e12.

Ma, D, Zerangue, N, Lin, YF, Collins, A, Yu, M, Jan, YN, and Jan, LY (2001). Role of ER export signals in controlling surface potassium channel numbers. Science (80-) 291, 316–319.

Ma, W, and Goldberg, J (2013). Rules for the recognition of dilysine retrieval motifs by coatomer. EMBO J 32, 926–937.

Marchese, A, Paing, MM, Temple, BRS, and Trejo, J (2008). G protein-coupled receptor sorting to endosomes and lysosomes. Annu Rev Pharmacol Toxicol 48, 601–629.

Margeta-Mitrovic, M, Jan, YN, and Jan, LY (2000). A trafficking checkpoint controls GABA(B) receptor heterodimerization. Neuron 27, 97–106.

McVey, M, Ramsay, D, Kellett, E, Rees, S, Wilson, S, Pope, AJ, and Milligan, G (2001). Monitoring receptor oligomerization using time-resolved fluorescence resonance energy transfer and bioluminescence resonance energy transfer. The human delta -opioid receptor displays constitutive oligomerization at the cell surface, which is not regulate. J Biol Chem 276, 14092–14099.

Michelsen, K, Schmid, V, Metz, J, Heusser, K, Liebel, U, Schwede, T, Spang, A, and Schwappach, B (2007). Novel cargo-binding site in the β and δ subunits of coatomer. J Cell Biol.

Michelsen, K, Yuan, H, and Schwappach, B (2005). Hide and run. EMBO Rep 6, 717–722.

Mittal, N et al. (2013). Select G-protein coupled receptors modulate agonist-induced signaling via a ROCK, LIMK and β-arrestin 1 pathway. Cell Rep 5.

Nash, CA, Wei, W, Irannejad, R, and Smrcka, A V. (2019). Golgi localized βi-adrenergic receptors stimulate golgi PI4P hydrolysis by PLCε to regulate cardiac hypertrophy. Elife 8.

Paek, J, Kalocsay, M, Staus, DP, Wingler, L, Pascolutti, R, Paulo, JA, Gygi, SP, and Kruse, AC (2017). Multidimensional Tracking of GPCR Signaling via Peroxidase-Catalyzed Proximity Labeling. Cell 169, 338-349.e11.

Patwardhan, AM, Berg, KA, Akopain, AN, Jeske, NA, Gamper, N, Clarke, WP, and Hargreaves, KM (2005). Bradykinin-Induced Functional Competence and Trafficking of the ʕ -Opioid Receptor in Trigeminal Nociceptors. 25, 8825–8832.

Pei, G, Kieffer, BL, Lefkowitz, RJ, and Freedman, NJ (1995). Agonist-dependent phosphorylation of the mouse delta-opioid receptor: involvement of G protein-coupled receptor kinases but not protein kinase C. Mol Pharmacol 48.

Pettinger, L, Gigout, S, Linley, JE, and Gamper, N (2013). Bradykinin Controls Pool Size of Sensory Neurons Expressing Functional ʕ -Opioid Receptors. 33, 10762–10771.

Pradhan, A, Smith, M, McGuire, B, Evans, C, and Walwyn, W (2013). Chronic inflammatory injury results in increased coupling of delta opioid receptors to voltage-gated Ca2+ channels. Mol Pain 9, 8.

Puthenveedu, MA, and von Zastrow, M (2006). Cargo Regulates Clathrin-Coated Pit Dynamics. Cell 127, 113–124.

Ramírez, JL, Mouchantaf, R, Kumar, U, Otero Corchon, V, Rubinstein, M, Low, MJ, and Patel, YC (2002). Brain Somatostatin Receptors Are Up-Regulated In Somatostatin-Deficient Mice. Mol Endocrinol 16, 1951–1963.

Roth, BL, Laskowski, MB, and Coscia, CJ (1981). Evidence for distinct subcellular sites of opiate receptors. Demonstration of opiate receptors in smooth microsomal fractions isolated from rat brain. J Biol Chem 256, 10117–10123.

Rueden, CT, Schindelin, J, Hiner, MC, DeZonia, BE, Walter, AE, Arena, ET, and Eliceiri, KW (2017). ImageJ2: ImageJ for the next generation of scientific image data. BMC Bioinformatics 18, 529.

Salahpour, A, Angers, S, Mercier, JF, Lagacé, M, Marullo, S, and Bouvier, M (2004). Homodimerization of the β2-adrenergic receptor as a prerequisite for cell surface targeting. J Biol Chem 279, 33390–33397.

Sarret, P, Esdaile, MJ, McPherson, PS, Schonbrunn, A, Kreienkamp, HJ, and Beaudet, A (2004). Role of Amphiphysin II in Somatostatin Receptor Trafficking in Neuroendocrine Cells. J Biol Chem 279, 8029–8037.

Schindelin, J et al. (2012). Fiji: An open-source platform for biological-image analysis. Nat Methods 9, 676–682.

Scott, DB, Blanpied, TA, Swanson, GT, Zhang, C, and Ehlers, MD (2001). An NMDA receptor ER retention signal regulated by phosphorylation and alternative splicing. J Neurosci 21, 3063–3072.

Shiwarski, DJ, Darr, M, Telmer, CA, Bruchez, MP, and Puthenveedu, MA (2017a). PI3K class II α regulates δ-opioid receptor export from the trans-Golgi network. Mol Biol Cell 28, 2202–2219.

Shiwarski, DJ, Tipton, A, Giraldo, MD, Schmidt, BF, Gold, MS, Pradhan, AA, and Puthenveedu, MA (2017b). A PTEN-regulated checkpoint controls surface delivery of σ opioid receptors. J Neurosci 37, 3741–3752.

Sorkin, A, and Von Zastrow, M (2002). Signal transduction and endocytosis: Close encounters of many kinds. Nat Rev Mol Cell Biol 3, 600–614.

St-Louis, É, Degrandmaison, J, Grastilleur, S, Génier, S, Blais, V, Lavoie, C, Parent, J-L, and Gendron, L (2017). Involvement of the coatomer protein complex I in the intracellular traffic of the delta opioid receptor. Mol Cell Neurosci 79, 53–63.

Stoeber, M, Jullié, D, Lobingier, BT, Schiller, PW, Manglik, A, Von, M, and Correspondence, Z (2018). A Genetically Encoded Biosensor Reveals Location Bias of Opioid Drug Action. Neuron 98, 963-976.e5.

Stroh, T, Kreienkamp, HJ, and Beaudet, A (1999). Immunohistochemical distribution of the somatostatin receptor subtype 5 in the adult rat brain: Predominant expression in the basal forebrain. J Comp Neurol 412, 69–82.

Tsao, PI, and Von Zastrow, M (2000). Type-specific sorting of G protein-coupled receptors after endocytosis. J Biol Chem 275, 11130–11140.

Tsvetanova, NG, and von Zastrow, M (2014). Spatial encoding of cyclic AMP signaling specificity by GPCR endocytosis. Nat Chem Biol 10, 1061–1065.

Wang, H, and Pickel, VM (2001). Preferential cytoplasmic localization of delta-opioid receptors in rat striatal patches: comparison with plasmalemmal mu-opioid receptors. J Neurosci 21, 3242–3250.

Weinberg, ZY, Zajac, AS, Phan, T, Shiwarski, DJ, and Puthenveedu, MA (2017). Sequence-Specific Regulation of Endocytic Lifetimes Modulates Arrestin-Mediated Signaling at the μ Opioid Receptor. Mol Pharmacol 91, 416–427.

Wente, W, Stroh, T, Beaudet, A, and Richter, D (2005). Interactions with PDZ Domain Proteins PIST / GOPC and PDZK1 Regulate Intracellular Sorting of the Somatostatin

Receptor Subtype 5 *. 280, 32419–32425.

Whistler, JL, Enquist, J, Marley, A, Fong, J, Gladher, F, Tsuruda, P, Murray, SR, and Von Zastrow, M (2002). Modulation of postendocytic sorting of G protein-coupled receptors. Science 297, 615–620.

Yuan, H, Michelsen, K, and Schwappach, B (2003). 14-3-3 Dimers Probe the Assembly Status of Multimeric Membrane Proteins. Curr Biol 13, 638–646.

Von Zastrow, M, and Kobilka, BK (1992). Ligand-regulated internalization and recycling of human β2-adrenergic receptors between the plasma membrane and endosomes containing transferrin receptors. J Biol Chem 267, 3530–3538.

Zerangue, N, Malan, MJ, Fried, SR, Dazin, PF, Jan, YN, Jan, LY, and Schwappach, B (2001). Analysis of endoplasmic reticulum trafficking signals by combinatorial screening in mammalian cells. Proc Natl Acad Sci U S A 98, 2431–2436.

Zerangue, N, Schwappach, B, Jan, YN, Jan, LY, Isaac, JTR, and Roche, KW (1999). A new ER trafficking signal regulates the subunit stoichiometry of plasma membrane K(ATP) channels. Neuron 22, 537–548.

Zhang, M, Davis, JE, Li, C, Gao, J, Huang, W, Lambert, NA, Terry, A V., and Wu, G (2016). GGA3 Interacts with a G Protein-Coupled Receptor and Modulates Its Cell Surface Export. Mol Cell Biol 36, 1152–1163.

Zhang, X, Dong, C, Wu, QJ, Balch, WE, and Wu, G (2011). Di-acidic motifs in the membrane-distal C termini modulate the transport of angiotensin II receptors from the endoplasmic reticulum to the cell surface. J Biol Chem 286, 20525–20535.

Zhu, S, Zhang, M, Davis, JE, Wu, WH, Surrao, K, Wang, H, and Wu, G (2015). A single mutation in helix 8 enhances the angiotensin II type 1a receptor transport and signaling. Cell Signal 27, 2371–2379.

Chapter 3: Conformational Specificity of the Delta Opioid Receptor Is Determined by Subcellular Location Irrespective of Agonist

This chapter was published as and adapted from[3]:

Crilly, SE, Ko, W, Weinberg, ZY, and Puthenveedu, MA (2021). Conformational specificity of opioid receptors is determined by subcellular location irrespective of agonist. Elife 10: e67478.

Abstract

The prevailing model for the variety in drug responses is that they stabilize distinct active states of their G protein-coupled receptor (GPCR) targets, allowing coupling to different effectors. However, whether the same ligand can produce different GPCR active states based on the environment of receptors in cells is a fundamental unanswered question. Here we address this question using live cell imaging of conformational biosensors that read out distinct active conformations of the delta opioid receptor (DOR), a physiologically relevant GPCR localized to the Golgi and plasma membrane in neurons. We show that, although Golgi and plasma membrane pools of DOR regulated cAMP, the two pools differentially engaged conformational biosensors in response to the same ligand. Further, DOR recruited arrestin on the plasma membrane but not the Golgi. Our results suggest that the same agonist could drive different conformations of a GPCR at different locations, allowing receptor coupling to distinct effectors at different locations.

[3] Statement of others' contributions to this work:
I performed all live cell biosensor, arrestin, and FRET sensor imaging and analysis. Wooree Ko and I performed fixed cell imaging experiments and analysis. Zara Weinberg contributed to assay design and data analysis methods. I wrote the published manuscript along with Manoj Puthenveedu and input from Wooree Ko and Zara Weinberg. I adapted the published manuscript for this chapter.

Introduction

A given GPCR can generate a diverse array of signaling responses, underscoring the physiological and clinical relevance of this class of proteins. Endogenous and synthetic ligands which “bias” the responses of a given receptor towards one response or another are a key aspect of this signaling diversity (Wootten *et al.*, 2018). This diversity in responses provides several opportunities to target specific GPCR signaling responses to reduce potential adverse effects while managing a variety of clinical conditions. However, using bias to precisely tune GPCR signaling has been difficult, suggesting that we are missing some key piece in our understanding. Understanding the cellular mechanisms that contribute to individual components of the integrated signaling response is therefore of profound importance to understanding GPCR pharmacology.

The specific conformations adopted by GPCRs, which preferentially allow coupling to distinct effectors, is likely a key determinant of which specific downstream signaling response is amplified (Okude *et al.*, 2015; Latorraca *et al.*, 2017; Wingler *et al.*, 2019; Suomivuori *et al.*, 2020). Recent studies support an allosteric model of coupling in which binding to both agonist and G protein stabilizes an active state of the receptor, among a number of states which a given receptor may sample (Nygaard *et al.*, 2013; Manglik *et al.*, 2015; Okude *et al.*, 2015; Ye *et al.*, 2016; Weis and Kobilka, 2018). In addition to canonical G protein effectors, β-arrestins interact with GPCRs through additional receptor conformations and can serve as scaffolds for kinase signaling pathways (Liu *et al.*, 2012; Gurevich and Gurevich, 2019b; Wingler *et al.*, 2020). However, efforts to develop compounds which stabilize one set of conformations and therefore bias the receptor response to specific pathways have been promising but difficult to translate to *in vivo* models (Luttrell *et al.*, 2015; Viscusi *et al.*, 2019; Gillis *et al.*, 2020).

One hypothesis that could explain this difficulty is that the same agonist could drive coupling of the same receptor to different core signaling proteins based on the immediate subcellular environment of receptors. While an exciting idea with profound implications, this hypothesis has been difficult to test using traditional methods, because

receptor signaling readouts at the cellular level are complex and have been difficult to separate based on location.

Here we use the delta opioid receptor (DOR), a physiologically and clinically relevant GPCR, as a model to test this hypothesis. DOR localizes to intracellular compartments, including the Golgi, in neuronal cells, with a small amount on the plasma membrane (PM) (Zhang *et al.*, 1998; Cahill *et al.*, 2001a; Wang and Pickel, 2001; Kim and von Zastrow, 2003; Mittal *et al.*, 2013; Shiwarski *et al.*, 2017b, 2017a). DOR can be activated both on the PM and the Golgi by synthetic agonists, but whether the two activation states are different is not clear (Stoeber *et al.*, 2018). Relocating DOR from intracellular compartments to the PM increases the ability of DOR agonists to relieve pain (Cahill *et al.*, 2001b; Patwardhan *et al.*, 2005; Mittal *et al.*, 2013; Pradhan *et al.*, 2013; Shiwarski *et al.*, 2017b), illustrating the importance of understanding whether DOR activation on the Golgi is different from that on the PM.

Here we leverage conformational biosensors and high-resolution imaging to test whether DOR activation on the Golgi is different from that on the PM. We show that DOR on the PM, when activated by the selective DOR agonist SNC80, can recruit both a nanobody-based sensor and a G protein-based sensor that reads out active DOR conformations, as well as β-arrestins. In contrast, DOR in the Golgi apparatus, when activated by the same ligand, recruits the nanobody sensor, but not the G protein-based sensor or β-arrestins. Nevertheless, Golgi-localized DOR is competent to inhibit cAMP. Together these data demonstrate that these biosensors could be used to read out subtle differences in GPCR conformations even if signaling readouts are similar. Our results that the downstream effectors recruited by the same GPCR, activated by the same ligand, depend on the location of the receptor, suggest that subcellular location could be a master regulator of GPCR coupling to specific effectors and signaling for any given GPCR-ligand pair.

Results

Nanobody and miniG protein biosensors are emerging as powerful tools to study the effects of ligand-induced receptor conformational changes at the molecular and

cellular level (Manglik *et al.*, 2017; Wan *et al.*, 2018; Crilly and Puthenveedu, 2020). These sensors differentially engage the μ-opioid receptor (MOR) and κ-opioid receptor (KOR) activated by different agonists *in vitro* (Livingston *et al.*, 2018) or in the PM (Stoeber *et al.*, 2020), suggesting that they can provide a readout of conformational heterogeneity in agonist-stabilized active states. Because DOR is highly similar to MOR and KOR in the intracellular regions recognized by the sensors (Chen *et al.*, 1993), we asked whether these sensors could be optimized to read out specific active DOR conformations at distinct subcellular locations. We used the nanobody biosensor, Nb39 which recognizes opioid receptor active conformations through residues conserved across MOR, KOR, and DOR (Huang *et al.*, 2015; Che *et al.*, 2018), and the miniGsi biosensor, which mimics the interaction of the Gαi protein with GPCRs (Nehmé *et al.*, 2017; Wan *et al.*, 2018), as two orthogonal readouts of DOR conformations.

As an initial step, we first tested whether these sensors report active DOR conformations on the PM, similar to what has been reported for MOR and KOR. We used total internal fluorescence reflection microscopy (TIR-FM), which uses an evanescent wave to specifically excite fluorescent proteins on the PM to a depth of approximately 100nm into the cell (Hellen and Axelrod, 1991), to visualize sensor recruitment to activated DOR on the PM with high sensitivity **(Figure 3.1A)**. When cells were treated with either small molecule agonist SNC80 or peptide DPDPE, Nb39 **(Figure 3.1B-C)** and miniGsi **(Figure 3.1D-E)** were rapidly recruited to DOR on the plasma membrane (PM DOR), as observed by a rapid increase in fluorescence. Fluorescence of both sensors increased significantly after treatment with either agonist, but not inverse agonist ICI174864 (ICI) **(Figure 3.1F)**, indicating specificity of both sensors for an agonist-induced active conformation. Furthermore, recruitment of Nb39 and miniGsi to PM DOR was concentration-dependent and saturated at the concentration of SNC80 used in these experiments (10μM) **(Figure 3.1G)**. Concentration-response curves also revealed that miniGsi was more potently recruited to PM DOR than Nb39 in response to the agonist SNC80.

Interestingly, DPDPE recruited Nb39 to PM DOR more strongly than SNC80 **(Figure 3.1C,F)**, whereas the opposite trend was observed for miniGsi **(Figure 3.1E-F)**,

suggesting that these sensors might report selective conformations of DOR induced by different agonists. MiniGs, which mimics Gαs protein interaction with Gs-coupled GPCRs, was not recruited to PM DOR **(Figure 3.1F)**, suggesting that the miniGsi sensor specifically reports activation of the Gi-coupled DOR. DOR expression levels were overall comparable across conditions **(Figure 3.S1A)**. Overall, our data show that Nb39 and miniGsi report agonist-induced active conformations of PM DOR.

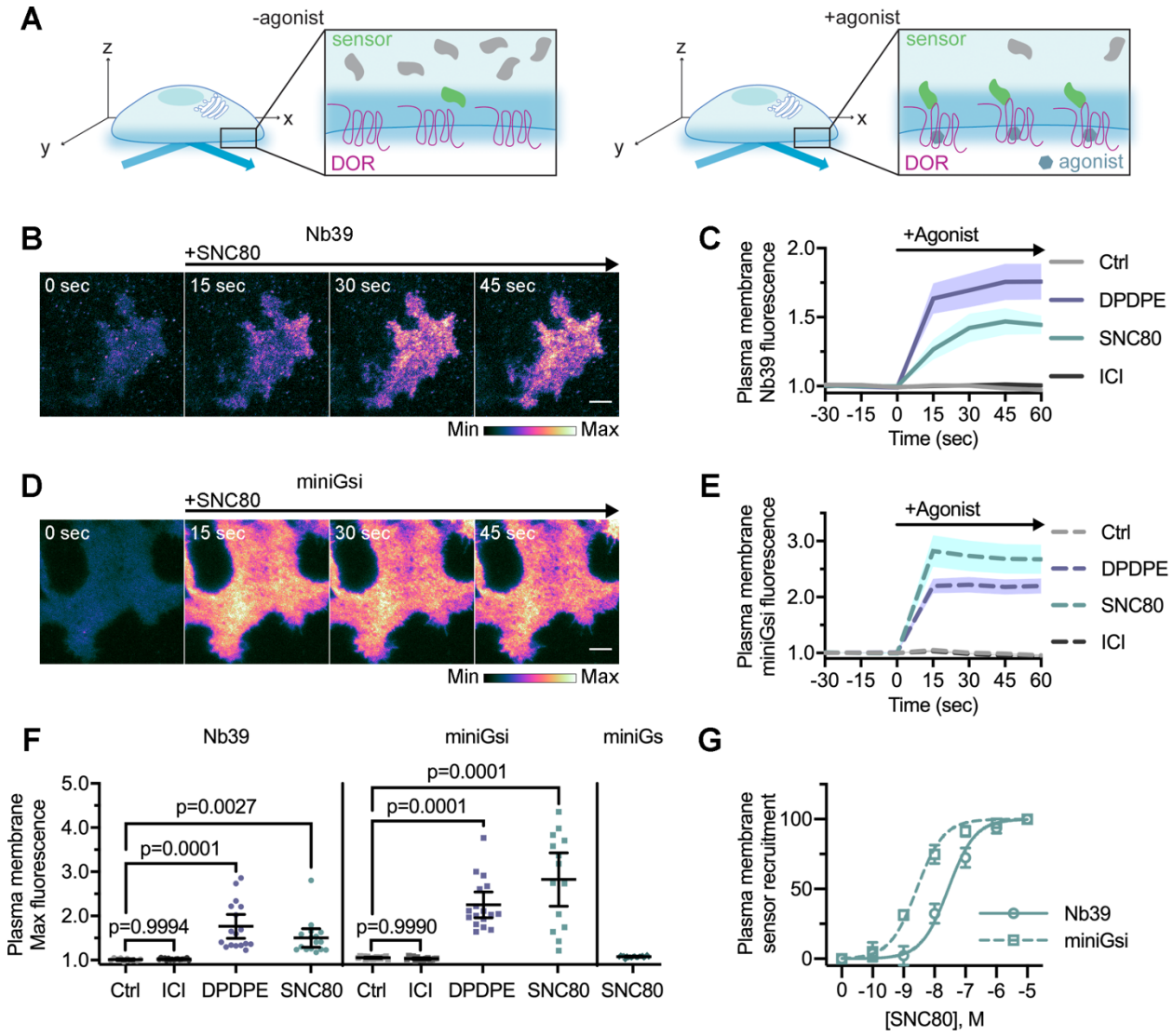

Figure 3.1. Nb39 and miniGsi are recruited to plasma membrane DOR.
(A) Schematic of biosensor recruitment to DOR in the PM using total internal reflection fluorescence microscopy (TIR-FM). Only fluorescent proteins within the evanescent wave close to the PM are excited, such that baseline fluorescence is low when biosensors are diffuse in the cell but increases upon agonist addition as biosensors recruited to active

DOR in the plasma membrane. **(B)** Nb39-mVenus in PC12 cells expressing SNAP-DOR imaged using TIR-FM to capture recruitment to the PM after addition of 10μM SNC80 (scale bar = 5μm). **(C)** Increase in Nb39-mVenus fluorescence by TIR-FM normalized to the mean baseline fluorescence over time after addition of 10μM DOR agonist, DPDPE or SNC80, 10μM inverse agonist, ICI174864 (ICI), or vehicle control (Ctrl, n=10 cells; ICI, n=17 cells; DPDPE, n=17 cells; SNC80, n=16 cells; all across 3 biological replicates defined as coverslips prepared and imaging independently; solid line indicates mean, shading +/- SEM). **(D)** Venus-miniGsi in PC12 cells expressing SNAP-DOR imaged using TIR-FM to capture recruitment to the PM after addition of 10μM SNC80 (scale bar = 5μm). Calibration bars indicate relative fluorescence values in scaled images. **(E)** Increase in Venus-miniGsi fluorescence by TIR-FM normalized to the mean baseline fluorescence over time after addition of 10μM DPDPE or SNC80, 10μM inverse agonist ICI, or vehicle control (Ctrl, n=17 cells; ICI, n=15 cells; DPDPE, n=17 cells; SNC80, n=14 cells; all across 3 biological replicates; dashed line indicates mean, shading +/- SEM). **(F)** Nb39 max PM biosensor fluorescence significantly increases over baseline within 60 seconds of addition of either agonist DPDPE or SNC80 but not with addition of inverse agonist ICI, by one-way ANOVA ($p<0.0001$) with p-values from Dunnett's multiple comparisons test to vehicle control reported in the figure. miniGsi max PM biosensor fluorescence significantly increases over baseline within 60 seconds of addition of either agonist DPDPE or SNC80 but not with addition of inverse agonist ICI, by one-way ANOVA ($p<0.0001$) with p-values from Dunnett's multiple comparisons test to vehicle control reported in the figure. Venus-miniGs, a sensor for Gs coupling, fluorescence does not visibly increase after addition of 10μM SNC80. (Nb39: Ctrl, n=10 cells; ICI, n=17 cells; DPDPE, n=17 cells; SNC80, n=16 cells; miniGsi: Ctrl, n=17 cells; ICI, n=15 cells; DPDPE, n=17 cells; SNC80, n=14 cells; miniGs-SNC80, n=20 cells; all across 3 biological replicates; mean +/- 95% CI, points represent individual cells). **(G)** Concentration-response curves for Nb39 (EC_{50}=22.7nM) and miniGsi (EC_{50}=2.284nM) plasma membrane recruitment measured in TIR-FM, in cells treated with increasing concentrations of SNC80 ranging from 0.1nM to 10μM. Responses are normalized from 0 to 100 for cells within each condition. (Nb39, n=13 cells; miniGsi, n=7 cells; symbols indicate mean normalized response for cells in each condition with error bars indicating +/- 95% CI; solid and dashed lines indicate fitted non-linear curves with a standard slope of 1, for Nb39 and miniGsi, respectively).

To test whether DOR localized to an intracellular compartment engages Nb39 or miniGsi differently upon activation by the same agonist, we took advantage of the fact that newly-synthesized DOR is retained in an intracellular compartment in neurons and PC12 cells **(Figure 3.2B, yellow arrows)** acutely treated with nerve growth factor (NGF) (Kim and von Zastrow, 2003; Shiwarski *et al.*, 2017b). The presence of both PM

and intracellular pools of DOR in these cells allowed us to measure sensor recruitment to DOR at both of these locations.

We first tested whether the two different biosensors were differentially recruited to DOR in intracellular compartments (IC DOR) vs. PM DOR by confocal imaging **(Figure 3.2A)**. When cells were treated with 10μM SNC80, a membrane permeable, small molecule agonist, Nb39 was rapidly recruited to intracellular SNAP-tagged DOR, within 30 sec **(Figure 3.2B)**. When quantitated, Nb39 fluorescence in the region of the cell defined by intracellular DOR rapidly and significantly increased after SNC80 addition **(Figure 3.2D-E)**. This Nb39 recruitment was dynamic and required DOR activation, as the DOR antagonist Naltrindole rapidly reversed this effect **(Figure 3.S2A-B)**. In striking contrast to Nb39, miniGsi was not recruited to IC DOR in the same time frame **(Figure 3.2C-D)**, despite comparable levels of IC DOR **(Figure 3.S1B)**. MiniGsi fluorescence in the region of the cell defined by IC DOR did not increase in cells treated with SNC80 **(Figure 3.2D-E)**. As a control, miniGs was also not recruited to IC DOR in cells treated with SNC80 **(Figure 3.2E)**.

Both sensors were recruited to PM DOR, as seen by confocal imaging in the same cells in which we measured recruitment to IC DOR, although the sensitivity of detection was lower in confocal imaging **(Figure 3.2B-C, yellow arrowheads and Figure 3.2F)**. MiniGsi was recruited to PM DOR more strongly than Nb39 **(Figure 3.1F, 3.2F)**, consistent with the TIR-FM results, which makes the absence of miniGsi recruitment to IC DOR in response to SNC80 is even more striking. These results indicate that SNC80 promotes an active DOR conformation preferentially recognized by Nb39 in intracellular compartments, and a distinct active DOR conformation preferentially recognized by miniGsi at the PM, suggesting location-specific conformational effects of SNC80 on DOR.

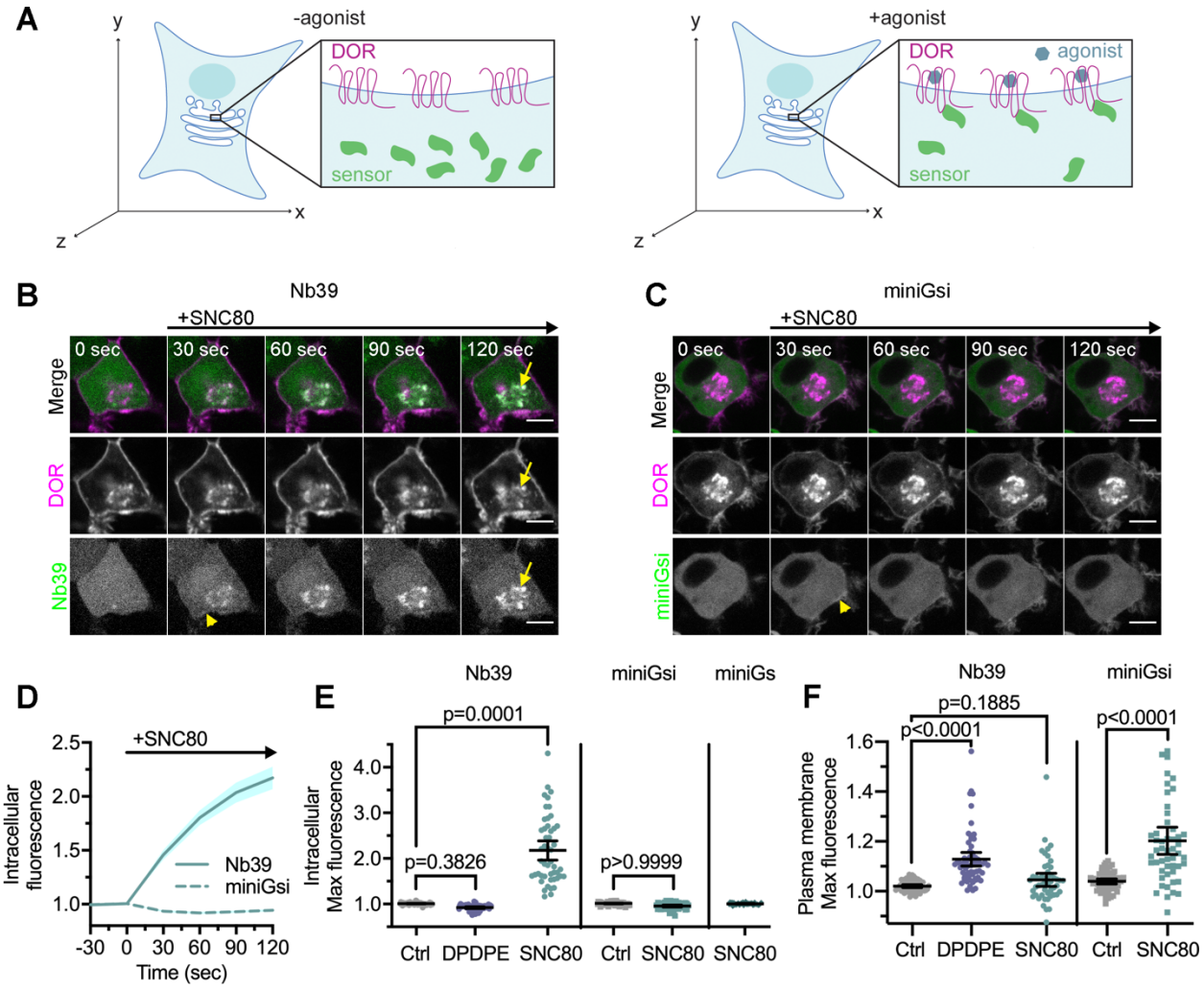

Figure 3.2. Nb39 and miniGsi are differentially recruited to Golgi DOR.
(A) Schematic of biosensor recruitment to DOR in intracellular compartments upon addition of a cell permeable agonist. Both Nb39 and miniGsi biosensors are diffuse throughout the cytoplasm in the absence of agonist (left), but are expected to localize to membranes containing active receptor upon agonist addition (right). **(B)** PC12 cells expressing SNAP-DOR (magenta in merge) and Nb39-mVenus (green in merge) were treated with 10μM SNC80 and imaged live by confocal microscopy. Treatment with SNC80 leads to an increase in Nb39-mVenus signal in a perinuclear region (yellow arrow) which colocalizes with intracellular DOR (white in merge). A small amount of Nb39 recruitment is also visible at the PM (yellow arrowhead) (scale bar=5μm). **(C)** PC12 cells expressing SNAP-DOR (magenta in merge) and Venus-miniGsi (green in merge) were treated with 10μM SNC80 and imaged live by confocal microscopy. miniGsi does not localize to intracellular DOR after agonist treatment, though a small amount of minGsi recruitment is visible at the PM (yellow arrowhead) (scale bar=5μm). **(D)** Nb39 (solid line indicates mean, shading +/- SEM) and miniGsi (dashed line, shading +/- SEM) fluorescence in the region of the cell defined by intracellular DOR normalized to mean

baseline fluorescence over time after addition of 10μM SNC80 (Nb39, n=49 cells across 4 biological replicates; miniGsi, n=51 cells across 3 biological replicates). **(E)** Max intracellular biosensor fluorescence in the region of the cell defined by intracellular DOR within 120 seconds of agonist addition shows a significant increase in Nb39 recruitment with addition of permeable agonist SNC80 but not with peptide agonist DPDPE, by one-way ANOVA ($p<0.0001$) with p-values from Dunnett's multiple comparison test to vehicle control reported in the figure. In contrast, miniGsi intracellular max fluorescence does not increase upon addition of 10μM SNC80 by one-tailed student's t-test compared to vehicle control. miniGs intracellular max fluorescence also does not visibly increase upon SNC80 treatment. (Nb39: Ctrl, n=61 cells; DPDPE, n=61 cells; SNC80, n=49 cells; miniGsi: Ctrl, n=57 cells; SNC80, n=51 cells; miniGs: SNC80, n=36 cells; all across a minimum of 3 biological replicates; mean +/- 95% CI, points represent individual cells). **(F)** Max plasma membrane biosensor fluorescence in the region of the cell defined by plasma membrane DOR for the same cells quantified in **(E)** shows a significant increase in Nb39 recruitment with addition of DPDPE and a small but non-significant increase upon addition of SNC80, by one-way ANOVA ($p<0.0001$). P-values from Dunnett's multiple comparison test to vehicle control are reported. MiniGsi plasma membrane max fluorescence also significantly increases upon addition of SNC80, as estimated by one-tailed student's t-test, compared to vehicle control. (Nb39: Ctrl, n=61 cells; DPDPE, n=61 cells; SNC80, n=49 cells; miniGsi: Ctrl, n=57 cells; SNC80, n=51 cells; miniGs: SNC80, n=36 cells; all across a minimum of 3 biological replicates; mean +/- 95% CI, points represent individual cells with one outlier in the miniGsi SNC80 condition equal to 2.0167 not shown in the graph).

Differential biosensor recruitment to IC DOR did not depend on the method used to cause DOR retention in this compartment **(Figure 3.S3A)**, and recruitment to PM DOR was unaffected by the presence of IC DOR **(Figure 3.S3B)**. Further, recruitment of either sensor was not significantly correlated with sensor expression level **(Figure 3.S3C-D)**, as miniGsi failed to show recruitment to IC DOR across a broad range of expression levels **(Figure 3.S3D)**.

When cells were treated with 10μM peptide agonist DPDPE, which does not readily cross the PM over short time scales (Stoeber *et al.*, 2018), Nb39 was not recruited to IC DOR **(Figure 3.2E)**. This suggests that activation of PM DOR is not sufficient for recruitment of Nb39 to IC DOR. We next tested whether PM DOR activation was required for differential sensor recruitment to IC DOR. Cells were pre-treated with a high concentration (100μM) of DOR inverse agonist ICI174864 (ICI), a

peptide restricted to the extracellular space (Stoeber *et al.*, 2018), to pharmacologically block PM DOR. Nb39 recruitment to IC DOR after 100nM SNC80 addition was then measured. Nb39 was robustly recruited to IC DOR, even when PM DOR was pharmacologically blocked, indicating that recruitment to IC DOR does not require activation of PM DOR **(Figure 3.3A, top, 3.3B, C)**. When PM DOR was pharmacologically blocked, miniGsi again remained diffuse throughout the cell and was not recruited to IC DOR **(Figure 3.3A, bottom, 3.3B, C)**, indicating that the absence of miniGsi recruitment to IC DOR is not due to sequestration of sensor at PM DOR. To test whether activation of endogenous G proteins was restricting miniGsi recruitment, cells were pretreated with pertussis toxin (PTX) to inactivate endogenous Gi/o proteins. Even in PTX-treated cells, miniGsi was not recruited to IC DOR, suggesting that competition with endogenous Gαi/o protein effectors for interaction with DOR is not responsible for the lack of recruitment of miniGsi to IC DOR **(Figure 3.3C)**.

Immunofluorescence microscopy showed that Nb39 was recruited to IC DOR localized to the Golgi. Using a similar approach as described above, PC12 cells expressing Flag-tagged DOR and either Nb39 or miniGsi were pretreated for 15 minutes with 10μM β-chlornaltrexamine (CNA), an irreversible, cell impermeable antagonist (Virk and Williams, 2008; Shiwarski *et al.*, 2017b), to irreversibly block PM DOR, before treating with 10μM SNC80 for 5 minutes. Cells were stained for TGN-38, a marker for the trans-Golgi network, which was previously shown to colocalize with IC DOR (Shiwarski *et al.*, 2017b). Consistent with live cell imaging data, only Nb39 and not miniGsi was recruited to IC DOR in a region of the cell colocalizing with the TGN-38 marker **(Figure 3.3D, E)** in cells treated with CNA and SNC80. CNA alone did not cause recruitment of either sensor. Sensor fluorescence in the region of the cell defined by TGN-38 staining was normalized to sensor fluorescence in the cell outside this region, as a measure of sensor enrichment in the Golgi. Treatment with CNA and SNC80 significantly increased Nb39 Golgi enrichment **(Figure 3.3F)**, whereas miniGsi enrichment was not significantly different from control cells **(Figure 3.3G)**. These results confirm differential biosensor recruitment to IC DOR specifically localized to the Golgi and reiterate that PM DOR activation is not required for differential biosensor recruitment to Golgi DOR.

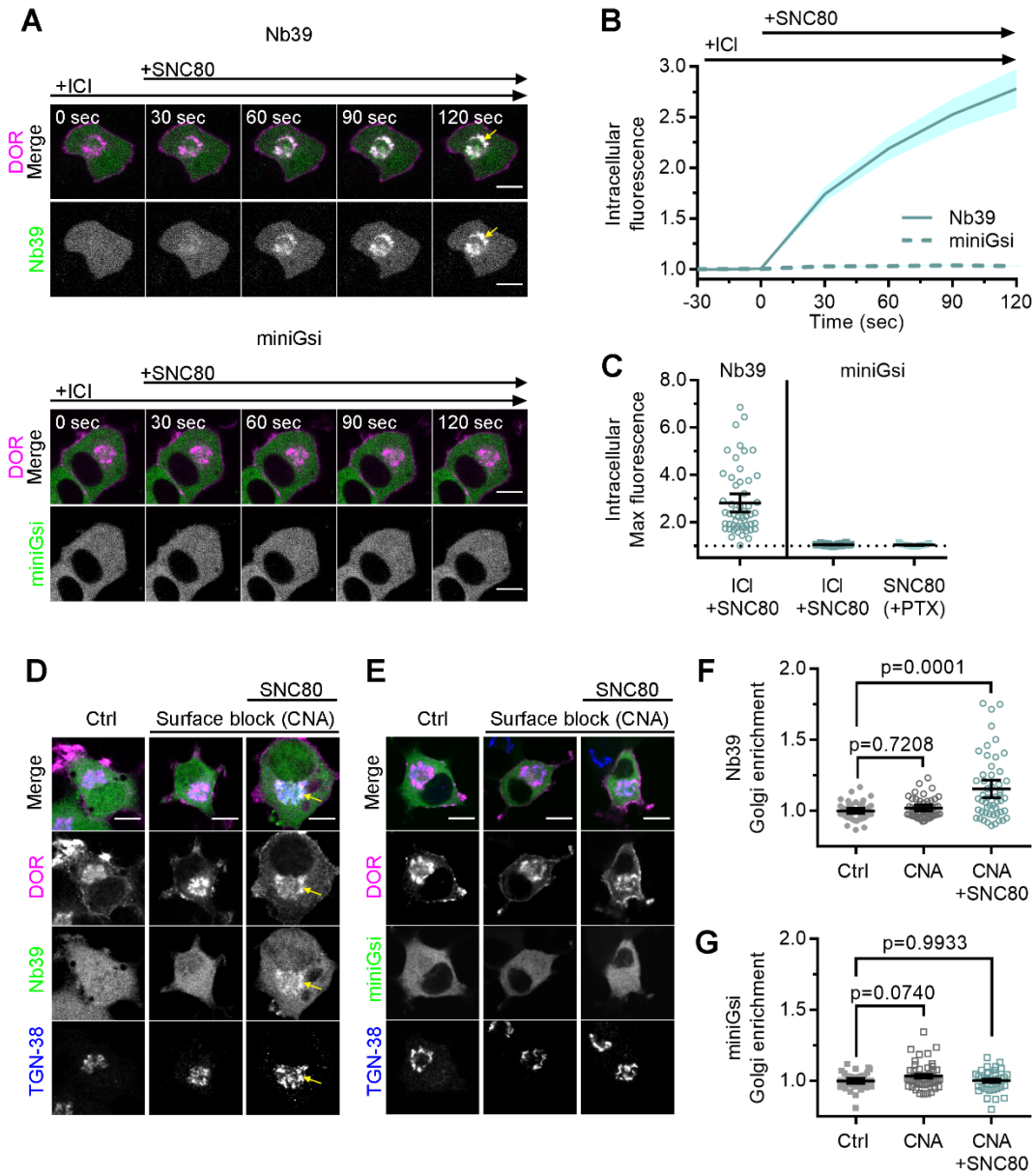

Figure 3.3. Differential sensor recruitment to Golgi DOR is independent of plasma membrane DOR activation.

(A) PC12 cells expressing SNAP-DOR (magenta in merge) and Nb39-mVenus or Venus-miniGsi (green in merge) were imaged live by confocal microscopy with 100μM ICI present in the media before addition of 100nM SNC80. After SNC80 treatment, Nb39-mVenus fluorescence increases in a perinuclear region (yellow arrow) which colocalizes with intracellular DOR (white in merge), whereas Venus-miniGsi remains diffuse through the cell (scale bar=5μm). **(B)** Nb39 (solid line indicates mean, shading +/- SEM) or miniGsi (dashed line, shading +/- SEM) fluorescence in the region of the cell defined by intracellular DOR normalized to mean baseline fluorescence in cells treated with 100μM ICI and 100nM SNC80 (Nb39, n=54 cells across 3 biological replicates; miniGsi, n=58 cells across 4 biological replicates). **(C)** Nb39-mVenus max intracellular fluorescence

increases over baseline within 120 seconds of SNC80 in cells treated with 100μM ICI and 100nM SNC80. In contrast, miniGsi intracellular max fluorescence does not visibly increase over baseline in cells treated with ICI and SNC80, nor in cells pretreated with pertussis toxin (PTX) and SNC80 (Nb39: ICI+SNC80, n=54 cells; miniGsi: ICI+SNC80, n=58 cells; PTX+SNC80, n=33 cells; mean +/- 95% CI, points represent individual cells). **(D)** PC12 cells expressing Flag-DOR and Nb39-mVenus or Venus-miniGsi, **(E),** (green in merge) were treated with either 10μM β-chlornaltrexamine (CNA) alone for 15 minutes or 10μM CNA for 15 minutes followed by 10μM SNC80 for 5 minutes, then fixed and stained for Flag (magenta in merge) and *trans*-Golgi network marker TGN-38 (blue in merge) (scale bar = 5μm). Colocalization of DOR, Nb39, and TGN-38 is visible in white and light blue (yellow arrow) in cells treated with CNA and SNC80, but not CNA alone. **(F)** Normalized Nb39-mVenus fluorescence enriched in the Golgi, expressed as sensor fluorescence in the region of the cell defined by the TGN-38 staining divided by sensor fluorescence in the region of the cell not containing TGN-38 staining. Nb39 Golgi enrichment is significantly increased in cells treated with CNA and SNC80, but not CNA alone, by one-way ANOVA ($p<0.0001$) with p-values reported in the figure from Dunnett's multiple comparisons test compared to control cells (Ctrl, n=46 cells; CNA, n=49; CNA+SNC80, n=52; all across 2 biological replicates; points indicate individual cells with bars representing mean +/- 95% CI). **(G)** Venus-miniGsi Golgi enrichment is not significantly increased in cells treated with either CNA and SNC80 or CNA alone, by one-way ANOVA ($p=0.0654$) with p-values reported in the figure from Dunnett's multiple comparisons test compared to control cells (Ctrl, n=40 cells; CNA, n=50; CNA+SNC80, n=37; all across 2 biological replicates; points indicate individual cells with bars representing mean +/- 95% CI).

In addition to heterotrimeric G proteins, DOR and other GPCRs interact with other proteins and signaling effectors after agonist-induced conformational changes. Agonist-dependent differential biosensor recruitment to MOR and KOR in the PM correlates with recruitment of other receptor effectors, specifically G protein-coupled receptor kinase 2 (GRK2), which mediates receptor desensitization (Stoeber *et al.*, 2020). Given differential recruitment of Nb39 and miniGsi to IC DOR, we hypothesized that Golgi localization may also influence coupling to other downstream signaling effectors. β-arrestins interact with DOR and other GPCRs after activation by agonists and receptor phosphorylation by GRKs to mediate receptor desensitization and internalization from the PM (Zhang *et al.*, 1999, 2005; Gurevich and Gurevich, 2019a). β-arrestins can also scaffold kinase signaling complexes from GPCRs at the PM and

endosomes (DeFea *et al.*, 2000b, 2000a; McDonald *et al.*, 2000; Peterson and Luttrell, 2017; Weinberg *et al.*, 2017).

To test whether β-arrestin effectors are recruited to active IC DOR, we monitored recruitment of fluorescently tagged β-arrestin1 or β-arrestin2 to IC DOR. Similar to miniGsi, neither β-arrestin-1 nor β-arrestin-2 were recruited to IC DOR in cells treated with SNC80, and no increase in fluorescence in the region of the cell defined by IC DOR was detected **(Figure 3.4A-C)**. In contrast, both β-arrestins were visibly recruited to the PM by confocal imaging **(Figure 3.4A, B, yellow arrowheads)** and by quantitation of TIR-FM imaging **(Figure 3.4D-F)** in response to SNC80 treatment. Together, these data indicate that like miniGsi, β-arrestins interact with only agonist-activated DOR present in the PM.

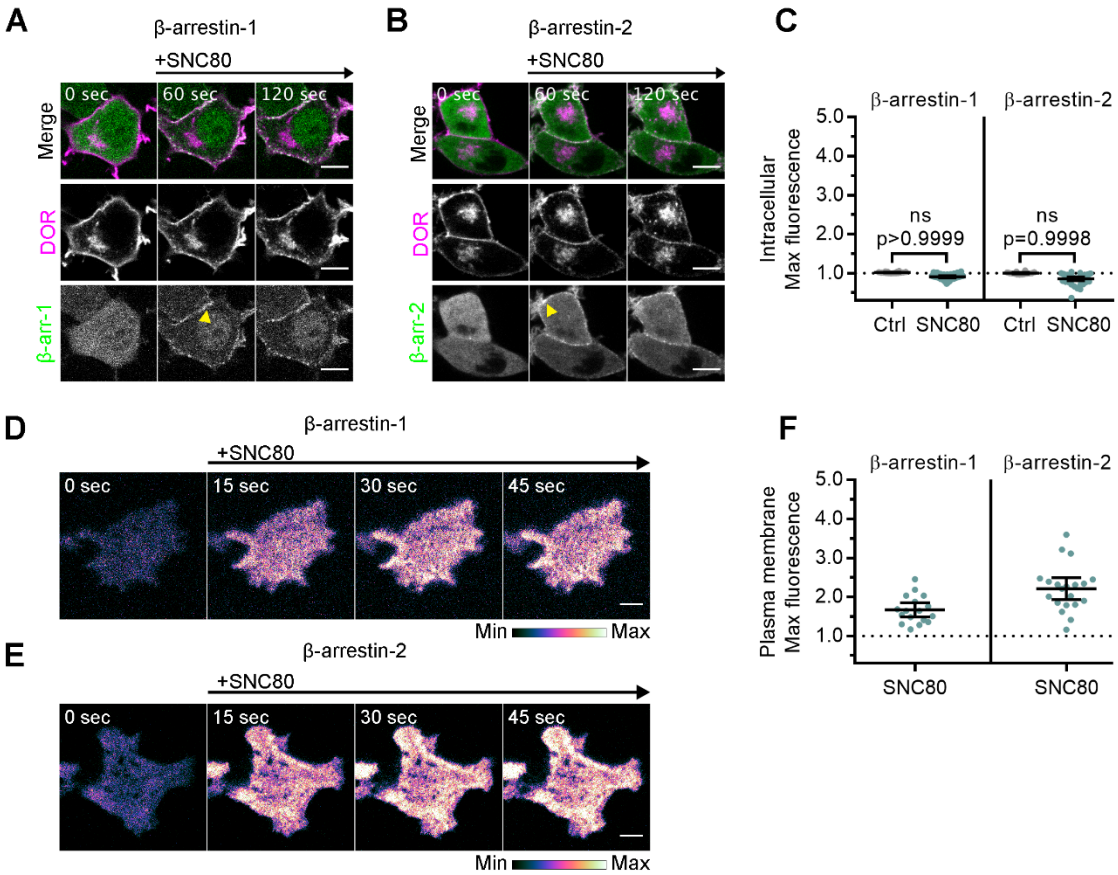

Figure 3.4. Arrestins are differentially recruited to plasma membrane and intracellular DOR.
(A) PC12 cells expressing SNAP-DOR (magenta in merge) and β-arrestin-1-mScarlet (green in merge) were treated with 10μM SNC80 and imaged live by confocal microscopy.

β-arrestin-1-mScarlet signal increases at the PM (yellow arrowhead) but not at sites colocalized with intracellular DOR upon 10μM SNC80 treatment (scale bar=5μm). **(B)** PC12 cells expressing SNAP-DOR (magenta in merge) and β-arrestin-2-tdTomato (green in merge). β-arrestin-2-tdTomato signal increases at the PM (yellow arrowhead) but not at sites colocalized with intracellular DOR upon 10μM SNC80 treatment (scale bar=5μm). **(C)** Neither β-arrestin-1-mScarlet nor β-arrestin-2-tdTomato max intracellular fluorescence significantly increases within 120 seconds of SNC80 addition by one-tailed student's t-test compared to control cells (β-arr-1: Ctrl, n=16 cells; SNC80, n=33 cells; β-arr-2: Ctrl, n=14 cells; SNC80, n=37 cells; with control conditions across 1 biological replicate and SNC80 conditions across 3 biological replicates; mean +/- 95% CI, points represent individual cells). **(D)** β-arrestin-1-mScarlet in PC12 cells expressing SNAP-DOR imaged using TIR-FM to capture recruitment to the PM after addition of 10μM SNC80 (scale bar = 5μm). **(E)** β-arrestin-2-tdTomato in PC12 cells expressing SNAP-DOR imaged using TIR-FM to capture recruitment to the PM after addition of 10μM SNC80 (scale bar = 5μm). Calibration bars indicate relative fluorescence values in scaled images. **(F)** Both β-arrestin-1-mScarlet and β-arrestin-2-tdTomato max PM fluorescence increases within 60 seconds of 10μM SNC80 addition (β-arr-1: SNC80, n=17 cells; β-arr-2: SNC80, n=20 cells; all across 3 biological replicates; mean +/- 95% CI, points represent individual cells).

Given differential recruitment of active conformation biosensors, Nb39 and miniGsi, and the absence of β-arrestin recruitment to IC DOR, we asked whether the active conformation of IC DOR allows for signaling through G proteins. Like the other opioid receptors, DOR couples primarily to Gi/o proteins which inhibit adenylyl cyclase activity to decrease cAMP (Gendron *et al.*, 2016). We used a Forster resonance energy transfer (FRET) sensor, ICUE3, to monitor cAMP levels in single cells in real time (DiPilato and Zhang, 2009). In PC12 cells expressing ICUE3 and SNAP-DOR, addition of adenylyl cyclase activator forskolin (Fsk, 2μM) caused a rapid increase in the CFP/FRET ratio over the baseline ratio **(Figure 3.5A-B)**. Pretreatment with 100nM SNC80 prior to Fsk addition decreased the Fsk-stimulated cAMP response **(Figure 3.5C-D)**, consistent with DOR activation inhibiting adenylyl cyclase activity.

We next specifically tested whether IC DOR was sufficient for cAMP inhibition. Cells expressing DOR were treated with cycloheximide (CHX) to ensure that, in the absence of NGF, newly synthesized DOR transiting the Golgi was cleared out and that no residual DOR remained in the Golgi. In cells pre-treated with NGF before CHX, the

pool of IC DOR was maintained even after CHX treatment, consistent with previous results (Kim and von Zastrow, 2003; Shiwarski *et al.*, 2017b). Under these conditions, the overall Fsk response and SNC80-mediated inhibition in cells treated with NGF were comparable to untreated cells **(Figure 3.S4A)**. To isolate the contribution of IC DOR to cAMP inhibition, we pharmacologically blocked PM DOR with 100μM ICI. In cells with PM DOR only, SNC80 failed to decrease Fsk-stimulated cAMP in the presence of ICI **(Figure 3.5E-F)**. Neither the total cAMP levels, measured as area under the curve, nor the endpoint cAMP levels, measured as the change in endpoint cAMP levels over baseline, were significantly different from cells treated with Fsk alone **(Figure 3.5I-J)**. In contrast, in cells with IC DOR, SNC80 decreased Fsk-stimulated cAMP even in the presence of ICI (Figure 4G-H), and significantly decreased endpoint and total cAMP levels **(Figure 3.5I-J)**. IC DOR activation suppressed Fsk-stimulated cAMP to approximately half the degree suppressed by combined PM and IC DOR **(Figure 3.5I-J, 2.S4A)**. As a control, ICI alone did not significantly affect endpoint or total cAMP levels **(Figure 3.5I-J)**. These results indicate that Golgi DOR activation is sufficient for cAMP inhibition.

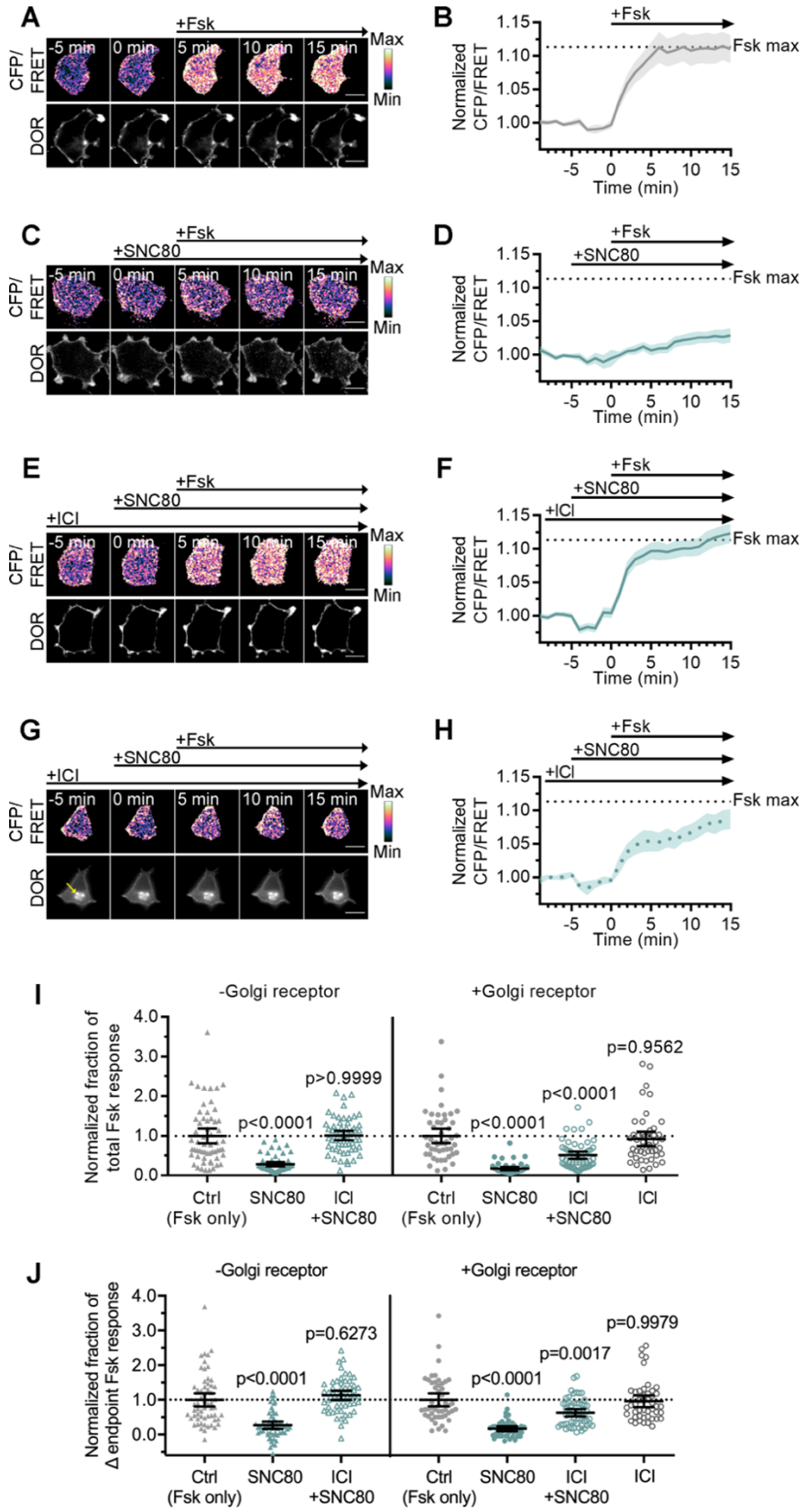

Figure 3.5. Golgi DOR inhibits cAMP.

(A-H) Ratiometric CFP/FRET and receptor images, along with corresponding trace of mean cellular CFP/FRET ratios (solid line indicates mean, shading +/- 95% CI), in PC12 cells expressing the ICUE3 cAMP FRET sensor and SNAP-DOR (scale bar=10μm). Calibration bars indicate relative fluorescence values in scaled images. **(A-B)** In cells without intracellular DOR, CFP/FRET ratio increases over baseline upon treatment with 2μM forskolin (Fsk), consistent with increase in cellular cAMP levels. **(C-D)** Treatment with DOR agonist SNC80 (100nM) decreases Fsk-stimulated increase in CFP/FRET ratio. **(E-F)** In cells without intracellular DOR, SNC80-dependent decrease in Fsk-stimulated CFP/FRET ratio is reversed when peptide inverse agonist ICI (100μM) is present in media. **(G-H)** In cells containing intracellular DOR (**G**, yellow arrow), SNC80 decreases Fsk-stimulated CFP/FRET ratio even when ICI is present in media. **(I-J)** Fsk-stimulated total cAMP levels (area under the curve) **(I)** and endpoint CFP/FRET ratios **(J)**, normalized to mean of control treated cells within -Golgi receptor and +Golgi receptor groups. Treatment with 100nM SNC80 significantly decreases total Fsk-stimulated cAMP and endpoint ratios. ICI and SNC80 treatment of cells without Golgi DOR does not significantly decrease total cAMP or endpoint ratios. In contrast, ICI and SNC80 treatment of cells with Golgi DOR significantly decreases total cAMP and endpoint ratios. ICI treatment alone in cells with Golgi DOR does not significantly decrease total cAMP and endpoint ratios. (-Golgi receptor: control, n= 59 cells; SNC80, n=58; ICI+SNC80, n=57; +Golgi DOR: control, n=48; SNC80, n=50; ICI+SNC80, n=55; ICI, n=47; all across 2 biological replicates; one-way ANOVA (total cAMP, $p<0.0001$; endpoint cAMP, $p<0.0001$) with p-values reported in the figure from Sidak's multiple comparisons test for each condition compared to control cells within –Golgi receptor and +Golgi receptor groups).

As an independent method to induce an intracellular pool of DOR, we used LY294002, a small molecule inhibitor of PI3K that causes DOR retention in the Golgi independent of NGF (Shiwarski *et al.*, 2017a). Similar to results obtained in NGF-treated cells, the permeable small molecule agonist SNC80 decreased Fsk-stimulated cAMP **(Figure 3.S4B-D)** even in the presence of ICI, reiterating that Golgi DOR activation is sufficient for cAMP inhibition. The total and endpoint cAMP levels decreased significantly compared to cells treated with Fsk alone **(Figure 3.S4G-H)**. Again, IC DOR alone suppresses Fsk-stimulated cAMP to approximately half the degree suppressed by combined PM and IC DOR **(Figure 3.S4B, G-H)**. As a control, the peptide DPDPE agonist did not decrease the Fsk response in the presence of ICI **(Figure 3.S4B, E-F)**.

Discussion

Together, our data indicate that DOR activation by the same agonist in different subcellular compartments drives differential engagement of effectors and interacting proteins, including active state biosensors and arrestins. The conventional model suggests that distinct GPCR conformations can drive coupling to distinct effectors, which determine subsequent downstream signaling responses. This relationship between structure and function has been a subject of great interest due to its potential to explain the pleiotropic effects of GPCR activation by any given ligand. Our results suggest that the subcellular location in which receptors are activated might determine the conformational landscapes that receptors can adopt upon activation, because the immediate environment of receptors varies between these locations.

Conformational biosensors like Nb39 and miniGsi used here are valuable tools to study how location could bias receptor conformations. The possibility that Nb39 and miniGsi could recognize distinct conformations is supported by structures of agonist-bound homologous MOR and KOR in complex with Nb39 or MOR in complex with the heterotrimeric G protein complex, $G\alpha_{i1}\beta_1\gamma_2$. Structures of MOR with agonist BU72 and KOR with agonist MP1104 share the outward shift of transmembrane helix (TM) 6 which is characteristic of active GPCR structures (Huang *et al.*, 2015; Che *et al.*, 2018). Nb39 appears to stabilize this conformation via contacts with intracellular loops (ICL) 2 and ICL3, as well as the 8th helix through residues conserved across MOR, KOR, and DOR (Huang *et al.*, 2015; Che *et al.*, 2018). The structure of MOR in complex with agonist DAMGO and the nucleotide free Gαi protein is very similar to the MOR-Nb39 structure with the exception of a greater displacement of TM6 toward TM7 and decreased extension of ICL3 (Koehl *et al.*, 2018). The miniGsi sensor does not contain all regions of Gαi which contact the receptor, but many of the residues which interact with MOR ICL2 and ICL3 via the Gαi C-terminal α5 helix are present in miniGsi, and previous reports show that miniGs and Gαs contact Gs-coupled GPCRs similarly (Carpenter *et al.*, 2016; Nehmé *et al.*, 2017). Though Nb39 and Gαi contact opioid receptors in similar regions and share two interaction residues, each also makes additional distinct contacts with TM domains and the 8th helix. Distinct interactions with these intracellular domains important for effector coupling and unique stabilization of TM6 and ICL3 by Nb39 could

suggest that these sensors differentially report distinct conformations relevant to receptor function. Structures of agonist-bound DOR in complex with Nb39 or miniGsi would enable direct comparison between receptor conformations recognized by each sensor. Additionally, structural data is limited to a single static view of opioid receptor active conformation, and the ability of Nb39 and miniGsi to discriminate between additional distinct intermediate or active conformations will be an exciting area for future study.

One clear difference between compartments is the composition of specific phospholipids that make up the membranes (Ikonen, 2008; Van Meer *et al.*, 2008; Balla, 2013). Phospholipids differing in charge can stabilize active or inactive conformations of the β_2-adrenergic receptor, stabilize G protein coupling, and modulate G protein selectivity (Dawaliby *et al.*, 2016; Yen *et al.*, 2018; Strohman *et al.*, 2019). The contribution of phospholipids to differential recruitment of sensors and effectors by DOR could be tested using similar approaches (Dawaliby *et al.*, 2016; Livingston *et al.*, 2018; Strohman *et al.*, 2019). Reconstituting DOR into lipoparticles with defined lipid compositions which mimic the PM or Golgi membrane and measuring sensor association and dissociation kinetics or interactions with G proteins could provide important insight into how membrane composition affects DOR interactions with these proteins. Lipid composition can also directly influence recruitment of effectors like β-arrestins which bind $PI(4,5)P_2$, a phospholipid species enriched in the PM (Gaidarov *et al.*, 1999), potentially contributing to the lack of observed arrestin recruitment to Golgi DOR. To date, β-arrestin recruitment to active GPCRs in the Golgi has not been reported, and the impact of receptor localization to this compartment on desensitization, β-arrestin recruitment, and β-arrestin biased signaling is not known.

Other compartment-specific factors including ion concentrations and GPCR interacting proteins could influence receptor conformations and effector coupling. The Golgi lumen is more acidic than the extracellular space, pH 6.4 vs pH 7.4 (Kim *et al.*, 1996; Llopis *et al.*, 1998; Miesenböck *et al.*, 1998), which could affect ligand binding and GPCR activation (Pert and Snyder, 1973; Ghanouni *et al.*, 2000; Vetter *et al.*, 2006; Meyer *et al.*, 2019). Estimated concentrations of sodium in the Golgi are closer to

cytosolic sodium concentrations (12-27mM) than high extracellular sodium concentrations (100mM) (Hooper and Dick, 1976; Chandra *et al.*, 1991). Sodium acts as an allosteric modulator of class A GPCRs, and DOR specifically has been crystallized with a coordinated sodium ion, which stabilizes the inactive receptor conformation and is required for receptor activation and signaling (Fenalti *et al.*, 2014; Zarzycka *et al.*, 2019), suggesting Golgi sodium concentrations could affect DOR activity. Ligand concentrations of a permeable agonist like SNC80 may also differ between the Golgi lumen and the extracellular space. A lower SNC80 concentration in the Golgi, however, is unlikely to explain the differential recruitment we observe, as miniGsi is more potently recruited to PM DOR than Nb39 **(Figure 3.1G)**. Additionally, DOR interacting proteins which regulate DOR trafficking and localize to the Golgi, like the COPI complex and Rab10, could also regulate receptor conformations and effector coupling (St-Louis *et al.*, 2017; Shiwarski *et al.*, 2019; Degrandmaison *et al.*, 2020).

Our results suggest that the conformational space sampled by any given GPCR, even when activated by the same agonist, could differ based on the precise subcellular location of the receptor. Compartmental effects on GPCR conformations may also be specific to individual GPCRs. In contrast to DOR, both an active state nanobody and miniGs are recruited to active Gs-coupled β_1-adrenergic receptor (B1AR) in the Golgi, suggesting the local Golgi environment may influence DOR and B1AR energy landscapes differently (Irannejad *et al.*, 2017; Nash *et al.*, 2019). Additionally, the A_1-adenosine receptor, when expressed exogenously can localize to the Golgi and recruits miniGsi to this compartment upon adenosine treatment (Wan *et al.*, 2018). This result demonstrates that miniGsi can in fact report active conformations of Gαi-coupled receptors in the Golgi, which emphasizes the absence of miniGsi recruitment to IC DOR that we observe. These GPCR specific effects may reflect important differences in pharmacology among individual GPCRs and emphasize the importance of characterizing compartmental effects for each GPCR.

These results also provide a new perspective into drug development efforts, by highlighting the effects that the subcellular location of receptors could have on the integrated effects of any given drug. The majority of these efforts largely rely on assays

using conventional readouts of signaling in model cells, where GPCR localization could be different from that of physiologically relevant cells *in vivo*. This difference is especially true for DOR, which exhibits robust surface localization in model cell lines, but high levels of intracellular pools in many neuronal subtypes. Traditional signaling assays, which rely on whole-cell readouts of primary signaling pathways such as cAMP, will not distinguish between the contributions of different pools of receptors, which could signal differently via pathways outside the primary readouts (Costa-Neto *et al.*, 2016). Therefore, the potentially distinct effects of ligands at spatially distinct pools of receptors in the integrated response should be an important consideration for measuring the outcomes of receptor activation.

Materials and Methods

DNA constructs

SSF-DOR construct consists of an N-terminal signal sequence followed by a Flag tag followed by the mouse DOR sequence in a pcDNA3.1 vector backbone. To create SNAP-DOR, the full-length receptor sequence was amplified from the SSF-DOR construct by PCR with compatible cut sites (BamHI and XbaI). The SNAP tag (New England Biolabs, Ipswich, MA) was amplified by PCR with compatible cut sites (HindIII and BamHI) and both were ligated into a pcDNA3.1 vector backbone to produce the final construct containing an N-terminal signal sequence, followed by the SNAP tag and then the receptor. β-arrestin-1 was generated from a geneblock (Integrated DNA Technologies, Coralville, IA) containing the human cDNA (ENST00000420843) for hARRB1 with HindIII and AgeI cut sites. mScarlet was amplified by PCR from pmScarlet_alphaTubulin_C1 a gift from Dorus Gadella (Addgene plasmid #85045) (Bindels *et al.*, 2016), with AgeI and XbaI cut sites. Both were then ligated into a pcDNA3.1 vector backbone to produce a C-terminally tagged β-arrestin-1. β-arrestin 2 tagged with tdTomato was generated from β-arrestin 2-GFP via restriction site cloning (Weinberg *et al.*, 2017). Nb39-mVenus was a gift from Drs. Bryan Roth and Tao Che (Che *et al.*, 2020). Venus-miniGsi and Venus-miniGs were gifts from Drs. Greg Tall and

Nevin Lambert. pcDNA3-ICUE3 was a gift from Dr. Jin Zhang (Addgene plasmid #61622) (DiPilato and Zhang, 2009).

Cell culture and transfection

Pheochromocytoma-12 cells (PC12 cells, ATCC #CRL-1721) were used for all experiments. Cells were maintained at 37ºC with 5% CO2 and culture in F-12K media (Gibco, #21127), with 10% horse serum and 5% fetal bovine serum (FBS). Cells were grown in flasks coated with CollagenIV (Sigma-Aldrich, #C5533) to allow for adherence. PC12 cells were transiently transfected at 90% confluency according to manufacturer's guidelines with Lipofectamine 2000 (Invitrogen, #11668) with 1.5ug of each DNA construct to be expressed. The transfection mixture was incubated with cells in Opti-MEM media (Gibco, #31985) for 5 hours then removed and replaced with normal culture media until imaging 48-72 hours following transfection.

Live cell imaging with fluorescent biosensors

PC12 cells transfected with SNAP-DOR and the appropriate biosensor were plated and imaged in single-use MatTek dishes (MatTek Life Sciences, #P35G-1.5-14-C) coated with 20µg/mL poly-D-lysine (Sigma-Aldrich, #P7280) for 1 hour. For experiments requiring a Golgi pool of DOR, cells were pretreated with 100ng/mL of NGF (Gibco, #13257) or 10µM LY294002 (Tocris, #1130) or 20µM PI4K inhibitor MI 14 (Tocris, #5604) for 1 hour prior to imaging, as described previously (Kim and von Zastrow, 2003; Shiwarski *et al.*, 2017b, 2017a). Cells were labeled with 500nM SNAP-Surface 649 (New England Biolabs, #S9159S) for 5 minutes at 37ºC for TIR-FM imaging or 1µM permeable SNAP-Cell 647-SiR (New England Biolabs, #S9102S) for 15 minutes followed by a 15 minute wash in cell culture media for confocal imaging. Cells were imaged on a Nikon TiE inverted microscope using a 60x/1.49 Apo-TIRF (Nikon Instruments, Melville, NY) objective in CO_2-independent Leibovitz's L-15 media (Gibco, #11415), supplemented with 1% FBS in a 37ºC heated imaging chamber (In Vivo Scientific). RFP (β-arrestin-1 and β-arrestin-2, 561 nm excitation, 620 emission filter), YFP (Nb39-mVenus and Venus-miniGsi, 488nm excitation, 446/523/600/677 quad-band

filter) and the SNAP labeled DOR (647nm excitation, 700 emission filter when imaged with RFP or 446/523/600/677 quad-band filter when imaged with YFP) were excited with solid state lasers and collected with an iXon + 897 EMCCD camera (Andor, Belfast, UK).

Immunofluorescence and fixed cell imaging

PC12 cells transfected with Flag-DOR and either Nb39-mVenus or Venus-miniGsi were plated on poly-D-lysine coated coverslips and grown at 37ºC for 48 hours. To induce intracellular accumulation of newly synthesized DOR, cells were treated with NGF (100ng/mL) for 1 hour prior to treatment for 15 minutes with 10μM β-chlornaltrexamine (CNA, Sigma-Aldrich, #O001) or CNA followed by 10μM SNC80 (Tocris, #0764) for 5 minutes. Cells were fixed with 4% paraformaldehyde, pH 7.4, for 20 minutes at 25ºC followed by blocking with phosphate-buffered saline (PBS) with 5% fetal bovine serum (FBS), 5% glycine, 0.75% Triton-X-100, 1mM magnesium chloride, and 1mM calcium chloride. Primary and secondary antibody incubations were performed for 1 hour at 25ºC in blocking buffer with anti-Flag-M1 (Sigma-Aldrich, #F3040, 1:1000) conjugated with Alexa-647 (Molecular Probes, #A20186) and anti-TGN-38 rabbit polyclonal antibody (Sigma-Aldrich, #T9826, 1:1000), and goat anti-Rabbit IgG conjugated to Alexa-568 (ThermoFisher, #A-11011, 1:1000), respectively. Cells were washed with blocking buffer without Triton-X-100 after primary and secondary incubations. Coverslips were mounted on glass slides using Prolong Diamond Reagent (Molecular Probes, #P36962). Cells were imaged on a Nikon TiE inverted microscope using a 60x/1.49 Apo-TIRF (Nikon Instruments, Melville, NY) objective and iXon + 897 EMCCD camera (Andor, Belfast, UK).

Live cell FRET imaging

PC12 cells transfected with SNAP-DOR and the ICUE3 FRET sensor were plated and imaged in MatTek dishes (MatTek Life Sciences, #P35G-1.5-14-C) coated with poly-D-lysine. For experiments comparing inhibition of Fsk-stimulated cAMP in cells with and without Golgi DOR, cells in all conditions were treated with cycloheximide

(3μg/mL) for 1 hour before imaging to chase out any receptor transiting through the biosynthetic pathway. To induce a Golgi pool, cells were treated with NGF for 1 hour prior to cycloheximide treatment to build up a pool of internal receptors which is maintained even in the absence of new protein synthesis with NGF maintained in the media during the subsequent cycloheximide incubation (Shiwarski *et al.*, 2017b). Cycloheximide, NGF, and 100μM ICI174864 (ICI, Tocris, #0820), when appropriate, were present in the media for the duration of the experiment. For experiments comparing the signaling of DPDPE (Tocris, #1431) peptide agonist and SNC80 small molecule agonist with and without a surface block, cells in all conditions were treated with 10μM LY294002 for 1hr prior to imaging to induce a Golgi pool of receptor, and LY294002 was maintained in the media throughout the duration of the experiment. Cells were labeled with 1μM permeable SNAP-Cell 647-SiR for 15 minutes followed by a 15 minute wash to visualize receptor. Cells were imaged in L-15 media supplemented with 1% FBS at 25°C in a temperature-controlled imaging chamber (In Vivo Scientific) at 60 second intervals. Imaging was conducted on a Ti2 inverted microscope (Nikon Instruments, Melville, NY) with a 60x NA 1.49 Apo-TIRF objective (Nikon Instruments, Melville, NY). CFP (405 nm excitation, 400 emission filter), YFP or FRET (405nm excitation, 514 emission filter) and the SNAP tagged isoform (647-nm excitation, 700 emission filter) were collected with a iXon-888 Life EMCCD camera (Andor, Belfast, UK) every 30 sec with 5 frames of baseline before 2μM Fsk (Sigma-Aldrich, #F3917) addition to stimulate adenylyl cyclase activity.

Image quantification

All image quantification was performed using ImageJ/Fiji (National Institutes of Health, Bethesda, MD) (Schindelin *et al.*, 2012; Rueden *et al.*, 2017). To quantify biosensor recruitment to intracellular DOR or plasma membrane DOR, the receptor channel at each timepoint was thresholded and used to create a binary mask to isolate only pixels containing receptor signal. The receptor mask from each timepoint was then applied to the corresponding timepoint in the biosensor channel to produce an image of biosensor fluorescence in regions of the cell containing receptor. A region of interest

corresponding to intracellular receptor was selected in confocal images, and in TIRF images a region of interest capturing the entire cell was selected. Mean fluorescence intensity was then measured in these images over time and normalized to average baseline fluorescence before drug addition.

A similar approach was used to measure biosensor recruitment to the Golgi in cells fixed and stained for TGN-38. In these images, TGN-38 was used to create the binary mask, which was then applied to the biosensor channel to isolate biosensor fluorescence in the Golgi region of the cell. An inverse mask of the TGN-38 channel was also created and applied to the biosensor channel to isolate biosensor fluorescence in all other regions of the cell. Biosensor enrichment in the Golgi is expressed as the mean fluorescence intensity in the Golgi region, divided by the mean fluorescence intensity in the rest of the cell. FRET images were analyzed in ImageJ as previously described (Shiwarski *et al.*, 2017b; Weinberg *et al.*, 2017). Briefly, the CFP channel was divided by the FRET channel at each timepoint. A region of interest was defined for each cell in a given field and the resulting CFP/FRET ratio measured at each timepoint. The CFP/FRET ratio was normalized to the mean baseline ratio before drug addition for each cell. Endpoint CFP/FRET ratios (measured as the change of the endpoint value from the baseline of 1) and total cAMP responses (measured as area under the curve) for all cells were normalized to the average of cells in the control condition for each experimental replicate.

Acknowledgements

The authors would like to thank Dr. Alan Smrcka, Dr. Lois Weisman, Dr. Bing Ye, and Candilianne Serrano Zayas for valuable feedback on this project. We also thank Drs. Bryan Roth, Tao Che, Greg Tall, and Nevin Lambert for essential reagents. SEC was supported by National Science Foundation Graduate Research Fellowship under Grant DGE 1256260. MAP was supported by NIH grant GM117425 and National Science Foundation (NSF) grant 1935926.

Supplementary Figures

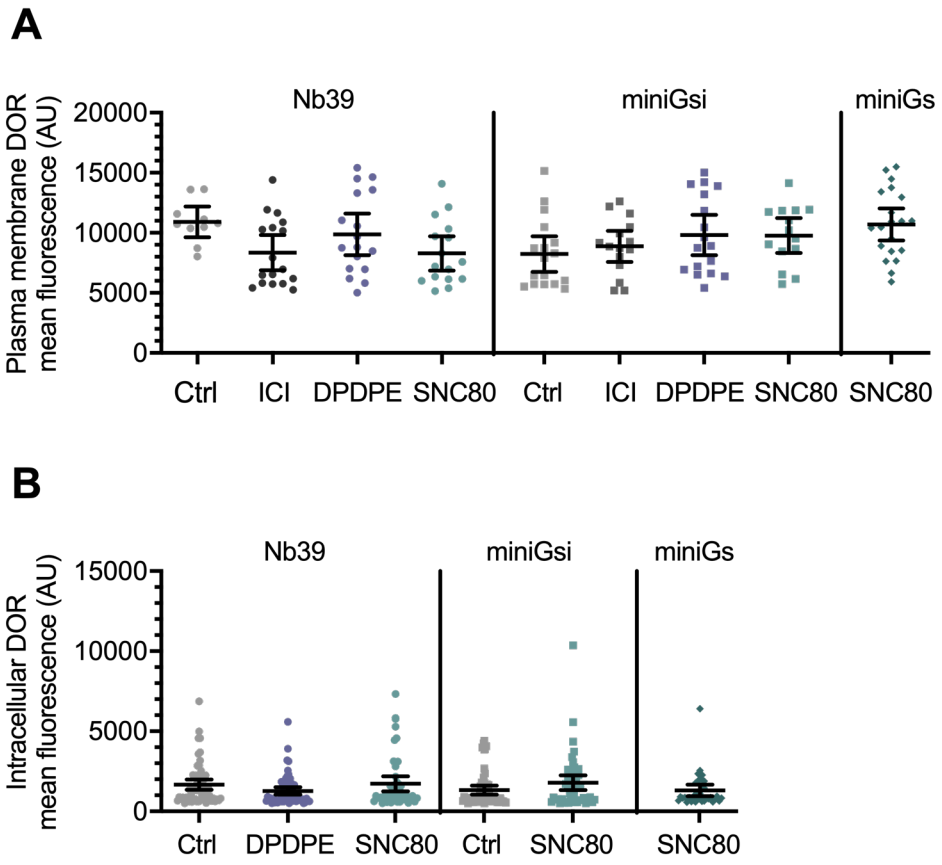

Figure 3.S1. DOR expression levels are similar across treatment conditions.
(A) Plasma membrane DOR expression levels in cells expressing Nb39, miniGsi, or miniGs are similar across untreated or 10μM agonist treatment conditions control (Nb39: Ctrl, n=10 cells; ICI, n=17 cells; DPDPE, n=17 cells; SNC80, n=16 cells; miniGsi: Ctrl, n=17 cells; ICI, n=15 cells; DPDPE, n=17 cells; SNC80, n=14 cells; miniGs-SNC80, n=20 cells; across a minimum of 3 biological replicates; mean +/- 95% CI, points represent individual cells). **(B)** Intracellular DOR expression levels in cells expressing Nb39, miniGsi, or miniGs are similar across untreated or 10μM agonist treatment conditions (Nb39: Ctrl, n=61 cells; DPDPE, n=61 cells; SNC80, n=49 cells; miniGsi: Ctrl, n=57 cells; SNC80, n=51 cells; miniGs: SNC80, n=36 cells; all across 3 biological replicates; mean +/- 95% CI, points represent individual cells).

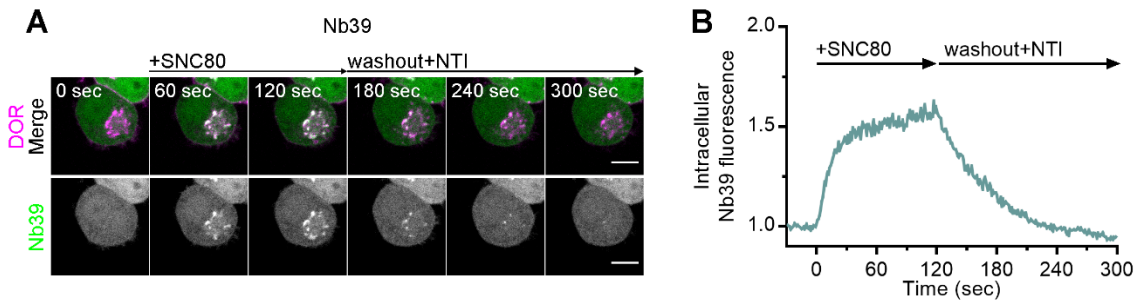

Figure 3.S2. Nb39 recruitment to active DOR is reversible.
(A) PC12 cells expressing SNAP-DOR (magenta in merge) and Nb39-mVenus (green in merge) were imaged live by confocal microscopy. Cells were pretreated with irreversible, impermeable antagonist CNA (1μM) for 15 minutes prior to imaging to inhibit plasma membrane DOR activation and internalization. After 1μM SNC80 treatment, Nb39-mVenus fluorescence increases in a perinuclear region which colocalizes with intracellular DOR (white in merge), and this recruitment is reversed upon a washout, introducing fresh imaging media containing permeable antagonist naltrindole (NTI, 10μM) (scale bar=5μm). **(B)** Representative trace of Nb39 fluorescence in the region of the cell defined by intracellular DOR normalized to mean baseline fluorescence for the cell shown in **(A).**

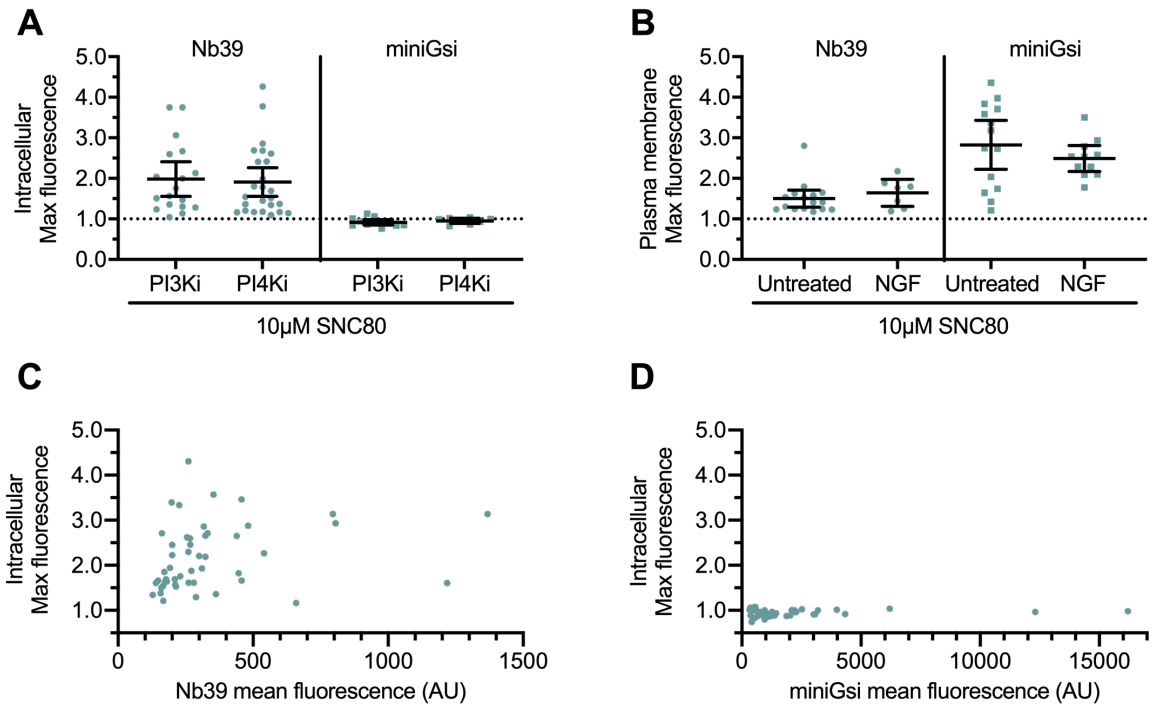

Figure 3.S3. Mechanism of DOR Golgi retention does not influence sensor recruitment to Golgi or PM DOR, and sensor recruitment to intracellular DOR is not correlated with sensor expression.

(A) Nb39, but not miniGsi, max intracellular fluorescence increases over baseline within 120 seconds of 10μM SNC80 addition in cells treated with 10μM PI3K inhibitor LY294002 or 20μM PI4K inhibitor MI14 to induce DOR retention in the Golgi through a DOR specific and non-specific mechanism (Wang *et al.*, 2003; Malhotra and Campelo, 2011), respectively (Nb39: PI3Ki, n=18 cells; PI4Ki, n=25 cells; miniGsi: PI3Ki, n=12 cells; PI4Ki, n=8 cells; all across 1 biological replicate; mean +/- 95% CI, points represent individual cells). **(B)** Nb39 and miniGsi max plasma membrane fluorescence increases to a similar degree within 60 seconds of 10μM SNC80 addition in untreated cells without Golgi DOR and NGF-treated cells with Golgi DOR (Nb39: Untreated, n=16 cells; NGF, n=7 cells; miniGsi: Untreated, n=14cells; NGF, n=11 cells; all across 1 biological replicate; mean +/- 95% CI, points represent individual cells). **(C)** Scatterplot of max intracellular fluorescence increase and corresponding mean Nb39 fluorescence as a measure of sensor expression (n=49 cells, points represent individual cells). Linear regression analysis indicates no significant correlation between max intracellular fluorescence increase and Nb39 expression (R^2=0.05745, p=0.0972). **(D)** Scatterplot of max intracellular fluorescence increase and corresponding mean miniGsi fluorescence as a measure of sensor expression (n=51 cells, points represent individual cells). Linear regression analysis indicates no significant correlation between max intracellular fluorescence increase and miniGsi expression (R^2=0.005465, p=0.6062).

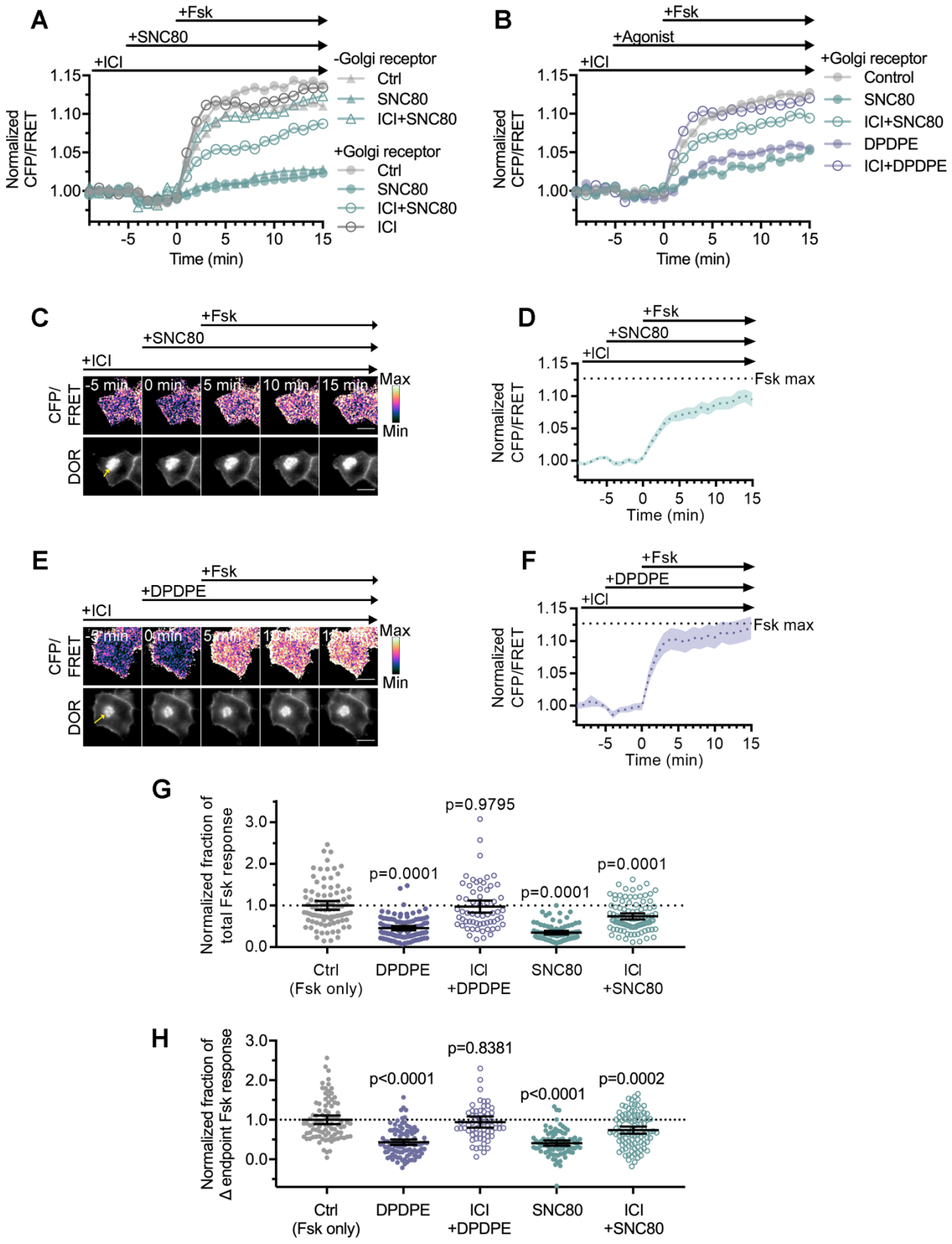

Figure 3.S4. Golgi DOR inhibits cellular cAMP.

(A) Trace of mean cellular cAMP levels in PC12 cells expressing SNAP-DOR and cAMP FRET sensor ICUE3 with and without Golgi receptor. (-Golgi receptor: control, n= 59 cells; SNC80, n=58; ICI+SNC80, n=57; +Golgi DOR: control, n=48; SNC80, n=50; ICI+SNC80, n=55; ICI, n=47). **(B)** Trace of mean cellular cAMP levels in PC12 cells expressing SNAP-DOR and ICUE3 with Golgi receptor and treated with either small molecule agonist SNC80 or peptide agonist DPDPE. (control, n=89 cells; DPDPE, n=101; ICI+DPDPE, n=62; SNC80, n=87; ICI+SNC80, n=95). **(C-F)** Ratiometric CFP/FRET and receptor images, along with corresponding trace of mean cellular CFP/FRET ratios (solid line indicates mean, shading +/- 95% CI), in PC12 cells expressing the ICUE3 cAMP FRET sensor and SNAP-DOR (scale bar=10μm). Calibration bars indicate relative fluorescence values in scaled images. **(C-D)** In cells containing Golgi DOR (**E**, yellow arrow), SNC80 (100nM) decreases Fsk-stimulated cAMP levels even when peptide inverse agonist ICI (100μM) is present in media. **(E-F)** In cells containing Golgi DOR (**C**, yellow arrow), peptide agonist DPDPE (100nM) does not decrease Fsk-stimulated cAMP levels when peptide inverse agonist ICI (100μM) is present in media. **(G-H)** Fsk-stimulated total cAMP levels (area under the curve) **(G)** and endpoint CFP/FRET ratios **(H),** normalized to the mean of control treated cells. Cells in all conditions have intracellular DOR. Total and endpoint cAMP responses are significantly decreased in cells treated with 100nM peptide agonist DPDPE or small molecule agonist SNC80. Total and endpoint cAMP responses are significantly decreased only in cells treated with membrane permeable agonist SNC80 and not DPDPE when 100μM ICI is present in media. (Ctrl, n=89 cells; DPDPE, n=101; ICI+DPDPE, n=62; SNC80, n=87; ICI+SNC80, n=95; all across 3 biological replicates; one-way ANOVA (total, $p<0.0001$; endpoint, $p<0.0001$) with p-values reported in the figure from Dunnett's multiple comparison test for each condition compared to control (Fsk only) condition).

References

Balla, T (2013). Phosphoinositides: Tiny lipids with giant impact on cell regulation. Physiol Rev 93, 1019–1137.

Bindels, DS et al. (2016). MScarlet: A bright monomeric red fluorescent protein for cellular imaging. Nat Methods 14, 53–56.

Cahill, CM, McClellan, KA, Morinville, A, Hoffert, C, Hubatsch, D, O'Donnell, D, and Beaudet, A (2001a). Immunohistochemical distribution of delta opioid receptors in the rat central nervous system: Evidence for somatodendritic labeling and antigen-specific cellular compartmentalization. J Comp Neurol 440, 65–84.

Cahill, CM, Morinville, A, Lee, MC, Vincent, JP, Collier, B, and Beaudet, A (2001b). Prolonged morphine treatment targets delta opioid receptors to neuronal plasma membranes and enhances delta-mediated antinociception. J Neurosci 21, 7598–7607.

Carpenter, B, Nehmé, R, Warne, T, Leslie, AGW, and Tate, CG (2016). Structure of the adenosine A2A receptor bound to an engineered G protein. Nature 536, 104–107.

Chandra, S, Kable, EP, Morrison, GH, and Webb, WW (1991). Calcium sequestration in the Golgi apparatus of cultured mammalian cells revealed by laser scanning confocal microscopy and ion microscopy. J Cell Sci 100.

Che, T et al. (2018). Structure of a nanobody-stabilized active state of the kappa opioid receptor HHS Public Access. Cell 172, 55–67.

Che, T et al. (2020). Nanobody-enabled monitoring of kappa opioid receptor states. Nat Commun 11.

Chen, Y, Mestek, A, Liu, J, and Yu, L (1993). Molecular cloning of a rat κ opioid receptor reveals sequence similarities to the μ and δ opioid receptors. Biochem J 295, 625–628.

Costa-Neto, CM, Parreiras-E-Silva, LT, and Bouvier, M (2016). A pluridimensional view of biased agonism. Mol Pharmacol 90, 587–595.

Crilly, SE, and Puthenveedu, MA (2020). Compartmentalized GPCR Signaling from Intracellular Membranes. J Membr Biol.

Dawaliby, R, Trubbia, C, Delporte, C, Masureel, M, Van Antwerpen, P, Kobilka, BK, and Govaerts, C (2016). Allosteric regulation of G protein-coupled receptor activity by phospholipids. Nat Chem Biol 12, 35–39.

DeFea, KA, Vaughn, ZD, O'Bryan, EM, Nishijima, D, Déry, O, and Bunnett, NW

(2000a). The proliferative and antiapoptotic effects of substance P are facilitated by formation of a β-arrestin-dependent scaffolding complex. Proc Natl Acad Sci U S A 97, 11086–11091.

DeFea, KA, Zalevsky, J, Thoma, MS, Dery, O, Mullins, RD, and Bunnett, NW (2000b). β-Arrestin-dependent endocytosis of proteinase-activated receptor 2 is required for intracellular targeting of activated ERK1/2. J Cell Biol 148, 1267–1281.

Degrandmaison, J et al. (2020). In vivo mapping of a GPCR interactome using knockin mice. Proc Natl Acad Sci U S A 117, 13105–13116.

DiPilato, LM, and Zhang, J (2009). The role of membrane microdomains in shaping β2-adrenergic receptor-mediated cAMP dynamics. Mol Biosyst 5, 832.

Fenalti, G, Giguere, PM, Katritch, V, Huang, X-P, Thompson, AA, Cherezov, V, Roth, BL, and Stevens, RC (2014). Molecular control of d-opioid receptor signalling.

Gaidarov, I, Krupnick, JG, Falck, JR, Benovic, JL, and Keen, JH (1999). Arrestin function in G protein-coupled receptor endocytosis requires phosphoinositide binding.

Gendron, L, Cahill, CM, Zastrow, M Von, Schiller, PW, and Pineyro, G (2016). Molecular Pharmacology of d -Opioid Receptors. 68, 631–700.

Ghanouni, P, Schambye, H, Seifert, R, Lee, TW, Rasmussen, SGF, Gether, U, and Kobilka, BK (2000). The effect of pH on β2 adrenoceptor function. Evidence for protonation- dependent activation. J Biol Chem 275, 3121–3127.

Gillis, A, Kliewer, A, Kelly, E, Henderson, G, Christie, MJ, Schulz, S, and Canals, M (2020). Critical Assessment of G Protein-Biased Agonism at the μ-Opioid Receptor. Trends Pharmacol Sci 41, 947–959.

Gurevich, V V., and Gurevich, E V. (2019a). GPCR signaling regulation: The role of GRKs and arrestins. Front Pharmacol 10.

Gurevich, V V., and Gurevich, E V. (2019b). The structural basis of the arrestin binding to GPCRs. Mol Cell Endocrinol 484, 34–41.

Hellen, EH, and Axelrod, D (1991). Kinetics of Epidermal Growth Factor/Receptor Binding on Cells Measured by Total Internal Reflection/Fluorescence Recovery After Photobleaching.

Hooper, G, and Dick, DAT (1976). Nonuniform distribution of sodium in the rat hepatocyte. J Gen Physiol 67, 469–474.

Huang, W et al. (2015). Structural insights into μ-opioid receptor activation. Nature 524, 315–321.

Ikonen, E (2008). Cellular cholesterol trafficking and compartmentalization. Nat Rev Mol Cell Biol 9, 125–138.

Irannejad, R, Pessino, V, Mika, D, Huang, B, Wedegaertner, PB, Conti, M, and von Zastrow, M (2017). Functional selectivity of GPCR-directed drug action through location bias. Nat Chem Biol 13, 799–806.

Kim, JH, Lingwood, CA, Williams, DB, Furuya, W, Manolson, MF, and Grinstein, S (1996). Dynamic measurement of the pH of the Golgi complex in living cells using retrograde transport of the verotoxin receptor. J Cell Biol 134, 1387–1399.

Kim, K, and von Zastrow, M (2003). Neurotrophin-regulated sorting of opioid receptors in the biosynthetic pathway of neurosecretory cells. J Neurosci 23, 2075–2085.

Koehl, A et al. (2018). Structure of the μ-opioid receptor-G i protein complex.

Latorraca, NR, Venkatakrishnan, AJ, and Dror, RO (2017). GPCR dynamics: Structures in motion. Chem Rev 117, 139–155.

Liu, JJ, Horst, R, Katritch, V, Stevens, RC, and Wüthrich, K (2012). Biased signaling pathways in β2-adrenergic receptor characterized by 19F-NMR. Science (80-) 335, 1106–1110.

Livingston, KE, Mahoney, JP, Manglik, A, Sunahara, RK, and Traynor, JR (2018). Measuring ligand efficacy at the mu-opioid receptor using a conformational biosensor. Elife 7.

Llopis, J, McCaffery, JM, Miyawaki, A, Farquhar, MG, and Tsien, RY (1998). Measurement of cytosolic, mitochondrial, and Golgi pH in single living cells with green fluorescent proteins. Proc Natl Acad Sci U S A 95, 6803–6808.

Luttrell, LM, Maudsley, S, and Bohn, LM (2015). Fulfilling the promise of “biased” g protein-coupled receptor agonism. Mol Pharmacol 88, 579–588.

Malhotra, V, and Campelo, F (2011). PKD regulates membrane fission to generate TGN to cell surface transport carriers. Cold Spring Harb Perspect Biol 3, 1–9.

Manglik, A et al. (2015). Structural insights into the dynamic process of β2-adrenergic receptor signaling. Cell 161, 1101–1111.

Manglik, A, Kobilka, BK, and Steyaert, J (2017). Nanobodies to Study G Protein–Coupled Receptor Structure and Function. Annu Rev Pharmacol Toxicol 57, 19–37.

McDonald, PH, Chow, C-W, Miller, WE, Laporte, SA, Field, ME, Lin, F-T, Davis, RJ, and Lefkowitz, RJ (2000). beta -Arrestin 2: A Receptor-Regulated MAPK Scaffold for the Activation of JNK3. Science (80-) 290, 1574–1577.

Van Meer, G, Voelker, DR, and Feigenson, GW (2008). Membrane lipids: Where they are and how they behave. Nat Rev Mol Cell Biol 9, 112–124.

Meyer, J, Del Vecchio, G, Seitz, V, Massaly, N, and Stein, C (2019). Modulation of μ-opioid receptor activation by acidic pH is dependent on ligand structure and an ionizable amino acid residue. Br J Pharmacol 176, 4510–4520.

Miesenböck, G, De Angelis, DA, and Rothman, JE (1998). Visualizing secretion and synaptic transmission with pH-sensitive green fluorescent proteins. Nature 394, 192–195.

Mittal, N et al. (2013). Select G-protein coupled receptors modulate agonist-induced signaling via a ROCK, LIMK and β-arrestin 1 pathway. Cell Rep 5.

Nash, CA, Wei, W, Irannejad, R, and Smrcka, A V. (2019). Golgi localized βi-adrenergic receptors stimulate golgi PI4P hydrolysis by PLCε to regulate cardiac hypertrophy. Elife 8.

Nehmé, R, Carpenter, B, Singhal, A, Strege, A, Edwards, PC, White, CF, Du, H, Grisshammer, R, and Tate, CG (2017). Mini-G proteins: Novel tools for studying GPCRs in their active conformation. PLoS One 12.

Nygaard, R et al. (2013). The dynamic process of β2-adrenergic receptor activation. Cell 152, 532–542.

Okude, J et al. (2015). Identification of a Conformational Equilibrium That Determines the Efficacy and Functional Selectivity of the μ-Opioid Receptor. Angew Chemie - Int Ed 54, 15771–15776.

Patwardhan, AM, Berg, KA, Akopain, AN, Jeske, NA, Gamper, N, Clarke, WP, and Hargreaves, KM (2005). Bradykinin-Induced Functional Competence and Trafficking of the ʕ -Opioid Receptor in Trigeminal Nociceptors. 25, 8825–8832.

Pert, CB, and Snyder, SH (1973). Properties of opiate receptor binding in rat brain. Proc Natl Acad Sci U S A 70, 2243–2247.

Peterson, YK, and Luttrell, LM (2017). The Diverse Roles of Arrestin Scaffolds in G Protein-Coupled Receptor Signaling. Pharmacol Rev 69, 256–297.

Pradhan, A, Smith, M, McGuire, B, Evans, C, and Walwyn, W (2013). Chronic inflammatory injury results in increased coupling of delta opioid receptors to voltage-gated Ca2+ channels. Mol Pain 9, 8.

Rueden, CT, Schindelin, J, Hiner, MC, DeZonia, BE, Walter, AE, Arena, ET, and Eliceiri, KW (2017). ImageJ2: ImageJ for the next generation of scientific image data. BMC Bioinformatics 18, 529.

Schindelin, J et al. (2012). Fiji: An open-source platform for biological-image analysis. Nat Methods 9, 676–682.

Shiwarski, DJ, Crilly, SE, Dates, A, and Puthenveedu, MA (2019). Dual RXR motifs regulate nerve growth factor–mediated intracellular retention of the delta opioid receptor. Mol Biol Cell 30, 680–690.

Shiwarski, DJ, Darr, M, Telmer, CA, Bruchez, MP, and Puthenveedu, MA (2017a). PI3K class II α regulates δ-opioid receptor export from the trans-Golgi network. Mol Biol Cell 28, 2202–2219.

Shiwarski, DJ, Tipton, A, Giraldo, MD, Schmidt, BF, Gold, MS, Pradhan, AA, and Puthenveedu, MA (2017b). A PTEN-regulated checkpoint controls surface delivery of σ opioid receptors. J Neurosci 37, 3741–3752.

St-Louis, É, Degrandmaison, J, Grastilleur, S, Génier, S, Blais, V, Lavoie, C, Parent, J-L, and Gendron, L (2017). Involvement of the coatomer protein complex I in the intracellular traffic of the delta opioid receptor. Mol Cell Neurosci 79, 53–63.

Stoeber, M, Jullié, D, Li, J, Chakraborty, S, Majumdar, S, Lambert, NA, Manglik, A, and von Zastrow, M (2020). Agonist-selective recruitment of engineered protein probes and of GRK2 by opioid receptors in living cells. Elife 9.

Stoeber, M, Jullié, D, Lobingier, BT, Laeremans, T, Steyaert, J, Schiller, PW, Manglik, A, and von Zastrow, M (2018). A Genetically Encoded Biosensor Reveals Location Bias of Opioid Drug Action. Neuron 98, 963-976.e5.

Strohman, MJ, Maeda, S, Hilger, D, Masureel, M, Du, Y, and Kobilka, BK (2019). Local membrane charge regulates β2 adrenergic receptor coupling to Gi3. Nat Commun 10, 1–10.

Suomivuori, CM et al. (2020). Molecular mechanism of biased signaling in a prototypical

G protein-coupled receptor. Science (80-) 367, 881–887.

Vetter, I, Kapitzke, D, Hermanussen, S, Monteith, GR, and Cabot, PJ (2006). The Effects of pH on Beta-Endorphin and Morphine Inhibition of Calcium Transients in Dorsal Root Ganglion Neurons. J Pain 7, 488–499.

Virk, MS, and Williams, JT (2008). Agonist-specific regulation of μ-opioid receptor desensitization and recovery from desensitization. Mol Pharmacol 73, 1301–1308.

Viscusi, ER, Skobieranda, F, Soergel, DG, Cook, E, Burt, DA, and Singla, N (2019). APOLLO-1: A randomized placebo and activecontrolled phase iii study investigating oliceridine (TRV130), a G protein-biased ligand at the μ-opioid receptor, for management of moderateto-severe acute pain following bunionectomy. J Pain Res 12, 927–943.

Wan, Q, Okashah, N, Inoue, A, Nehmé, R, Carpenter, B, Tate, CG, and Lambert, NA (2018). Mini G protein probes for active G protein-coupled receptors (GPCRs) in live cells. J Biol Chem, jbc.RA118.001975.

Wang, H, and Pickel, VM (2001). Preferential cytoplasmic localization of delta-opioid receptors in rat striatal patches: comparison with plasmalemmal mu-opioid receptors. J Neurosci 21, 3242–3250.

Wang, YJ, Wang, J, Sun, HQ, Martinez, M, Sun, YX, Macia, E, Kirchhausen, T, Albanesi, JP, Roth, MG, and Yin, HL (2003). Phosphatidylinositol 4 Phosphate Regulates Targeting of Clathrin Adaptor AP-1 Complexes to the Golgi. Cell 114, 299–310.

Weinberg, ZY, Zajac, AS, Phan, T, Shiwarski, DJ, and Puthenveedu, MA (2017). Sequence-Specific Regulation of Endocytic Lifetimes Modulates Arrestin-Mediated Signaling at the μ Opioid Receptor. Mol Pharmacol 91, 416–427.

Weis, WI, and Kobilka, BK (2018). The Molecular Basis of G Protein–Coupled Receptor Activation. Annu Rev Biochem 87, 897–919.

Wingler, LM, Elgeti, M, Hilger, D, Latorraca, NR, Lerch, MT, Staus, DP, Dror, RO, Kobilka, BK, Hubbell, WL, and Lefkowitz, RJ (2019). Angiotensin Analogs with Divergent Bias Stabilize Distinct Receptor Conformations. Cell 176, 468-478.e11.

Wingler, LM, Skiba, MA, McMahon, C, Staus, DP, Kleinhenz, ALW, Suomivuori, CM, Latorraca, NR, Dror, RO, Lefkowitz, RJ, and Kruse, AC (2020). Angiotensin and biased analogs induce structurally distinct active conformations within a GPCR. Science (80-) 367, 888–892.

Wootten, D, Christopoulos, A, Marti-Solano, M, Babu, MM, and Sexton, PM (2018). Mechanisms of signalling and biased agonism in G protein-coupled receptors. Nat Rev Mol Cell Biol 19, 638–653.

Ye, L, Van Eps, N, Zimmer, M, Ernst, OP, and Scott Prosser, R (2016). Activation of the A 2A adenosine G-protein-coupled receptor by conformational selection. Nature 533, 265–268.

Yen, HY et al. (2018). PtdIns(4,5)P2 stabilizes active states of GPCRs and enhances selectivity of G-protein coupling. Nature 559, 423–427.

Zarzycka, B, Zaidi, SA, Roth, BL, and Katritch, V (2019). Harnessing ion-binding sites for GPCR pharmacology. Pharmacol Rev 71, 571–595.

Zhang, J, Ferguson, SSG, Law, PY, Barak, LS, and Caron, MG (1999). Agonist-specific regulation of δ-opioid receptor trafficking by G protein-coupled receptor kinase and β-arrestin. In: Journal of Receptor and Signal Transduction Research, Marcel Dekker Inc., 301–313.

Zhang, X, Bao, L, Arvidsson, U, Elde, R, and Hökfelt, T (1998). Localization and regulation of the delta-opioid receptor in dorsal root ganglia and spinal cord of the rat and monkey: evidence for association with the membrane of large dense-core vesicles. Neuroscience 82, 1225–1242.

Zhang, X, Wang, F, Chen, X, Li, J, Xiang, B, Zhang, YQ, Li, BM, and Ma, L (2005). β-arrestin1 and β-arrestin2 are differentially required for phosphorylation-dependent and -independent internalization of δ-opioid receptors. J Neurochem 95, 169–178.

Chapter 4: Calcium Release From Intracellular Stores Is Regulated by Specific Subcellular Pools of the Delta Opioid Receptor in Rat Neuroendocrine Cells

Abstract[4]

The G protein-coupled receptor (GPCR) family of transmembrane signaling receptors transduce signals, including light, ions, and neurotransmitters, into a diverse array of cell signaling events. An active GPCR can modulate multiple second messenger signaling molecules in the cell which can vary based on the cellular context in which signaling occurs. The subcellular location in which GPCR signaling occurs has emerged as an important factor influencing GPCR signaling responses, but we lack a clear understanding of how GPCR localization alters signaling for many clinically relevant GPCRs. Here we use the delta opioid receptor (DOR), a clinically relevant GPCR for the treatment of pain which can localize to both the plasma membrane and the Golgi in neuronal cells, to investigate how DOR subcellular localization affects regulation of calcium, an important signaling molecule linked to DOR's pain-relieving effects. We show that DOR activation at the plasma membrane causes intracellular calcium release in a Gi/o, Gαq, and phospholipase C-dependent manner. Importantly, this calcium signaling response is specifically regulated by DOR localized to the plasma membrane and is not mediated by DOR localized to the Golgi. Though the mechanisms underlying subcellular-specific regulation of calcium by DOR are still being investigated, we present preliminary data to suggest that Golgi DOR does not activate PLC activity locally at the Golgi. Together these data provide important insight into how GPCR subcellular localization determines signaling pathways activated downstream of a GPCR.

[4] Statement of others' contributions to this work:
In addition to writing this chapter, I performed all experiments measuring calcium signaling with GCaMP6f, as well as YFP-DBD imaging experiments. Kasun Ratnayake performed all experiments measuring calcium signaling with Fluo-4 AM and provided helpful feedback on this written chapter. Zara Weinberg developed the Python script used to quantify GCaMP6f and Fluo-4 AM fluorescence changes.

Introduction

G protein-coupled receptors (GPCRs) transduce a wide variety of signals into diverse and complex cellular responses. These complex responses result from GPCR regulation of a wide array of cellular signaling events through activation of effector proteins, including heterotrimeric G proteins and arrestins (Weis and Kobilka, 2018; Wu *et al.*, 2019). The array of responses activated by a GPCR can be thought of as a signaling profile. This signaling profile is shaped by interaction of a GPCR with available effector proteins and the availability of cellular substrates of these effector proteins in a specific cellular context. Defining how this signaling profile is altered in different cellular contexts will improve our understanding of GPCR physiology and therapeutic targeting of these receptors.

The subcellular location of GPCR signaling has been recently identified as a contributor to the GPCR signaling profile (Crilly and Puthenveedu, 2020). Increasing evidence supports the idea that GPCRs can signal from multiple cellular locations in addition to the plasma membrane (PM) (Jong *et al.*, 2018; Lobingier and von Zastrow, 2019; Crilly and Puthenveedu, 2020), but the ways in which subcellular context alters the signaling profile of clinically relevant GPCRs are not fully understood.

Here we use the delta opioid receptor (DOR) as a prototype GPCR to study how receptor subcellular localization affects regulation of second messenger signaling molecules. DOR, a clinically relevant GPCR target for the treatment of pain and depression, localizes to both the PM and intracellular compartments, including the Golgi, in neuronal cells (Roth *et al.*, 1981; Cahill *et al.*, 2001; Wang and Pickel, 2001; Kim and von Zastrow, 2003; Shiwarski *et al.*, 2017b; Abdallah and Gendron, 2018; Dripps and Jutkiewicz, 2018). DOR modulation of second messenger signaling molecules, including cAMP and calcium, is linked to its pain-relieving effects, and DOR localization to the PM is associated with enhanced pain relieving effects of DOR agonists (Cahill *et al.*, 2003; Pradhan *et al.*, 2013; Gendron *et al.*, 2016; Shiwarski *et al.*, 2017b). Whether DOR localization to the PM versus intracellular compartments like the Golgi alters regulation of second messenger signaling molecules is an important unanswered question. Previous work from our lab and others has shown that DOR

inhibits cAMP production from both the PM and Golgi (Stoeber *et al.*, 2018; Crilly *et al.*, 2021), but the impact of DOR Golgi localization on calcium regulation is unknown.

We performed live cell imaging with calcium biosensors to define the signaling pathway by which DOR modulates calcium in rat neuroendocrine pheochromocytoma (PC12) cells. PC12 cells and neurons share common mechanisms regulating DOR localization to the Golgi which we use to test how DOR subcellular localization affects calcium signaling (Kim and von Zastrow, 2003; Shiwarski *et al.*, 2017a, 2017b). We have shown that DOR activation increases intracellular calcium levels in PC12 cells through a mechanism which requires Gi/o and Gαq/11 proteins, phospholipase C (PLC), and calcium release from intracellular stores. Modulation of calcium is specific to DOR signaling at the PM, highlighting the direct impact of DOR subcellular localization on its signaling profile.

Results

DOR activation increases intracellular calcium in PC12 cells

DOR regulates cellular calcium via multiple mechanisms many of which have been linked to the role of DOR in the nervous system and modulation of pain (Ohsawa *et al.*, 1998; Gendron *et al.*, 2016). We measured intracellular calcium in PC12 cells expressing SNAP-DOR and the calcium sensor GCaMP6f, which exhibits increased fluorescence when bound to calcium (Chen *et al.*, 2013). DOR localization to the Golgi is specifically and acutely regulated in PC12 cells in response to nerve growth factor (NGF) treatment, and in the absence of NGF, DOR localizes primarily to the PM **(Figure 4.1A, lower panel)** (Kim and von Zastrow, 2003; Shiwarski *et al.*, 2017b, 2019). We first characterized calcium signaling in the absence of NGF to define the signaling pathways by which PM DOR regulates calcium in PC12 cells.

When cells expressing DOR were treated with DOR agonist SNC80 (10μM), GCaMP6f fluorescence rapidly increases, before returning to baseline **(Figure 4.1A-B)**. Both small molecule agonist, SNC80, and peptide agonists, DADLE and DPDPE, increased the max fold change in GCaMP6f fluorescence over baseline after agonist addition **(Figure 4.1C)**. These increases were not observed in untransfected cells

treated with agonists **(Figure 4.1C)**, and the magnitude of calcium responses were positively correlated with DOR expression **(Figure 4.S1)**, indicating these responses are DOR-dependent. PC12 cells stably expressing FAP-DOR and treated with SNC80 also exhibited dose-dependent increases in cellular calcium indicated by fluorescence of calcium indicator dye Fluo-4 AM **(Figure 4.1D)**. Together, these data demonstrate that in PC12 cells, DOR couples to signaling pathways which increase intracellular calcium levels.

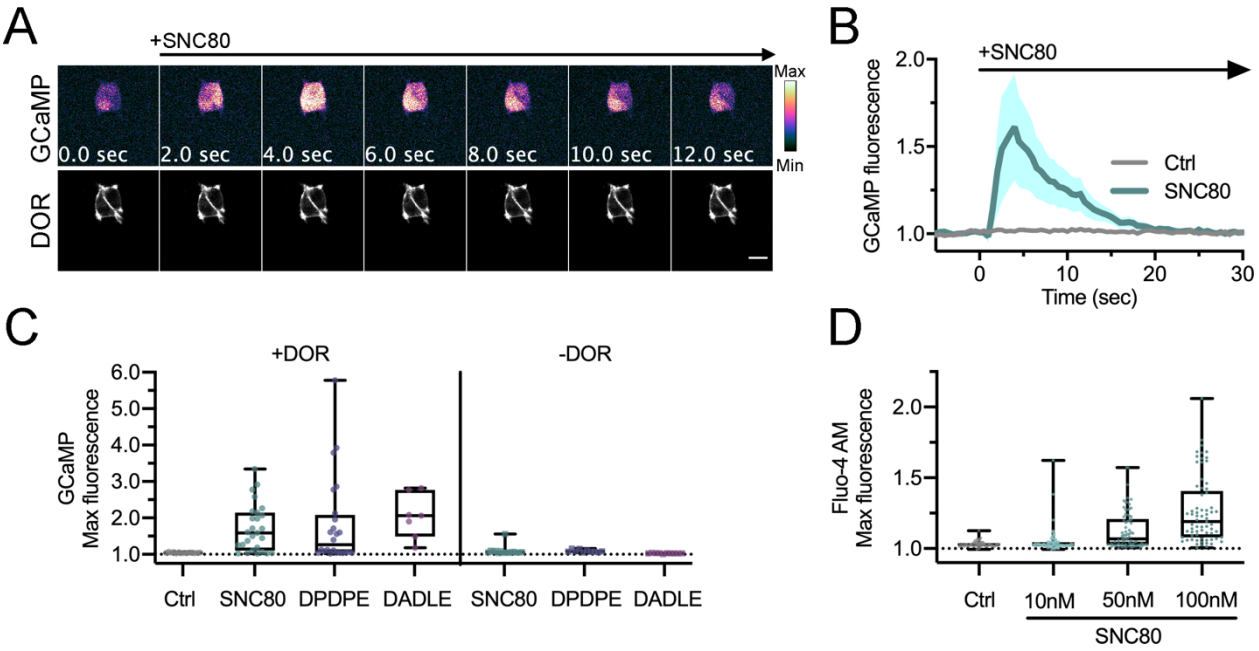

Figure 4.1. DOR agonists increase intracellular calcium levels in PC12 cells.
(A) PC12 cells expressing GCaMP6f (upper panel) and SNAP-DOR (lower panel) were imaged live by confocal microscopy. Calibration bar represents pixel values in scaled GCaMP image. Treatment with 10μM SNC80 leads to a rapid increase in GCaMP6f fluorescence, (Scale bar=15μM). **(B)** GCaMP6f fluorescence normalized to mean baseline fluorescence over time in cells treated with SNC80 (10μM) or DMSO control (Ctrl) (solid line indicates mean, shading +/- 95% CI; Ctrl n=14 cells; SNC80 n=27). **(C)** Maximum GCaMP6f fluorescence increases in cells transfected with SNAP-DOR in response to DOR agonists SNC80, DPDPE, and DADLE (10μM). This increase is not observed in untransfected cells (+DOR, Ctrl n=14, SNC80 n=27, DPDPE n=24, DADLE n=7; -DOR, SNC80 n=15, DPDPE n=10, DADLE n=10; box represents 25th to 75th percentiles, whiskers represent min to max, points represent individual cells). **(D)** Maximum Fluo-4 AM fluorescence increases in PC12 cells stably expressing FAP-DOR in a dose-dependent manner in response to SNC80 (Ctrl n=51, 10nM SNC80 n=85, 50nM SNC80 n=78, 100nM SNC80 n=69; box represents 25th to 75th percentiles, whiskers represent min to max, points represent individual cells).

DOR requires Gi/o, Gαq/11, and PLC to mobilize intracellular calcium stores

Gq/11 and Gi/o-coupled GPCRs can increase intracellular calcium levels (Ma *et al.*, 2017). Both Gβγ, dissociated from activated Gαi/o subunits, and free Gαq can activate phospholipase C (PLC) enzymes (Smrcka *et al.*, 1991; Chang Ho Lee *et al.*, 1992; Smrcka and Sternweis, 1993). PLC-induced hydrolysis of phosphatidylinositol-4,5-bisphosphate ($PI(4,5)P_2$) produces diacylglycerol (DAG) and inositol 1,4,5-trisphosphate (IP_3), the latter of which activates the IP_3 receptor (IP_3R) on the endoplasmic reticulum (ER) to promote calcium release from intracellular stores (Berridge, 2009). Gi/o and Gq-coupled GPCRs can also synergistically activate PLC enzymes, and this synergy may be essential for the activation of PLC-dependent signaling pathways by Gi/o-coupled GPCRs in cells (Philip *et al.*, 2010; Rebres *et al.*, 2011; Lyon and Tesmer, 2013; Pfeil *et al.*, 2020).

We tested the contribution of both Gαq/11 and Gi/o proteins to the DOR-dependent calcium response. We treated cells with bradykinin, an agonist for bradykinin receptors endogenously expressed in PC12 cells, as a control for Gq-coupled GPCR responses (Fasolato *et al.*, 1990; Reber *et al.*, 1992; Gafni *et al.*, 1997). In PC12 cells expressing SNAP-DOR and GCaMP6f the magnitude of the calcium response was much lower in cells treated with SNC80 compared to bradykinin **(Figure 4.2A-B)**. This relative difference in response magnitude is consistent with previous reports comparing calcium responses between Gq and Gi/o-coupled GPCRs (Jin *et al.*, 1994; Spencer *et al.*, 1997; Yoon *et al.*, 1999), suggesting DOR modulates calcium levels through Gi/o proteins. To test requirement of these G proteins specifically we treated cells with either the Gi/o inhibitor pertussis toxin (PTX) or the Gαq/11 inhibitor YM-254890 (YM) (Katada, 2012; Xiong *et al.*, 2019). PTX treatment completely abolished the SNC80 calcium response, but had no effect on the bradykinin calcium response **(Figure 4.2C)**. Interestingly, YM abolished both the SNC80 and bradykinin calcium responses. Given that calcium responses were correlated with DOR expression **(Figure 4.S1A)**, we measured DOR expression levels and found they were similar across treatment conditions as an important control **(Figure 4.S2A)**. These data are consistent with

bradykinin activation of Gq-coupled GPCRs and suggest that DOR-dependent regulation of calcium levels requires both Gi/o and Gαq/11 proteins.

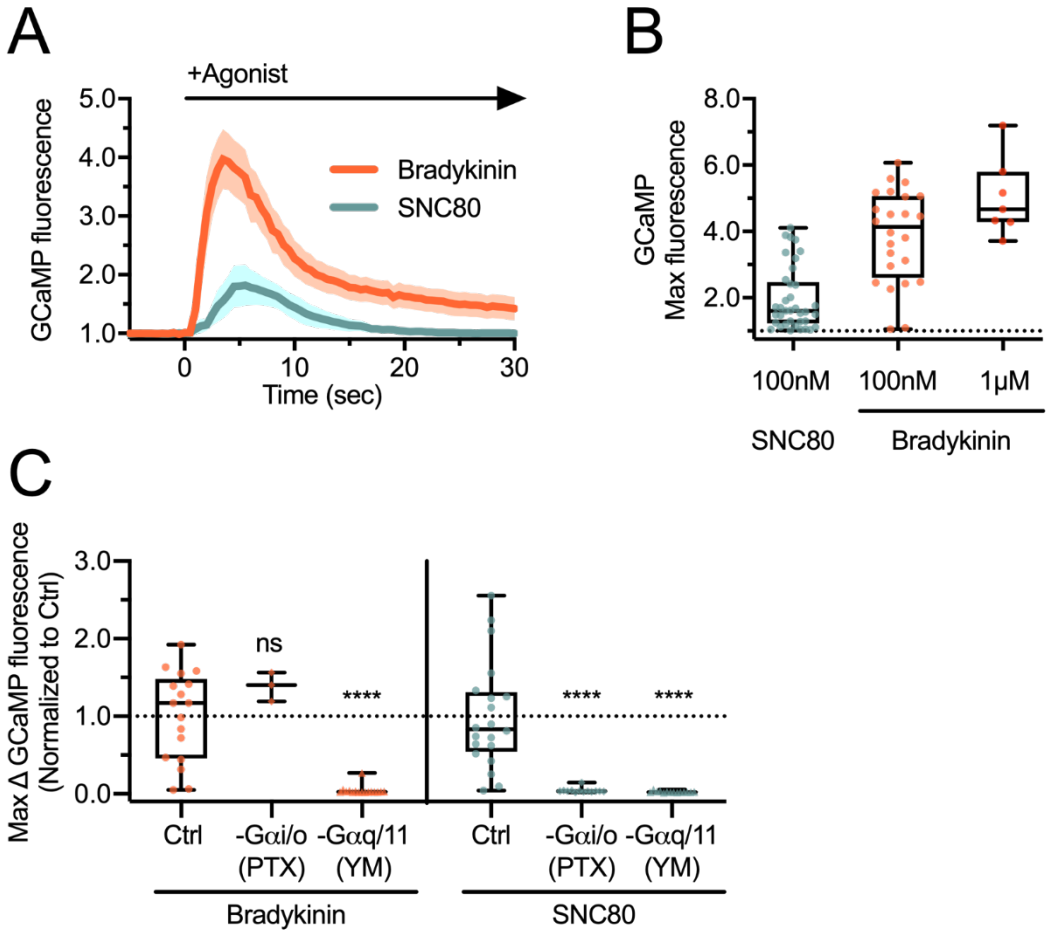

Figure 4.2. DOR-dependent calcium response requires both Gαi/o and Gαq/11. **(A)** GCaMP6f fluorescence normalized to mean baseline fluorescence over time after addition of either bradykinin (100nM) or SNC80 (100nM) (Bradykinin, n=24 cells; SNC80, n=37) (solid line indicates mean, shading +/- 95% CI). **(B)** Maximum GCaMP6f fluorescence increase over baseline in cells treated with SNC80 (100nM) or bradykinin (100nM or 1μM) (Bradykinin, 100nM, n=24, 1μM, n=7; SNC80, n=37). **(C)** Maximum change in GCaMP6f fluorescence over baseline, normalized to the respective control (Ctrl), 100nM bradykinin or 100nM SNC80. Pertussis toxin (PTX, 50ng/mL) treatment significantly decreased the change in GCaMP6f fluorescence in response to SNC80, but not bradykinin (one sample t-test compared to theoretical mean of 1; Bradykinin PTX, p=0.0696; SNC80 PTX, p<0.0001). YM-254890 (YM, 1μM) treatment significantly decreased the change in GCaMP6f fluorescence in response to both bradykinin and SNC80 (one sample t-test compared to a theoretical mean of 1, p<0.0001). (Bradykinin, Ctrl n=17, PTX n=3, YM n=16; SNC80, Ctrl n=20, PTX n=13, YM n=14; box represents 25th to 75th percentiles, whiskers represent min to max, points represent individual cells).

Because both Gi/o and Gq-coupled pathways converge on regulation of PLC and subsequent release of calcium from intracellular stores, we tested the requirement of this signaling pathway **(Figure 4.3A)** for DOR calcium responses. We treated PC12 cells expressing SNAP-DOR and GCaMP6f with PLC inhibitor U73122, or its negative control analog compound U73343 (Bleasdale *et al.*, 1990). U73122, but not U73343, significantly decreased the SNC80 calcium response, compared to control (Ctrl) cells treated with SNC80 alone **(Figure 4.3B)**. Additionally, depletion of ER calcium stores by treatment with thapsigargin (Treiman *et al.*, 1998) or inhibition of IP_3R with 2-APB (Bilmen and Michelangeli, 2002) significantly decreased the calcium response compared to control cells **(Figure 4.3B)**. DOR expression levels were similar across all treatment conditions **(Figure 4.S2B)**. These data indicate that both PLC and intracellular calcium stores are required for DOR calcium responses, consistent with known Gi/o and Gq-regulated signaling pathways.

To further confirm that DOR activates PLC, we used a fluorescently-tagged biosensor containing the DAG binding domain (DBD) of protein kinase Cβ to visualize DAG production at the PM following DOR activation (Gallegos *et al.*, 2006). PC12 cells expressing SNAP-DOR and YFP-DBD were imaged using total internal fluorescence reflection microscopy (TIRF-M) to visualize the sensor recruitment at the PM, as a readout of DAG production. Sensor fluorescence at the PM rapidly and transiently increased upon SNC80 addition **(Figure 4.3C-D)**, consistent with production of DAG following PLC hydrolysis of $PI(4,5)P_2$ at the PM. Maximum sensor fluorescence at the PM significantly increased in SNC80-treated cells compared to the vehicle-treated control cells **(Figure 4.3E)**. These data further support DOR-induced activation of PLC, consistent with the requirement of PLC activity for DOR-dependent calcium responses.

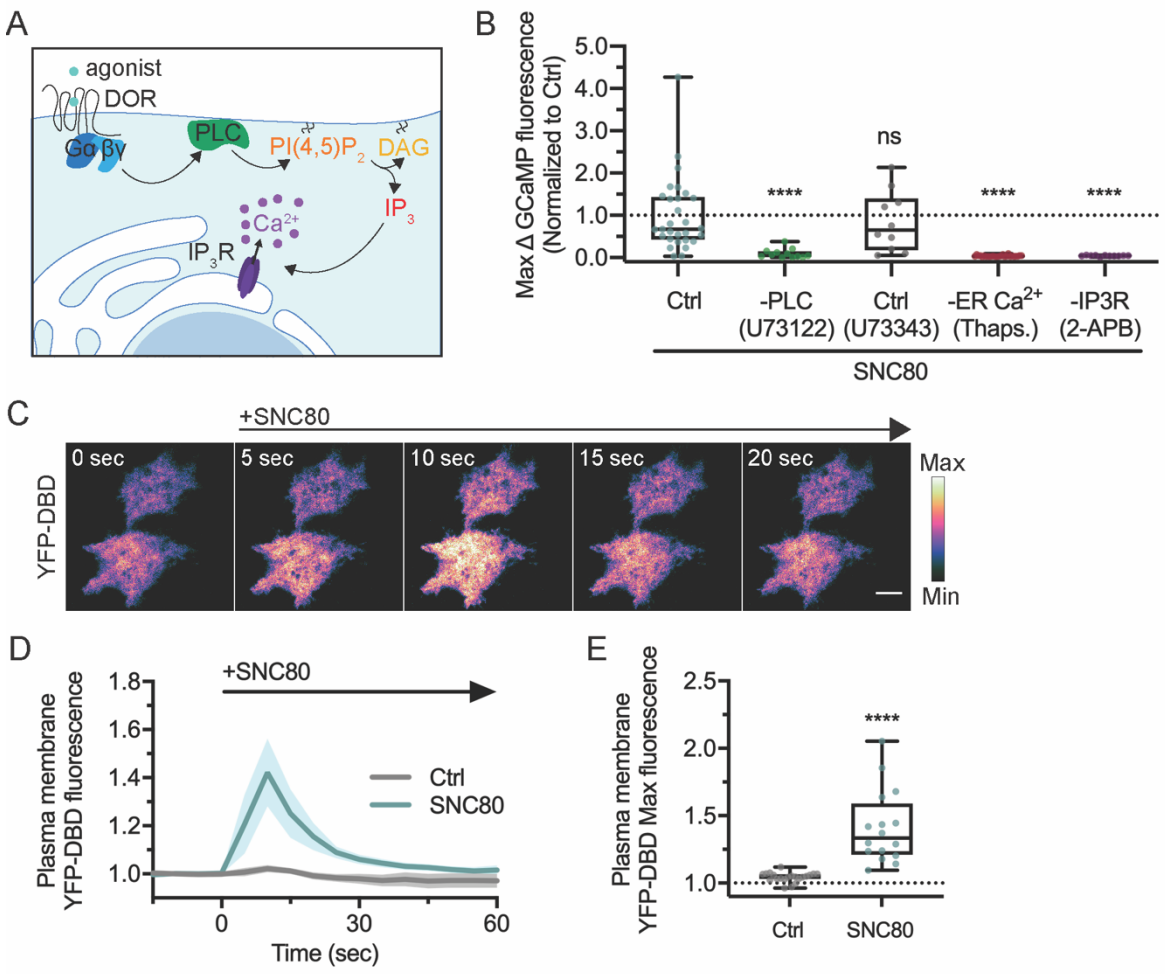

Figure 4.3. DOR mobilizes calcium from intracellular stores through a PLC-dependent pathway.

(A) PLC-dependent hydrolysis of PIP2 produces IP3 which acts on the IP3 receptor at the ER, promoting calcium release from intracellular stores into the cytoplasm. **(B)** Maximum change in GCaMP6f fluorescence over baseline, normalized to control (Ctrl), 100nM SNC80. Treatment with PLC inhibitor U73122 (10μM), but not control compound U73343 (10μM), significantly decreased the change in GCaMP6f fluorescence in response to SNC80 (one sample t-test compared to a theoretical mean of 1, U73122 $p<0.0001$, U73343 $p=0.5151$). Treatment with thapsigargin (Thaps., 1μM) to deplete ER calcium stores or IP3R antagonist 2-APB (500μM) also significantly decreased the change in GCaMP6f fluorescence in response to SNC80 (one sample t-test compared to a theoretical mean of 1, thapsigargin $p<0.0001$, 2-APB $p<0.0001$) (Ctrl n=29 cells; U73122 n=12; U73343 n=10; thapsigargin n=26; 2-APB n=11; box represents 25th to 75th percentiles, whiskers represent min to max, points represent individual cells). **(C)** YFP-DBD in PC12 cells expressing SNAP-DOR imaged using TIR-FM to capture recruitment to the PM after addition of DOR agonist SNC80 (100nM) (scale bar=5μm). Calibration bar indicates pixel values in scaled image. **(D)** Increase in YFP-DBD fluorescence by TIR-FM

normalized to the mean baseline fluorescence over time after addition of 100nM SNC80 (solid line indicates mean, shading +/- 95% CI). **(E)** Maximum PM YFP-DBD fluorescence increase over baseline after SNC80 addition is significantly increased compared to vehicle control (two tailed t-test, $p<0.0001$) (For **D** and **E**, Ctrl n=21, SNC80 n=16; box represents 25^{th} to 75^{th} percentiles, whiskers represent min to max, points represent individual cells).

Intracellular calcium release is specific to PM DOR signaling

Given increasing evidence that GPCRs activate numerous signaling pathways from intracellular compartments, and that Golgi DOR inhibits cAMP production (Stoeber *et al.*, 2018; Crilly *et al.*, 2021), suggestive of coupling to inhibitory G proteins, we next asked whether Golgi DOR promotes calcium release from intracellular stores, like PM DOR.

To specifically test the ability of Golgi DOR to regulate calcium release, we treated PC12 cells with NGF which acutely arrests Golgi export of newly synthesized DOR through mechanisms shared between PC12 cells and neurons (Kim and von Zastrow, 2003; Shiwarski *et al.*, 2017a, 2017b). All prior experiments **(Figures 4.1-4.3)** were performed in the absence of NGF with DOR localized primarily to the PM **(Figure 4.4A, lower panel)**. Following NGF treatment, cells contain both a PM and Golgi pool of DOR **(Figure 4.4B, lower panel, yellow arrow)**. We then used a paradigm developed previously in which high concentrations of peptide, membrane-impermeable inverse agonist ICI174,864 (ICI) were applied to pharmacologically block DOR binding sites at the PM (Stoeber *et al.*, 2018; Crilly *et al.*, 2021). Intracellular receptors were then activated by small molecule, membrane permeable agonist SNC80 to test their contribution to the signaling response. The signaling response to combined ICI and SNC80 treatment was then compared between cells in the absence of Golgi receptor (-Golgi) and presence of Golgi receptor (+Golgi, NGF treated).

In cells with and without Golgi DOR, treatment with only 100nM SNC80 produced similar increases in calcium **(Figure 4.4A-B, right panels, solid line)**. However, when 100μM ICI was present in the imaging media, the calcium response was completely abolished in cells with and without Golgi DOR **(Figure 4.4A-B, dotted lines)**. Indeed, in cells with and without Golgi DOR, inhibition of PM DOR with ICI significantly decreased

the SNC80-induced calcium increase compared to control cells treated with SNC80 alone **(Figure 4.4C)**. ICI alone caused no change in cellular calcium levels **(Figure 4.4C)**. We performed the same set of experiments using the peptide, membrane impermeable agonist DPDPE, and found similar results **(Figure 4.4D)**. DOR expression levels were similar across all treatment conditions **(Figure 4.S3)**.

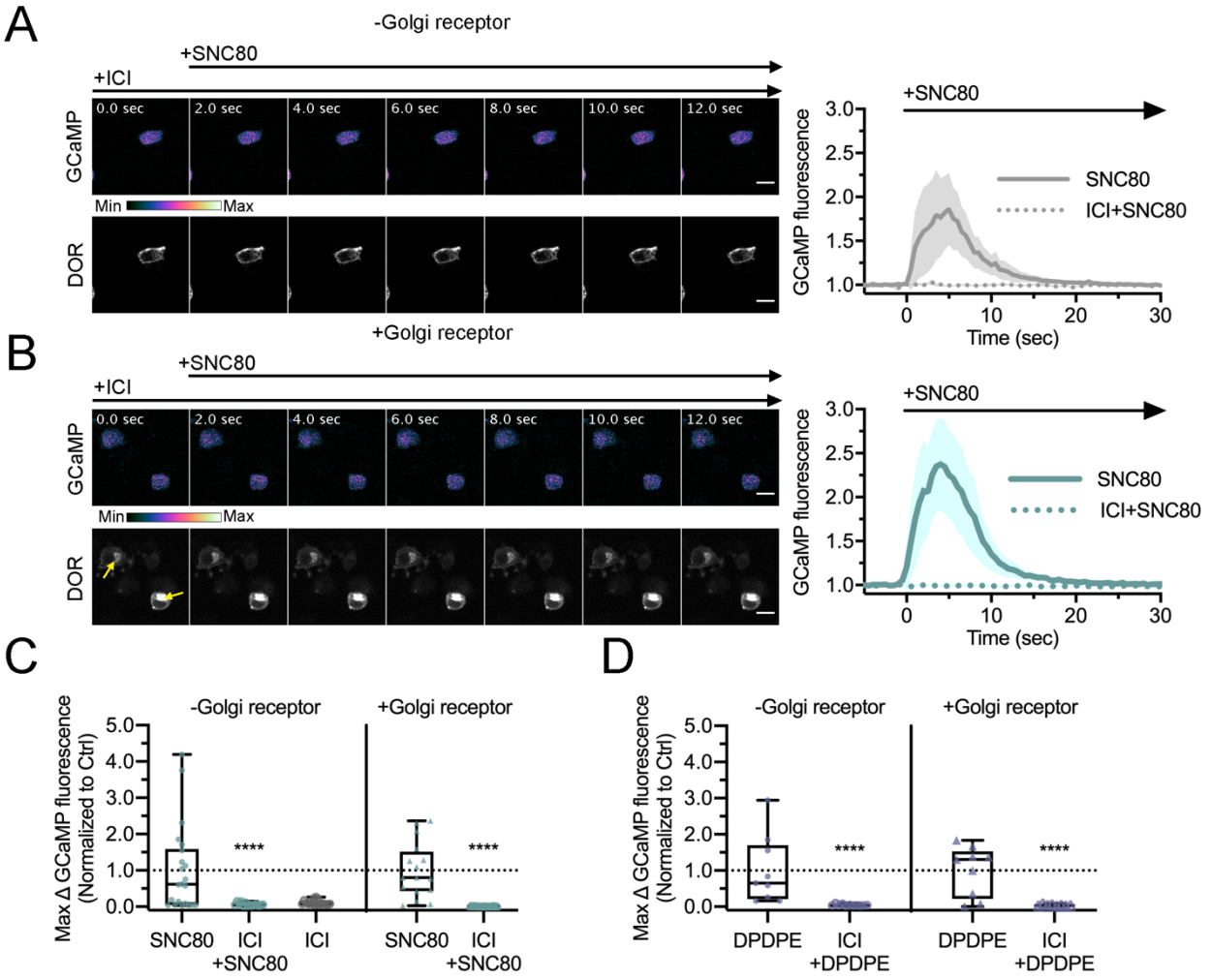

Figure 4.4. Intracellular calcium release is specific to PM DOR.
(A-B) PC12 cells expressing GCaMP6f and SNAP-DOR localized to the PM (**A**, upper panels), as well as cells expressing GCaMP6f and SNAP-DOR localized to the Golgi (**B**, lower panels, yellow arrows) were imaged live by confocal microscopy. Calibration bar indicates pixel values in scaled image. With 100μM ICI174864 (ICI) present in the media, addition of 100nM SNC80 to cells in either condition does not produce an increase in GCaMP6f fluorescence (Scale bar=15μm). Representative image is shown with corresponding trace of GCaMP6f fluorescence normalized to mean baseline fluorescence over time (solid line indicates mean, shading +/- 95% CI; -Golgi receptor, SNC80 n=22

cells, ICI+SNC80 n=14; +Golgi receptor, SNC80 n=16, ICI+SNC80 n=18). **(C-D)** Maximum change in GCaMP6f fluorescence over baseline, normalized to SNC80 **(C)** or DPDPE **(D)** treatment within each condition (+/- Golgi receptor). 100μM ICI present in the media significantly decrease the change in GCaMP6f fluorescence in response to SNC80 or DPDPE, regardless of whether a Golgi pool of DOR was present. ICI alone did not increase GCaMP6f fluorescence (one sample t-test compared to a theoretical mean of 1, -Golgi receptor ICI+SNC80 $p<0.0001$, +Golgi receptor ICI+SNC80 $p<0.0001$, -Golgi receptor ICI+DPDPE $p<0.0001$, +Golgi receptor ICI+DPDPE $p<0.0001$) (-Golgi receptor: SNC80 n=22, ICI+SNC80 n=14, ICI n=17; +Golgi receptor, SNC80 n=16, ICI+SNC80 n=18; -Golgi receptor: DPDPE n=9, ICI+DPDPE n=11; +Golgi receptor: DPDPE n=9, ICI+DPDPE n=8; box represents 25^{th} to 75^{th} percentiles, whiskers represent min to max, points represent individual cells).

These results are directly contrasted with results using the same experimental paradigm to measure Golgi DOR contributions to modulation of cellular cAMP (Stoeber *et al.*, 2018; Crilly *et al.*, 2021). Residual inhibition of cellular cAMP production was observed in cells with Golgi DOR activated with a cell permeable small molecule agonist (SNC80), but not an impermeable peptide agonist (DPDPE), despite pharmacological blockade of PM DOR with ICI. Here we observed no residual calcium response even when cells contained a Golgi pool of DOR, and results using a small molecule versus a peptide DOR agonist were indistinguishable. Together these data indicate that mobilization of calcium from intracellular stores is specific to PM DOR.

Discussion

We show that DOR activation by multiple agonists increases intracellular calcium levels in PC12 cells. This calcium response requires Gi/o proteins, Gαq/11, phospholipase C (PLC), and calcium release from intracellular stores. Importantly, modulation of this calcium response is specific to DOR signaling from the PM and is not detected downstream of DOR activation at the Golgi. These results contrast with previous findings that DOR in both locations regulates cAMP and highlight that DOR localization to the PM versus the Golgi divergently regulates signaling molecules.

To our knowledge we show for the first time that DOR mobilizes intracellular calcium stores in PC12 cells. DOR regulates calcium similarly in other neuronally

derived cell lines, including SH-SY5Y, NG108-15, and neuro2A cells, as well as primary dorsal root ganglion neurons (Jin *et al.*, 1994; Connor and Henderson, 1996; Spencer *et al.*, 1997; Bao *et al.*, 2003). Many of these studies have similarly implicated Gi/o proteins in this signaling response (Jin *et al.*, 1994; Connor and Henderson, 1996; Yoon *et al.*, 1999; Chen *et al.*, 2000). Specifically, Gβγ subunits liberated from activated Gi/o proteins modulate calcium signaling through actions on both PLC and calcium channels (Yoon *et al.*, 1999; Tennakoon *et al.*, 2021). We think DOR-dependent calcium responses likely require Gβγ, and ongoing experiments to inhibit Gβγ will clarify the role of Gβγ in the calcium signaling we have characterized. In some cellular contexts calcium influx through channels augments DOR-dependent intracellular calcium release (Jin *et al.*, 1992; Bao *et al.*, 2003). Our data showing a requirement for intracellular calcium stores and IP_3Rs suggest intracellular calcium stores are the primary source of the calcium increase, though further experiments testing the contribution of plasma membrane calcium channels specifically will clarify if they augment this response.

The requirement of Gαq/11 for DOR-dependent calcium responses is consistent with known synergy between Gq and Gi/o-coupled GPCRs, such as DOR and other opioid receptors (Okajima *et al.*, 1993; Connor and Henderson, 1996; Chen *et al.*, 2000). Gαq and Gβγ synergistically activate PLCβ2 and PLCβ3 isoforms (Philip *et al.*, 2010; Rebres *et al.*, 2011). We hypothesize that DOR couples primarily to inhibitory G proteins, but that basal signaling of endogenous Gq-coupled GPCRs is required to produce detectable increases in calcium upon DOR activation, as described for Gi/o-coupled GPCR calcium responses in multiple cell types (Okajima *et al.*, 1993; Pfeil *et al.*, 2020). The Gq-coupled GPCR serving this function in PC12 cells is not known. DOR calcium responses were independent of serum present in the imaging medium, suggesting Gq signaling may arise from an agonist secreted by the cells themselves or constitutive activity of a Gq-coupled GPCR. BRET sensors which report G protein activation at a cellular and subcellular level, such as TRUPATH and BERKY sensors (Maziarz *et al.*, 2020; Olsen *et al.*, 2020), could be used in the future to confirm DOR-G protein coupling specificity in PC12 cells.

Our findings that intracellular calcium levels are specifically regulated by PM DOR but not Golgi DOR provide important insight as to how DOR subcellular localization influences its signaling profile, though the mechanisms underlying this specificity remain unclear. It is interesting to speculate about the mechanisms by which regulation of calcium is specific to PM DOR. One possibility is that Golgi DOR does not couple to heterotrimeric G proteins to initiate this signaling. We think this is the least likely explanation, given the results showing both PM and Golgi DOR inhibit cAMP production, consistent with their known coupling to inhibitory G proteins (Stoeber *et al.*, 2018; Crilly *et al.*, 2021). However, we have not yet shown that DOR couples to endogenous G proteins in the Golgi or demonstrated a requirement of inhibitory G proteins for cAMP inhibition by Golgi DOR. Future experiments addressing these points will be essential to confirm functional coupling of DOR to G proteins in the Golgi.

Altered PLC activity or inefficient PLC activation downstream of Golgi DOR signaling is another possible mechanism conferring subcellular specificity to DOR calcium signaling. PLC substrate $PI(4,5P)_2$, which is hydrolyzed by PLC to produce DAG and IP_3, with the latter stimulating calcium release from ER stores, is most enriched at the PM (Balla, 2013). PLC enzymes can also hydrolyze phosphatidylinositol 4-phosphate (PI(4)P), the phospholipid most enriched at the Golgi, to produce DAG and IP_2, which will not activate IP_3Rs (Zhang *et al.*, 2013; Smrcka, 2015; Gil De Rubio *et al.*, 2018). Regardless of the phospholipid substrate, PLC activity on phospholipids in a membrane should produce DAG, an important signaling molecule, which can be used as a readout for PLC activity. Preliminary experiments using the YFP-DBD biosensor to monitor DAG production at the Golgi in response to Golgi DOR activation by SNC80, revealed no significant changes in sensor localization to the Golgi **(Figure 4.S4)**. These data are contrasted with recruitment of the sensor to the PM, upon DOR activation by SNC80 **(Figure 4.3C-E)** and suggest Golgi DOR activation may not locally activate PLC. Golgi DOR coupling to a different complement of Gβγ isoforms which can exert isoform-specific effects on effectors including PLCβ (Kankanamge *et al.*, 2021; Tennakoon *et al.*, 2021), could also influence local PLC activation. Subcellular localization of PLC enzymes through direct interactions of PLC enzyme with membranes or through scaffolding proteins, which can be expressed in a cell type-

specific manner (Adjobo-Hermans *et al.*, 2013; Lyon and Tesmer, 2013; Zhang *et al.*, 2013), could also affect local PLC activation. Clearly many factors could determine the subcellular specificity of DOR calcium signaling. In the immediate future, measurement of inositol phosphate levels upon Golgi DOR activation could provide a more sensitive readout of Golgi DOR stimulation of PLC activity to confirm our preliminary imaging data.

Taken together the data presented here and previous work support the idea that DOR subcellular localization to the PM versus the Golgi markedly alters the DOR signaling profile, with potentially profound impacts on DOR physiology and pharmacology. Both PM DOR and Golgi DOR inhibit cAMP production (Stoeber *et al.*, 2018; Crilly *et al.*, 2021). In contrast to PM DOR, Golgi DOR does not recruit β-arrestins (Crilly *et al.*, 2021), suggesting that kinase signaling may also be altered in the Golgi DOR signaling profile, similar to what we observed for calcium, though we have not investigated this directly. We have begun to probe the transcriptional effects downstream of PM DOR versus Golgi DOR activation, which could provide broader insights into subcellular signaling profile differences. Links between increased intracellular calcium, PLC activity, and DOR-mediated antinociception (Ohsawa *et al.*, 1998; Narita *et al.*, 2000) present the intriguing possibility that the association between DOR PM localization and enhanced pain relieving effects is due in part to a PM DOR specific signaling profile which promotes these effects.

Materials and Methods

DNA constructs

SNAP-DOR was cloned by restriction enzyme cloning as described (Crilly *et al.*, 2021). FAP-DOR was cloned as described (Shiwarski *et al.*, 2017a). GCaMP6f was a gift from Jonathan Ting (Addgene plasmid #51085). YFP-DBD was a gift from Alexandra Newton (Addgene plasmid #14874) via Alan Smrcka.

Cell culture and transfection

Pheochromocytoma-12 cells (PC12 cells, ATCC #CRL-1721) were maintained at 37C and 5% CO2. Cells were cultured in F12K media, supplemented with 10% horse serum and 5% fetal bovine serum (FBS). Cells were grown in flasks coated with Collagen IV to promote adherence. Cells were transfected using Lipofectamine 2000 (Invitrogen #11668) as described (Crilly *et al.*, 2021), and imaged 48-72 hours after transfection.

Live cell imaging

For calcium imaging experiments, PC12 cells transfected with SNAP-DOR and GCaMP6f or stably expressing FAP-DOR, were plated and imaged in single-use Mattek dishes (1.5 coverglass, 35mm, P35G-1.5-10-C) coated with poly-D-lysine. For Fluo-4 AM (Invitrogen F14201) loading, cells were washed once with HBSS, followed by incubation with Fluo-4 AM (3μM) in HBSS for 30 minutes at room temperature protected from light and washed three times with HBSS prior to imaging. In conditions requiring NGF treatment, cells were treated with 100ng/mL NGF for 1 hour prior to imaging with NGF maintained in imaging media. When imaging SNAP-DOR expressing cells, cells were labeled with 1μM cell permeable SNAP-Cell 647-SiR (NEB S9102S) for 15 minutes, followed by a 15 minute wash at 37°C immediately prior to imaging. Inhibitors requiring preincubation (YM-254890, U73122, U73343, Thapsigargin) were added to cells during this wash step. PTX was added to cells approximately 20-24 hours prior to imaging.

Cells were imaged in either Leibovitz's L-15 media (Gibco #11415) supplemented with 1% FBS or in HBSS. Cells were imaged on a Nikon TiE inverted microscope using a 20x objective (Nikon Instruments, Melville, NY) inside a 37°C heated imaging chamber (In Vivo Scientific). Cells were excited using 647-nm (SNAP-DOR) and 488-nm (GCaMP6f, Fluo-4) solid state lasers with a quad emission filter and images captured every 500ms on an iXon+897 EMCCD camera (Andor, Belfast, UK).

Imaging of PC12 cells expressing SNAP-DOR and YFP-DBD was performed on the same microscope system with a 60x-1.49 Apo-TIRF objective (Nikon Instruments,

Melville, NY). Cells were labeled with 500nM SNAP-647 surface for 5min at 37C prior to TIRF imaging. Cells were again excited with 647-nm and 488-nm solid state lasers and a quad emission filter , with images captured every 15sec on an iXon+897 EMCCD camera (Andor, Belfast, UK).

Image quantification

Quantification of GCaMP6f or Fluo4 calcium imaging was conducted using a custom Python script (Weinberg, 2020) that used numpy (Oliphant, 2006; Van Der Walt *et al.*, 2011), pandas (McKinney, 2010), matplotlib (Hunter, 2007), scikit-image (Van Der Walt *et al.*, 2014), Jupyter (Kluyver *et al.*, 2016), and seaborn (Waskom *et al.*, 2020), for data manipulation and StarDist (Schmidt *et al.*, 2018; Weigert *et al.*, 2020), for cell segmentation. Briefly, a StarDist segmentation model was trained on 25 hand-labeled images of GCaMP6f-expressing PC12 cells with varying levels of activation. This model was then used to segment all GCaMP6f movies. Cells were tracked across frames using centroids of detected objects in adjacent frames, allowing for gaps between detections. All tracked cells that were not detected in at least half the frames of a movie were discarded, as were cells whose mean GCaMP6f fluorescence was indistinguishable from background. Fluorescence was normalized to the mean of the first 100 frames of the movie, and drug response was taken as the max value detected between frames 101 and 200.

YFP-DBD recruitment to PM DOR or intracellular DOR was performed using ImageJ/Fiji (National Institutes of Health, Bethesda, MD) as previously described (Schindelin *et al.*, 2012; Crilly *et al.*, 2021). Briefly, mean fluorescence of the YFP-DBD channel was measured over time in the region of the cell defined by fluorescence in the SNAP-DOR channel. Change in mean fluorescence intensity is expressed as the fold change in mean fluorescence over baseline mean fluorescence before drug addition.

Statistics and data analysis

Data were plotted and statistically analyzed using GraphPad Prism 9 software. A p value of <0.05 was considered significant. Exact p values, statistical tests used, and

sample sizes are provided in the figure legends. Figures were assembled in Adobe Illustrator version 26.0.1.

Acknowledgements

SEC would like to thank Dr. Alan Smrcka, Dr. Lois Weisman, and Dr. Bing Ye for valuable feedback on this project. SEC would also like to thank Dr. Kasun Ratnayake for productive discussion and collaboration on this project and feedback during the writing of this chapter. Additional thanks to Dr. Alan Smrcka, Dr. Hoa Phan, and Gissell Sanchez for reagents and helpful discussion. SEC was supported by National Science Foundation Graduate Research Fellowship under Grant DGE 1256260. MAP was supported by NIH grant GM117425 and National Science Foundation (NSF) grant 1935926.

Supplementary Figures

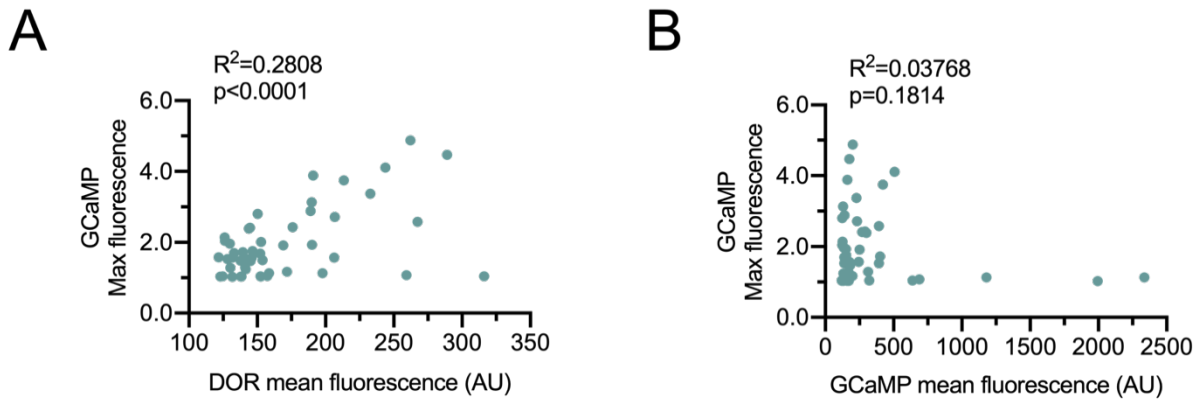

Figure 4.S1. DOR-dependent calcium response is positively correlated with DOR expression.
(A) Scatterplot of max GCaMP6f fluorescence increase after 100nM SNC80 addition and corresponding mean DOR fluorescence as a measure of DOR expression (n=49 cells, points represent individual cells). Linear regression analysis indicated a significant correlation between max GCaMP6f fluorescence increase and DOR expression (R^2=0.2808, p<0.0001). **(B)** Scatterplot of max GCaMP6f fluorescence increase after 100nM SNC80 addition and corresponding mean GCaMP6f baseline fluorescence as a measure of GCaMP6f expression (n=49 cells, points represent individual cells). Linear regression analysis indicated no significant correlation between max GCaMP6f fluorescence increase and GCaMP6f expression (R^2=0.03768, p=0.1814).

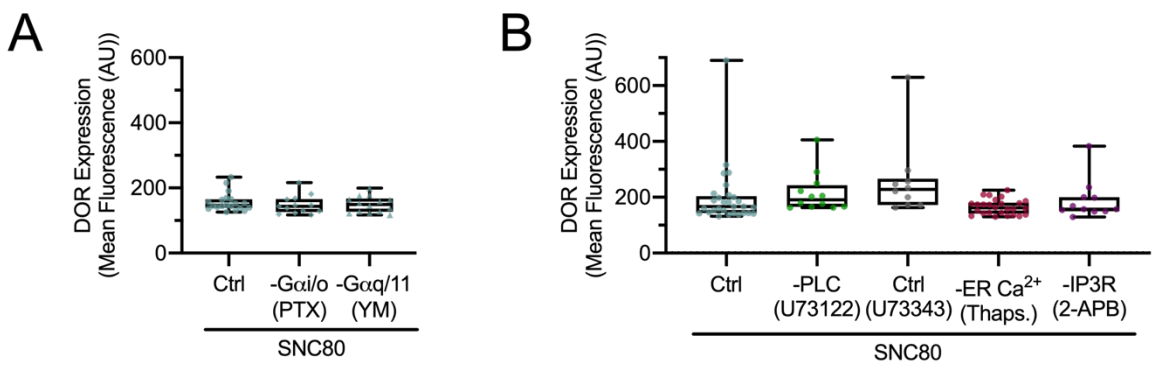

Figure 4.S2. DOR expression levels are similar across treatment conditions.
(A-B) Mean DOR fluorescence levels were similar across treatment conditions presented in **Figs. 2C,3B** (**A**: SNC80, Ctrl n=20 cells, PTX n=13, YM n=14; **B**: Ctrl n=29; U73122 n=12; U73343 n=10; thapsigargin n=26; 2-APB n=11; box represents 25th to 75th percentiles, whiskers represent min to max, points represent individual cells).

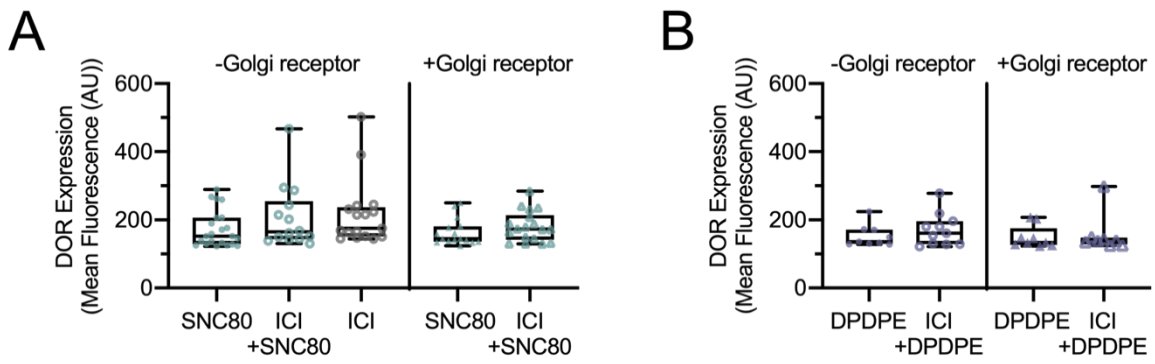

Figure 4.S3. DOR expression levels are similar in cells with and without Golgi receptor.

(A-B) Mean DOR fluorescence levels were similar across treatment conditions presented in **Fig. 4C-D** (**A**: -Golgi receptor, SNC80 n=22 cells, ICI+SNC80 n=14, ICI n=17; +Golgi receptor, SNC80 n=16, ICI+SNC80 n=18; **B**: -Golgi receptor: DPDPE n=9, ICI+DPDPE n=11; +Golgi receptor: DPDPE n=9, ICI+DPDPE n=8; box represents 25th to 75th percentiles, whiskers represent min to max, points represent individual cells).

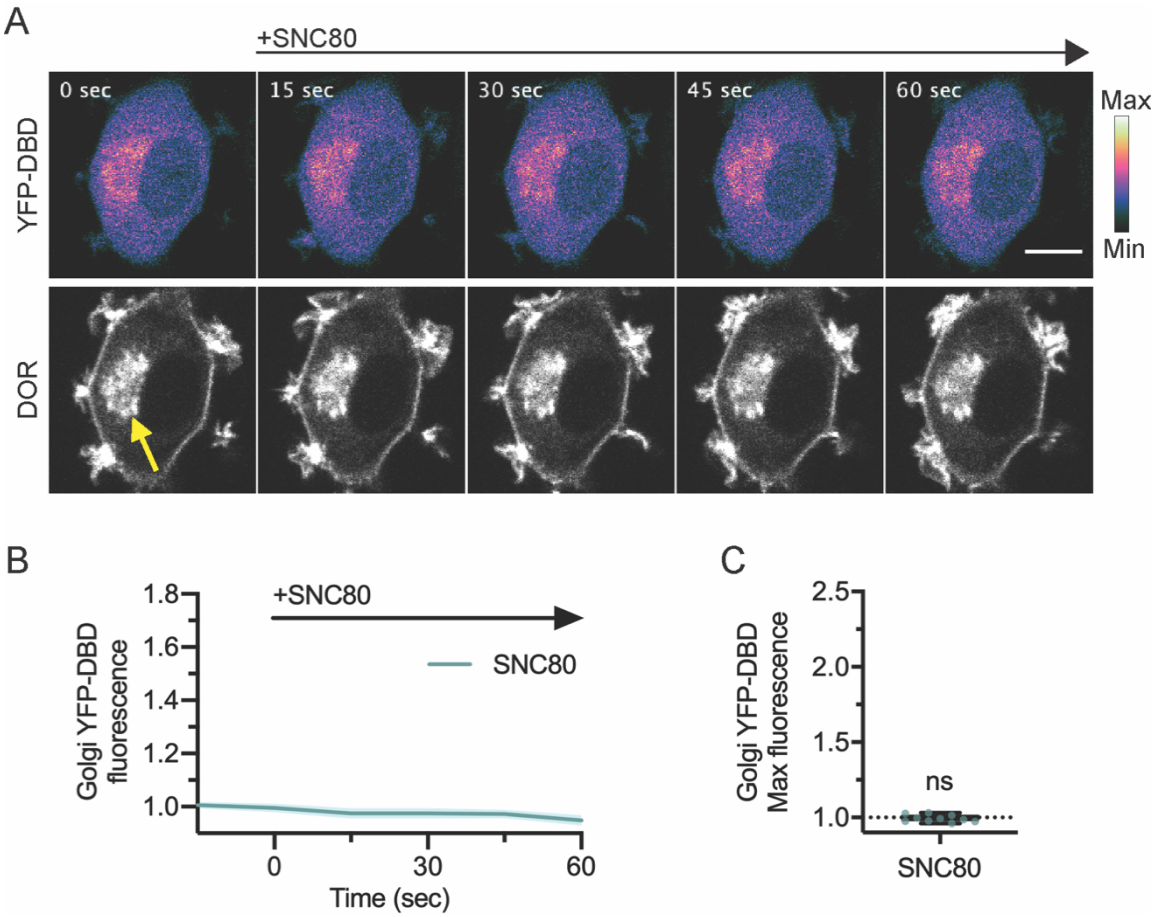

Figure 4.S4. DOR activation does not produce a detectable increase in Golgi DAG levels.

(A) YFP-DBD (upper panel) in PC12 cells expressing SNAP-DOR (lower panel) imaged by confocal microscopy to visualize changes in sensor recruitment to Golgi DOR (yellow arrow) DOR agonist SNC80 (10μM) (scale bar=5μm). Calibration bar indicates pixel values in scaled image. **(B)** Change in YFP-DBD fluorescence in the region of the cell defined by intracellular DOR normalized to the mean baseline fluorescence over time after addition of SNC80 (solid line indicates mean, shading +/- 95% CI). **(C)** Maximum Golgi YFP-DBD fluorescence does not significantly increase compared to baseline fluorescence within 60 seconds after SNC80 addition (one sample t-test compared to a theoretical mean of 1, p=0.2840) (SNC80 n=10 cells; box represents 25th to 75th percentiles, whiskers represent min to max, points represent individual cells).

References

Abdallah, K, and Gendron, L (2018). The delta opioid receptor in pain control. In: Handbook of Experimental Pharmacology, Springer New York LLC, 147–177.

Adjobo-Hermans, MJW, Crosby, KC, Putyrski, M, Bhageloe, A, van Weeren, L, Schultz, C, Goedhart, J, and Gadella, TWJ (2013). PLCβ isoforms differ in their subcellular location and their CT-domain dependent interaction with Gαq. Cell Signal 25, 255–263.

Balla, T (2013). Phosphoinositides: Tiny lipids with giant impact on cell regulation. Physiol Rev 93, 1019–1137.

Bao, L et al. (2003). Activation of delta opioid receptors induces receptor insertion and neuropeptide secretion. Neuron 37, 121–133.

Berridge, MJ (2009). Inositol trisphosphate and calcium signalling mechanisms. Biochim Biophys Acta - Mol Cell Res 1793, 933–940.

Bilmen, JG, and Michelangeli, F (2002). Inhibition of the type 1 inositol 1,4,5-trisphosphate receptor by 2-aminoethoxydiphenylborate. Cell Signal 14, 955–960.

Bleasdale, JE, Thakur, NR, Gremban, RS, Bundy, GL, Fitzpatrick, FA, Smith, RJ, and Bunting, S (1990). Selective inhibition of receptor-coupled phospholipase C-dependent processes in human platelets and polymorphonuclear neutrophils. J Pharmacol Exp Ther 255.

Cahill, CM, McClellan, KA, Morinville, A, Hoffert, C, Hubatsch, D, O'Donnell, D, and Beaudet, A (2001). Immunohistochemical distribution of delta opioid receptors in the rat central nervous system: Evidence for somatodendritic labeling and antigen-specific cellular compartmentalization. J Comp Neurol 440, 65–84.

Cahill, CM, Morinville, A, Hoffert, C, O'Donnell, D, and Beaudet, A (2003). Up-regulation and trafficking of delta opioid receptor in a model of chronic inflammation: implications for pain control. Pain 101, 199–208.

Chang Ho Lee, Park, D, Wu, D, Sue Goo Rhee, and Simon, MI (1992). Members of the G(q) α subunit gene family activate phospholipase C β isozymes. J Biol Chem 267, 16044–16047.

Chen, L, Zou, S, Lou, X, and Kang, HG (2000). Different stimulatory opioid effects on intracellular Ca2+ in SH-SY5Y cells. Brain Res 882, 256–265.

Chen, TW et al. (2013). Ultrasensitive fluorescent proteins for imaging neuronal activity. Nature 499, 295–300.

Connor, M, and Henderson, G (1996). δ- and μ-opioid receptor mobilization of intracellular calcium in SH-SY5Y human neuroblastoma cells. Br J Pharmacol 117, 333–340.

Crilly, SE, Ko, W, Weinberg, ZY, and Puthenveedu, MA (2021). Conformational specificity of opioid receptors is determined by subcellular location irrespective of

agonist. Elife 10.

Crilly, SE, and Puthenveedu, MA (2020). Compartmentalized GPCR Signaling from Intracellular Membranes. J Membr Biol.

Dripps, IJ, and Jutkiewicz, EM (2018). Delta opioid receptors and modulation of mood and emotion. In: Handbook of Experimental Pharmacology, Springer New York LLC, 179–197.

Fasolato, C, Pizzo, P, and Pozzan, T (1990). Receptor-mediated calcium influx in PC12 cells. ATP and bradykinin activate two independent pathways. J Biol Chem 265, 20351–20355.

Gafni, J, Munsch, JA, Lam, TH, Catlin, MC, Costa, LG, Molinski, TF, and Pessah, IN (1997). Xestospongins: Potent membrane permeable blockers of the inositol 1,4,5-trisphosphate receptor. Neuron 19, 723–733.

Gallegos, LL, Kunkel, MT, and Newton, AC (2006). Targeting protein kinase C activity reporter to discrete intracellular regions reveals spatiotemporal differences in agonist-dependent signaling. J Biol Chem 281, 30947–30956.

Gendron, L, Cahill, CM, Zastrow, M Von, Schiller, PW, and Pineyro, G (2016). Molecular Pharmacology of d -Opioid Receptors. 68, 631–700.

Gil De Rubio, R, Ransom, RF, Malik, S, Yule, DI, Anantharam, A, and Smrcka, A V (2018). Phosphatidylinositol 4-phosphate is a major source of GPCR-stimulated phosphoinositide production.

Hunter, JD (2007). Matplotlib: A 2D graphics environment. Comput Sci Eng 9, 99–104.

Jin, W, Lee, NM, Loh, HH, and Thayer, SA (1992). Dual excitatory and inhibitory effects of opioids on intracellular calcium in neuroblastoma x glioma hybrid NG108-15 cells. Mol Pharmacol 42.

Jin, W, Lee, NM, Loh, HH, and Thayer, SA (1994). Opioids Mobilize Calcium from Inositol 1,4,5-Trisphosphate-Sensitive Stores in NG 108-15 Cells.

Jong, YJI, Harmon, SK, and O'Malley, KL (2018). GPCR signalling from within the cell. Br J Pharmacol 175, 4026–4035.

Kankanamge, D, Ubeysinghe, S, Tennakoon, M, Pantula, PD, Mitra, K, Giri, L, and Karunarathne, A (2021). Dissociation of the G protein β? From the Gq-PLCβ complex partially attenuates PIP2 hydrolysis. J Biol Chem 296.

Katada, T (2012). The inhibitory G protein Gi identified as pertussis toxin-catalyzed ADP-ribosylation. Biol Pharm Bull 35, 2103–2111.

Kim, K, and von Zastrow, M (2003). Neurotrophin-regulated sorting of opioid receptors in the biosynthetic pathway of neurosecretory cells. J Neurosci 23, 2075–2085.

Kluyver, T et al. (2016). Jupyter Notebooks—a publishing format for reproducible computational workflows. In: Positioning and Power in Academic Publishing: Players,

Agents and Agendas - Proceedings of the 20th International Conference on Electronic Publishing, ELPUB 2016, IOS Press BV, 87–90.

Lobingier, BT, and von Zastrow, M (2019). When trafficking and signaling mix: How subcellular location shapes G protein-coupled receptor activation of heterotrimeric G proteins. Traffic 20, 130–136.

Lyon, AM, and Tesmer, JJG (2013). Structural insights into phospholipase C-β function. Mol Pharmacol 84, 488–500.

Ma, Q, Ye, L, Liu, H, Shi, Y, and Zhou, N (2017). An overview of Ca $^{2+}$ mobilization assays in GPCR drug discovery. Expert Opin Drug Discov 12, 511–523.

Maziarz, M, Park, JC, Leyme, A, Marivin, A, Garcia-Lopez, A, Patel, PP, and Garcia-Marcos, M (2020). Revealing the Activity of Trimeric G-proteins in Live Cells with a Versatile Biosensor Design. Cell 182, 770-785.e16.

McKinney, W (2010). Data Structures for Statistical Computing in Python. In: Proceedings of the 9th Python in Science Conference, 56–61.

Narita, M, Ohsawa, M, Mizoguchi, H, Aoki, T, Suzuki, T, and Tseng, LF (2000). Role of the phosphatidylinositol-specific phospholipase C pathway in δ-opioid receptor-mediated antinociception in the mouse spinal cord. Neuroscience 99, 327–331.

Ohsawa, M, Nagase, H, and Kamei, J (1998). Role of intracellular calcium in modification of Mu and delta opioid receptor-mediated antinociception by diabetes in mice. J Pharmacol Exp Ther 286, 780–787.

Okajima, F, Tomura, H, and Kondo, Y (1993). Enkephalin activates the phospholipase C/Ca2+ system through cross-talk between opioid receptors and P2-purinergic or bradykinin receptors in NG 108-15 cells: A permissive role for pertussis toxin-sensitive G-proteins. Biochem J 290, 241–247.

Oliphant, TE (2006). A guide to NumPy, USA: Trelgol Publishing.

Olsen, RHJ et al. (2020). TRUPATH, an open-source biosensor platform for interrogating the GPCR transducerome. Nat Chem Biol 16, 841–849.

Pfeil, EM et al. (2020). Heterotrimeric G Protein Subunit Gαq Is a Master Switch for Gβγ-Mediated Calcium Mobilization by Gi-Coupled GPCRs. Mol Cell 80, 940-954.e6.

Philip, F, Kadamur, G, Silos, RG, Woodson, J, and Ross, EM (2010). Synergistic activation of phospholipase C-β3 by Gαq and Gβγ describes a simple two-state coincidence detector. Curr Biol 20, 1327–1335.

Pradhan, A, Smith, M, McGuire, B, Evans, C, and Walwyn, W (2013). Chronic inflammatory injury results in increased coupling of delta opioid receptors to voltage-gated Ca2+ channels. Mol Pain 9, 8.

Reber, BFX, Neuhaus, R, and Reuter, H (1992). Activation of different pathways for calcium elevation by bradykinin and ATP in rat pheochromocytoma (PC 12) cells.

Pflügers Arch Eur J Physiol 420, 213–218.

Rebres, RA et al. (2011). Synergistic Ca2+ responses by Gαi- and Gαq-coupled G-protein-coupled receptors require a single PLCβ isoform that is sensitive to both Gβγ and Gαq. J Biol Chem 286, 942–951.

Roth, BL, Laskowski, MB, and Coscia, CJ (1981). Evidence for distinct subcellular sites of opiate receptors. Demonstration of opiate receptors in smooth microsomal fractions isolated from rat brain. J Biol Chem 256, 10117–10123.

Schindelin, J et al. (2012). Fiji: An open-source platform for biological-image analysis. Nat Methods 9, 676–682.

Schmidt, U, Weigert, M, Broaddus, C, and Myers, G (2018). Cell Detection with Star-Convex Polygons. In: Medical Image Computing and Computer Assisted Intervention (MICCAI) 2018-21st International Conference, Granada, Spain, September 16-20, 2018, Proceedings, Part II, 265–273.

Shiwarski, DJ, Crilly, SE, Dates, A, and Puthenveedu, MA (2019). Dual RXR motifs regulate nerve growth factor–mediated intracellular retention of the delta opioid receptor. Mol Biol Cell 30, 680–690.

Shiwarski, DJ, Darr, M, Telmer, CA, Bruchez, MP, and Puthenveedu, MA (2017a). PI3K class II α regulates δ-opioid receptor export from the trans-Golgi network. Mol Biol Cell 28, 2202–2219.

Shiwarski, DJ, Tipton, A, Giraldo, MD, Schmidt, BF, Gold, MS, Pradhan, AA, and Puthenveedu, MA (2017b). A PTEN-regulated checkpoint controls surface delivery of σ opioid receptors. J Neurosci 37, 3741–3752.

Smrcka, A V. (2015). Regulation of phosphatidylinositol-specific phospholipase C at the nuclear envelope in cardiac myocytes. J Cardiovasc Pharmacol 65, 203–210.

Smrcka, A V., Hepler, JR, Brown, KO, and Sternweis, PC (1991). Regulation of polyphosphoinositide-specific phospholipase C activity by purified Gq. Science (80-) 251, 804–807.

Smrcka, A V., and Sternweis, PC (1993). Regulation of purified subtypes of phosphatidylinositol-specific phospholipase C β by G protein α and βγ subunits. J Biol Chem 268, 9667–9674.

Spencer, RJ, Jin, W, Thayer, SA, Chakrabarti, S, Law, PY, and Loh, HH (1997). Mobilization of Ca2+ from intracellular stores in transfected neuro(2a) cells by activation of multiple opioid receptor subtypes. Biochem Pharmacol 54, 809–818.

Stoeber, M, Jullié, D, Lobingier, BT, Laeremans, T, Steyaert, J, Schiller, PW, Manglik, A, and von Zastrow, M (2018). A Genetically Encoded Biosensor Reveals Location Bias of Opioid Drug Action. Neuron 98, 963-976.e5.

Tennakoon, M, Senarath, K, Kankanamge, D, Ratnayake, K, Wijayaratna, D,

Olupothage, K, Ubeysinghe, S, Martins-Cannavino, K, Hébert, TE, and Karunarathne, A (2021). Subtype-dependent regulation of Gβγ signalling. Cell Signal 82.

Treiman, M, Caspersen, C, and Christensen, SB (1998). A tool coming of age: Thapsigargin as an inhibitor of sarco-endoplasmic reticulum Ca2+-ATPases. Trends Pharmacol Sci 19, 131–135.

Van Der Walt, S, Colbert, SC, and Varoquaux, G (2011). The NumPy array: A structure for efficient numerical computation. Comput Sci Eng 13, 22–30.

Van Der Walt, S, Schönberger, JL, Nunez-Iglesias, J, Boulogne, F, Warner, JD, Yager, N, Gouillart, E, and Yu, T (2014). Scikit-image: Image processing in python. PeerJ 2014, e453.

Wang, H, and Pickel, VM (2001). Preferential cytoplasmic localization of delta-opioid receptors in rat striatal patches: comparison with plasmalemmal mu-opioid receptors. J Neurosci 21, 3242–3250.

Waskom, M, Botvinnik, O, Ostblom, J, Gelbart, M, Lukauskas, S, and Hobson, P (2020). mwaskom/seaborn: v0.10.1 (April 2020) (Version v0.10.1). Zenodo. Available at: https://zenodo.org/record/3767070. Accessed September 17, 2020.

Weigert, M, Schmidt, U, Haase, R, Sugawara, K, and Myers, G (2020). Star-convex polyhedra for 3D object detection and segmentation in microscopy. In: Proceedings - 2020 IEEE Winter Conference on Applications of Computer Vision, WACV 2020, Institute of Electrical and Electronics Engineers Inc., 3655–3662.

Weis, WI, and Kobilka, BK (2018). The Molecular Basis of G Protein–Coupled Receptor Activation. Annu Rev Biochem 87, 897–919.

Wu, V, Yeerna, H, Nohata, N, Chiou, J, Harismendy, O, Raimondi, F, Inoue, A, Russell, RB, Tamayo, P, and Gutkind, JS (2019). Illuminating the Onco-GPCRome: Novel G protein-coupled receptor-driven oncocrine networks and targets for cancer immunotherapy. J Biol Chem 294, 11062–11086.

Xiong, XF, Zhang, H, Boesgaard, MW, Underwood, CR, Bräuner-Osborne, H, and Strømgaard, K (2019). Structure–Activity Relationship Studies of the Natural Product G q/11 Protein Inhibitor YM-254890. ChemMedChem 14.

Yoon, SH, Lo, TM, Loh, HH, and Thayer, SA (1999). δ-opioid-induced liberation of Gβγ mobilizes Ca2+ stores in NG108- 15 cells. Mol Pharmacol 56, 902–908.

Zhang, L, Malik, S, Pang, J, Wang, H, Park, KM, Yule, DI, Blaxall, BC, and Smrcka, A V (2013). Phospholipase Cε hydrolyzes perinuclear phosphatidylinositol 4-phosphate to regulate cardiac hypertrophy. Cell 153, 216–227.

Chapter 5: Concluding Remarks and Future Directions

This work contributes to a growing body of research investigating subcellular localization as an important variable influencing G protein-coupled receptor (GPCR) signaling and function. Using the delta opioid receptor (DOR) as a clinically relevant prototype GPCR, I have made novel discoveries regarding how GPCR subcellular localization is regulated and how subcellular location influences GPCR activation and signaling. The general principles by which DOR membrane trafficking and signaling within the biosynthetic pathway are regulated could be shared with other GPCRs. DOR specifically is a promising alternative target for the treatment of pain and depression (Abdallah and Gendron, 2018; Dripps and Jutkiewicz, 2018). DOR localizes to both the plasma membrane and the Golgi in neuronal cells, and its relocation from intracellular compartments to the plasma membrane enhances the pain-relieving effects of DOR agonists (Cahill *et al.*, 2003; Pradhan *et al.*, 2013; Shiwarski *et al.*, 2017). Therefore, these findings are also directly applicable to potential therapeutic strategies targeting DOR.

I have shown that DOR localization to the Golgi requires conserved dual RXR amino acid motifs which interact with coatomer protein I (COPI) retrograde trafficking machinery (Shiwarski *et al.*, 2019). From a cell biology perspective, these results provide a satisfying explanation for the steady-state localization of DOR to a dynamic organelle like the Golgi (Glick and Luini, 2011). From a translational perspective, identification of this interaction provides a targetable molecular interaction for therapeutic strategies to increase DOR localization to the plasma membrane. Additional work is necessary to further characterize the DOR-COPI interaction. Small molecules which disrupt this interaction could potentially increase DOR localization to the plasma membrane. We have also explored a genetic approach of overexpressing the DOR C-terminal tail to compete with DOR for binding to the cellular components responsible for

Golgi retention, thus allowing DOR to traffic to the plasma membrane. A genetic approach could provide greater specificity, both at the receptor and cellular level. This specificity may be especially important given preliminary data showing that Golgi localization of somatostatin receptor 5 may be regulated by similar mechanisms.

Using novel biosensors developed in the field within the past decade to detect specific GPCR conformations with high spatiotemporal resolution, I have shown that subcellular location drives distinct engagement of active conformation biosensors (Crilly *et al.*, 2021). These findings suggest the exciting possibility that these biosensors detect distinct receptor conformations and that subcellular location influences GPCR conformational landscapes. There has been a tremendous amount of interest in developing GPCR ligands which bias receptors toward specific conformations and associated effector interactions and signaling (Luttrell *et al.*, 2015). A possible spatial component of bias adds important context to development of new biased ligands which may act on GPCRs in multiple subcellular locations. Future experiments should specifically address whether these biosensors recognize distinct DOR conformations and how compartment-specific properties may drive these changes to receptor dynamics. Regardless, this work highlights the power of these biosensor tools to uncover new GPCR biology.

I have also shown that DOR in different subcellular locations differentially regulates second messenger signaling molecules, emphasizing the impact of subcellular localization on signaling. Specifically, DOR in both the plasma membrane and Golgi inhibits cAMP production (Crilly *et al.*, 2021), whereas modulation of calcium release from intracellular stores is specific to DOR signaling at the plasma membrane (Chapter 4). These data reveal how DOR subcellular localization alters the net signaling response at a cellular level. The mechanisms underlying DOR subcellular signaling specificity remain unclear. Future work should specifically test DOR coupling to G proteins in different subcellular locations. I have also performed preliminary experiments exploring how gene expression differs following DOR activation in the plasma membrane versus the Golgi. Among other GPCRs, differences in gene expression are a major downstream consequence of GPCR signaling from different locations (Jong *et al.*,

2009; Tsvetanova and von Zastrow, 2014; Godbole *et al.*, 2017; Jensen *et al.*, 2017; Gorvin *et al.*, 2018). These data could also broadly inform how signaling profiles change in response to DOR activation in different subcellular locations. Any differences in signaling also contribute to the idea of spatial bias and are relevant to development of new drugs which can act on GPCRs in multiple locations.

Rapid progress has been made in this field over the past decade. This progress has informed novel approaches to target GPCRs for the treatment of disease and is potentially paving the way for a new era of GPCR pharmacology. Proof-of-concept experiments have shown that targeting mechanisms regulating DOR Golgi retention increases DOR expression at the plasma membrane and enhances the antihyperalgesic effects of DOR agonists (Shiwarski *et al.*, 2017). These data suggest tuning GPCR function by altering GPCR localization may be a viable therapeutic strategy. Additionally, modified ligands which concentrate in endosomes have shown promise targeting endosomally localized GPCRs to more effectively treat pain (Jensen, Yarwood, Halls)(Jensen *et al.*, 2017; Yarwood *et al.*, 2017; Jimenez-Vargas *et al.*, 2020), and genetic approaches to specifically inhibit β_1-adrenergic receptor signaling at the Golgi may protect against cardiac hypertrophy (Nash *et al.*, 2019). Together these examples highlight the tremendous potential to apply a fundamental understanding of the links between GPCR location and signaling, such as that described in this dissertation, to design better therapeutics.

References

Abdallah, K, and Gendron, L (2018). The delta opioid receptor in pain control. In: Handbook of Experimental Pharmacology, Springer New York LLC, 147–177.

Cahill, CM, Morinville, A, Hoffert, C, O'Donnell, D, and Beaudet, A (2003). Up-regulation and trafficking of delta opioid receptor in a model of chronic inflammation: implications for pain control. Pain 101, 199–208.

Crilly, SE, Ko, W, Weinberg, ZY, and Puthenveedu, MA (2021). Conformational specificity of opioid receptors is determined by subcellular location irrespective of agonist. Elife 10.

Dripps, IJ, and Jutkiewicz, EM (2018). Delta opioid receptors and modulation of mood and emotion. In: Handbook of Experimental Pharmacology, Springer New York LLC,

179–197.

Glick, BS, and Luini, A (2011). Models for Golgi traffic: A critical assessment. Cold Spring Harb Perspect Biol 3.

Godbole, A, Lyga, S, Lohse, MJ, and Calebiro, D (2017). Internalized TSH receptors en route to the TGN induce local Gs-protein signaling and gene transcription. Nat Commun 8, 443.

Gorvin, CM et al. (2018). AP2σ Mutations Impair Calcium-Sensing Receptor Trafficking and Signaling, and Show an Endosomal Pathway to Spatially Direct G-Protein Selectivity. Cell Rep 22, 1054–1066.

Jensen, DD et al. (2017). Neurokinin 1 receptor signaling in endosomes mediates sustained nociception and is a viable therapeutic target for prolonged pain relief. Sci Transl Med 9.

Jimenez-Vargas, NN et al. (2020). Endosomal signaling of delta opioid receptors is an endogenous mechanism and therapeutic target for relief from inflammatory pain. Proc Natl Acad Sci, 202000500.

Jong, YJI, Kumar, V, and O'Malley, KL (2009). Intracellular metabotropic glutamate receptor 5 (mGluR5) activates signaling cascades distinct from cell surface counterparts. J Biol Chem 284, 35827–35838.

Luttrell, LM, Maudsley, S, and Bohn, LM (2015). Fulfilling the promise of "biased" g protein-coupled receptor agonism. Mol Pharmacol 88, 579–588.

Nash, CA, Wei, W, Irannejad, R, and Smrcka, A V. (2019). Golgi localized βi-adrenergic receptors stimulate golgi PI4P hydrolysis by PLCε to regulate cardiac hypertrophy. Elife 8.

Pradhan, A, Smith, M, McGuire, B, Evans, C, and Walwyn, W (2013). Chronic inflammatory injury results in increased coupling of delta opioid receptors to voltage-gated Ca2+ channels. Mol Pain 9, 8.

Shiwarski, DJ, Crilly, SE, Dates, A, and Puthenveedu, MA (2019). Dual RXR motifs regulate nerve growth factor-mediated intracellular retention of the delta opioid receptor. Mol Biol Cell 30, 680–690.

Shiwarski, DJ, Tipton, A, Giraldo, MD, Schmidt, BF, Gold, MS, Pradhan, AA, and Puthenveedu, MA (2017). A PTEN-regulated checkpoint controls surface delivery of σ opioid receptors. J Neurosci 37, 3741–3752.

Tsvetanova, NG, and von Zastrow, M (2014). Spatial encoding of cyclic AMP signaling specificity by GPCR endocytosis. Nat Chem Biol 10, 1061–1065.

Yarwood, RE et al. (2017). Endosomal signaling of the receptor for calcitonin gene-related peptide mediates pain transmission. Proc Natl Acad Sci U S A 114, 12309–12314.